

Property of
Flood Control District of MC Library
Please Return to
2801 W. Durango
Phoenix, AZ 85009

Generalized Computer Program

FLUVIAL-12

Mathematical Model for Erodible Channels

Users Manual

prepared by
Howard H. Chang, Ph.D., P.E.
San Diego, California
August 1986

CONTENTS

I. PROGRAM SUMMARY	1
II. INTRODUCTION	3
III. PHYSICAL FOUNDATION OF FLUVIAL PROCESS-RESPONSE	4
IV. CHANNEL WIDTH ADJUSTMENTS DURING SCOUR AND FILL	5
V. ANALYTICAL BASIS OF THE FLUVIAL MODEL	9
VI. WATER ROUTING	10
VII. SEDIMENT ROUTING	13
Determination of Sediment Discharge	13
Upstream Boundary Conditions for Sediment Inflow	15
Numerical Solution of Continuity Equation for Sediment	15
VIII. SIMULATION OF CHANGES IN CHANNEL WIDTH	16
Direction of Width Adjustment	17
Rate of Width Adjustment	17
IX. SIMULATION OF CHANGES IN CHANNEL-BED PROFILE	19
X. SIMULATION OF CHANGES DUE TO CURVATURE EFFECT	20
XI. TEST AND CALIBRATION OF MATHEMATICAL MODEL	22
APPENDIX A. REFERENCES	23
APPENDIX B. INPUT/OUTPUT INSTRUCTIONS FOR THE FLUVIAL MODEL	25
APPENDIX C. SAMPLE INPUT/OUTPUT LISTINGS	36
APPENDIX D. SAMPLE GRAPHIC OUTPUT FOR CROSS-SECTIONAL CHANGES	
APPENDIX E. TECHNICAL PAPERS DESCRIBING ANALYTICAL BACKGROUND OF MODEL	
Modeling of River Channel Changes	
Water and Sediment Routing through Curved Channels	
Computer-Based Design of River Bank Protection	

I. PROGRAM SUMMARY FOR FLUVIAL-12

The computer program FLUVIAL-12 is formulated and developed for water and sediment routing in natural and man-made channels. The combined effects of flow hydraulics, sediment transport and river channel changes are simulated for a given flow period.

River channels changes simulated by the model include channel bed scour and fill (or aggradation and degradation), width variation, and changes in bed topography induced by the curvature effect. These inter-related changes are coupled in the model for each time step. While this model is for erodible channels, physical constraints, such as bank protection, grade-control structures and bedrock outcroppings, may also be specified. Applications of this model include evaluations of general scour at bridge crossings, sediment delivery, channel responses to sand and gravel mining, channelization, etc. It has been applied to many designs for bank protection and grade-control structures which must extend below the potential channel bed scour and withstand the design flood.

This model is applicable to ephemeral rivers as well as rivers with long-term flow; it has also been tested and calibrated with field data from several rivers, in both semi-arid and humid regions. Because of the transient behavior in dynamic changes, ephemeral rivers require more complicated techniques in model formulation. This model may be used on any main frame computer; it may be used on a personal computer with adequate capacity, such as an IBM-PC-AT or -XT.

Development of the FLUVIAL computer model dates back to 1972. Several publications describing the physical foundation, analytical background, and applications are included in this manual. Publications documenting the successive stages of development of the model are listed in the following:

1. Chang, H. H., "Flood Plain Sedimentation and Erosion, Phase III," Dept. of Sanitation and Flood Control, Public Works Agency, County of San Diego, January, 1974, 78 pp.
2. Chang, H. H., "Flood Plain Sedimentation and Erosion, Phase VI," Dept.

of Sanitation and Flood Control, Public Works Agency, County of San Diego, July, 1975, 77 pp.

3. Chang, H. H., and Hill, J. C., "Computer Modeling of Erodible Flood Channels and Deltas," Journal of the Hydraulics Division, ASCE, Vol. 102, No. HY10, October, 1976, pp. 1461-75.
4. Chang, H. H., and Hill, J. C. "Minimum Stream Power for Rivers and Deltas," Journal of the Hydraulics Division, ASCE, Vol. 103, No. HY12, December, 1977, pp. 1375-89.
5. Chang, H. H., "Mathematical Model for Erodible Channels," Journal of the Hydraulics Division, ASCE, Vol. 108, No. HY5, May, 1982, pp.678-689.
6. Chang, H. H., "Modeling of River Channel Changes," Journal of Hydraulic Engineering, ASCE, Vol. 110, No. 2, February, 1984, pp. 157-172.
7. Chang, H. H., "Modeling General Scour at Bridge Crossings," Transportation Research Record, 950, Vol. 2, September, 1984, pp. 238-243, also presented at the Second Bridge Engineering Conference, Transportation Research Board, Minneapolis, Minnesota, September 24-26, 1984.
8. Chang, H. H., "Regular Meander Path Model", Journal of Hydraulic Engineering, ASCE, Vol. 110, No. 10, October, 1984, pp. 1398- 1411.
9. Chang, H. H., "Water and Sediment Routing through Curved Channels", Journal of Hydraulic Engineering, ASCE, Vol. 111, No. 4, April, 1985, pp. 644-658.
10. Chang, H. H., "Modeling Fluvial Processes in Streams with Gravel Mining", International Workshop on Problems of Sediment Transport in Gravel-Bed Rivers, Colorado State University, August 12-17, 1985.
11. Chang, H. H., Osmolski, Z. and Smutzer, D., "Computer-Based Design of River Bank Protection," Hydraulics and Hydrology in the Small Computer Age, Proceedings of the Hydraulic Specialty Conference, ASCE, Orlando, Florida, August 13-16, 1985, pp. 426-431.
12. Chang, H. H., "Channel Width Adjustment during Scour and Fill," Journal of Hydraulic Engineering, ASCE, Vol. 111, No. 10, October, 1985.
13. Chang, H. H., "River Channel Responses during Floods," Proceedings, The Third-International Symposium on river Sedimentation, Jackson, Mississippi, April, 1986.
14. Chang, H. H., and Osmolski, Z., "Fluvial Design of River Bank Protection for Santa Cruz River", Proceedings of Computational Hydrology '87, Computational Hydrology Institute, Irvine, Calif., June, 1987.

II. INTRODUCTION

Alluvial rivers are self-regulatory in that they adjust their characteristics in response to any change in the environment. These environmental changes may occur naturally, as in the case of climatic variation or changes in vegetative cover, or may be a result of such human activities as damming, river training, diversion, sand and gravel mining, channelization, bank protection, and bridge and highway construction. Such changes distort the natural quasi-equilibrium of a river; in the process of restoring the equilibrium, the river will adjust to the new conditions by changing its slope, roughness, bed-material size, cross-sectional shape, or meandering pattern. Within the existing constraints, any one or a combination of these characteristics may adjust as the river seeks to maintain the balance between its ability to transport and the load provided.

River channel behavior often needs to be studied for its natural state and responses to the aforementioned human activities. Studies of river hydraulics, sediment transport and river channel changes may be through physical modeling or mathematical modeling, or both. Physical modeling has been relied upon traditionally to obtain the essential design information. It nevertheless often involves large expenditure and is time consuming in model construction and experimentation. What limits the accuracy of physical modeling is the scale distortion which is almost unavoidable whenever it involves sedimentation.

Mathematical modeling of erodible channels has been advanced with the progress in the physics of fluvial processes and computer techniques. A evaluation of existing models was made by the National Academy of Sciences (1983). Recommendations in this report has been beneficial for subsequent model development. Since the actual size of a river is employed in mathematical modeling, there is no scale distortion. The applicability and accuracy of a model depend on the physical foundation and numerical techniques employed.

The traditional regime analyses of rivers are limited to regime rivers and their long-term adjustments in equilibrium. The hydraulic geometry,

flow and sediment transport processes exhibited in the process of adjustments are outside the scope of regime approach but they are included in the mathematical modeling. This manual addresses the more rapid process-response or the transient behavior of alluvial rivers. The subject is on unsteady flow and sediment transport in river channels with a changing boundary under given physical constraints. In the following, the physical foundation and numerical techniques for the transient process-response of the FLUVIAL model are described. The input/output instructions are provided. Applications of the FLUVIAL model are illustrated by examples given in the appendixes.

III. PHYSICAL FOUNDATION OF FLUVIAL PROCESS-RESPONSE

Mathematical modeling of river channel changes requires adequate and sufficient physical relationships for the fluvial processes. While the processes are governed by the principles of continuity, flow resistance, sediment transport and bank stability, such relations are insufficient to explain the time and spatial variations of channel width in an alluvial river. Generally, width adjustment occurs concurrently with changes in river bed profile, slope, channel pattern, roughness, etc. These changes are closely interrelated; they are delicately adjusted to establish or to maintain the dynamic state of equilibrium. While any factor imposed upon the river is usually absorbed by a combination of the above responses. The extent of each type of response is inversely related to the resistance to change.

The dynamic equilibrium is the direction toward which each river channel evolves. The transient behavior of an alluvial river undergoing changes must reflect its constant adjustment toward dynamic equilibrium, although, under the changing discharge, the true equilibrium may never be attained. For a short river reach of uniform discharge, the conditions for dynamic equilibrium are: (1) Equal sediment discharge along the channel, and (2) uniformity in power expenditure γQS , where γ is the unit weight of the water-sediment mixture, Q is the discharge, and S is the energy gradient. If the energy gradient is approximated by the water-surface slope, then uniform power expenditure or energy gradient is equivalent to the

linear (straight-line) water-surface profile along the channel. A river channel undergoing changes usually does not have a linear water-surface profile or uniform sediment discharge, but river channel adjustments are such that the non-uniformities in water-surface profile and sediment discharge are effectively reduced. The rate of adjustment is limited by the rate of sediment movement and subject to the rigid constraints such as grade-control structures, bank protection, abutments, bedrock, etc.

The energy gradient at a river cross section varies wildly. This variable is usually included in a hydraulic computation such as that of a HEC-2 study. The output of any HEC-2 study, even for a fairly uniform river channel, usually exhibits non-uniformity in energy gradient along the channel. This variation is much more pronounced in disturbed rivers. A mathematical modeler realizes that a river channel will change in order to attain streamwise uniformity in sediment load. It is equally important to perceive that it will also adjust toward equal energy gradient along the channel. Because sediment discharge is a direct function of $\gamma Q S$, channel adjustment in the direction of equal power expenditure also favors the uniformity in sediment discharge. The sediment discharge in the reach will match the inflow rate when the equilibrium is reached.

IV. CHANNEL WIDTH ADJUSTMENTS DURING SCOUR AND FILL

A stream channel's adjustment in the direction of equal power expenditure, or straight water-surface profile, provides the physical basis for the modeling of channel width changes. However, this adjustment does not necessarily mean movement toward uniformity in channel width. For one thing, the power expenditure is also affected by channel roughness and channel-bed elevation, in addition to the width. But, more importantly, the adjustment toward uniformity in power expenditure is frequently accomplished by significant streamwise variation in width. Such spatial width variation generally occurs concurrently with streambed scour or fill to be illustrated in the following by several examples.

The transient behavior can be more clearly demonstrated by more dramatic river channel changes in the short term. Field examples of this

nature are selected herein to illustrate how the significant spatial variation in width is related to river channel's adjustment toward uniform power expenditure. This example will also show why the regime approach may not be employed to simulate river channel changes.

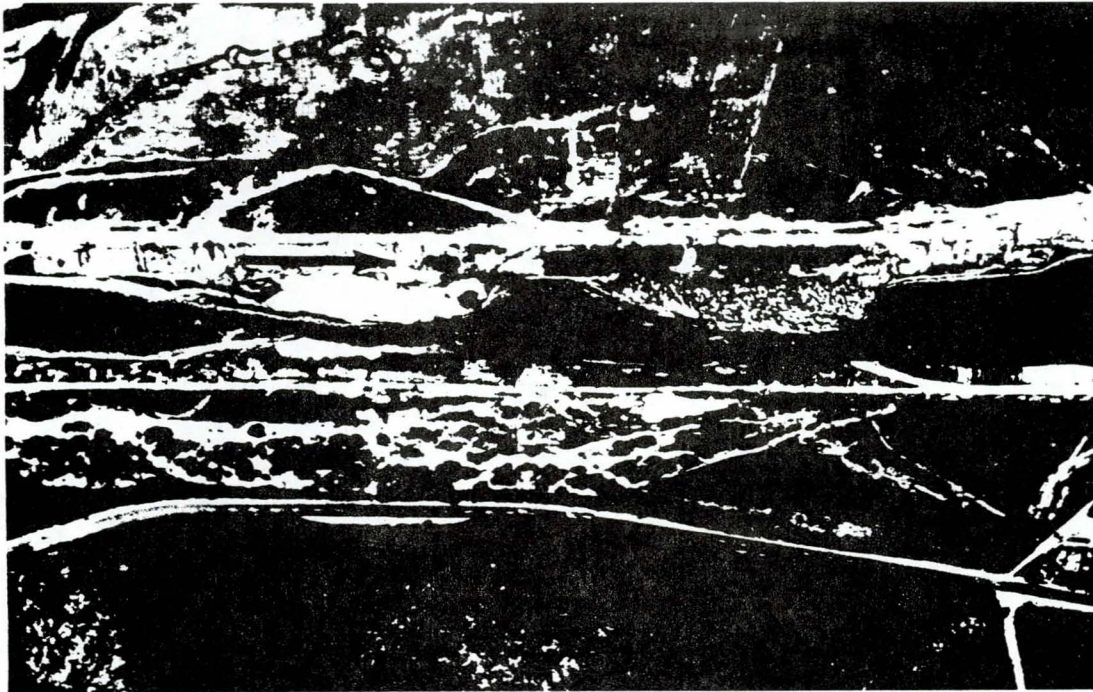


Fig. 1 Streamwise variation in width during stream channel adjustment toward establishing straight water-surface profile, San Diego River at Lakeside, California

Fig. 1 shows a short reach of the San Diego River at Lakeside, California on February 25, 1981 during the initial stage of a storm. The estimated discharge of 600 cfs persisted for several subsequent days. Prior to the storm, this sandy streambed was graded, due to sand mining, to a wavy profile. During the initial period of flow, the water-surface profile was not straight because its gradient was steeper over higher streambed areas than over lower areas. Gradually, these higher streambed areas were scoured while lower places filled. Small widths formed with streambed scour whereas large widths developed with fill as shown in the figure. The width development in this case was rapid in occurrence in the sandy material, its significant streamwise variation is depicted by the natural streamlines visible

on the water surface. This pattern of significant spatial variation in width actually represents the stream's adjustment toward equal energy gradient as explained in the following.

The streambed area undergoing scour had a steeper energy gradient (or water-surface slope) than its adjacent areas. Formation of a narrower and deeper channel was effective to reduce the energy gradient due to decreased boundary resistance and lowered streambed elevation. In addition, the cross section developed a somewhat circular shape which conserved power for being closer to the best hydraulic section. On the other hand, the streambed area undergoing fill had a lower streambed elevation and a flatter energy gradient. Channel widening at this area was effective to steepen its energy gradient due to the increasing boundary resistance and rising streambed elevation. In summary, these adjustments in channel width effectively reduced the spatial variation in power expenditure or non-linearity in water-surface profile. Because sediment discharge is a direct function of stream power $\gamma Q S$, channel adjustment in the direction of equal power expenditure also favors the equilibrium, or uniformity, in sediment discharge.

The significant spatial width variation shown in Fig. 1 was temporary. The small width lasted while streambed scour continued and the large width persisted with sustained fill. At a later stage when scour and fill ceased, the energy gradient or water-surface slope associated with the small width became flatter than that for the large width. The new profile of energy gradient or water surface became a reversal of the initial profile. Then, the small width started to grow wider while the large width began to slide back into the channel, resulting in a more uniform width along the channel.

The above example illustrates that a regime relationship for channel width may not be used in simulating transient river channel changes. Under the regime relationship, the width is a direct function of the discharge, i.e., $B \propto Q^{0.5}$; but under transient changes, the channel can have very different widths even though the discharge is essentially uniform along the channel.

The characteristic changes in channel width during channel-bed scour

and fill were also observed by Andrews (1982) on the East Fork river in Wyoming. This river was in its natural state, undisturbed by human activities. River channel changes were induced by the variation in discharge.

In 1906, the Associated Press filed a well-written report which seemed to end one of the world's most spectacular stories. In the story, the AP reported that the Colorado River flooded; the water moved from the All American Canal to the New River and poured down to the Salton Sea. The sea rose seven inches per day. The water became a cascade and its force cut back the banks. Soon the bank was receding faster and faster, moving upstream into the valley at a pace of 4,000 feet a day and widening the New River channel to a gorge of more than 1,000 feet. This example also illustrates the dramatic widening of river channel associated with a rising bed elevation.

A field study by the U. S. Bureau of Reclamation (1963) upstream of Milburn Diversion Dam on the Middle Loup River, Central Nebraska also exemplifies the aggradation of a channel and associated channel widening.

The construction of Milburn Diversion Dam was completed in May, 1956... By May 1957, two months after the reservoir was impounded for the first irrigation season, the channel had aggraded an average of 1.6 feet, with a rise in the channel thalweg elevation of 2.2 feet; and by October of the same year, the total rise in the streambed averaged 2.2 feet. The cross section obtained in December 1957, shows a continued rise in the thalweg elevation. During the same period, the width of the channel had increased by 70 feet, from 475 feet in 1951 to 545 feet in 1957. One-third of this increase occurred during the June, 1956 - December, 1957 period.

For these two case histories, both alluvial rivers entered reservoirs with a rising base level. The transient changes are characterized by rising channel bed and increasing channel width. Although measurements of the discharge and other parameters are not available, it is possible to describe, at least in trend, the nature of power transformation in the river channel.

At the river mouth, the base level was controlled in the reservoir. The rising base level first caused a lower velocity and energy gradient in the river channel near the mouth in relation to its upstream reach. In response to this change, channel adjustments through widening and aggradation near the mouth provided greater flow resistance and power expenditure at this location partly due to the increased boundary resistance. This process resulted in a more uniform power expenditure per unit channel length along the river.

A lowering base level, on the other hand, would result in a higher energy gradient in the river channel near the mouth. The higher energy gradient could be reduced through the development of a narrower and deeper channel at this location. This process would also result in a more uniform power expenditure along the channel. Such morphological features for deltas are also applicable to alluvial fans and hill slopes.

V. ANALYTICAL BASIS OF THE FLUVIAL MODEL

The FLUVIAL model with different versions has been developed for water and sediment routing in rivers while simulating river channel changes as documented in a series of publications listed in Section I. River channel changes simulated by the model include channel-bed scour and fill (or aggradation and degradation), width variation, and changes caused by curvature effects. Because changes in channel width and channel-bed profile are closely inter-related, modeling of erodible channels must include both changes. The analytical background of the FLUVIAL model is described in the following.

The FLUVIAL model has the following five major components: (1) Water routing, (2) sediment routing, (3) changes in channel width, (4) changes in channel-bed profile, and (5) changes in geometry due to curvature effect. These inter-related components are described in the following sections.

This model employs a space-time domain in which the space domain is represented by the discrete cross sections along the channel and the time domain is represented by discrete time increments. Temporal and spatial

variations in flow, sediment transport and channel geometry are computed following an iterative procedure. Water routing, which is coupled with the changing curvature, is assumed to be uncoupled from the sediment processes since sediment movement and changes in channel geometry are slow in comparison to the flow hydraulics. Flow chart showing major steps of the computation is given in Fig. 2.

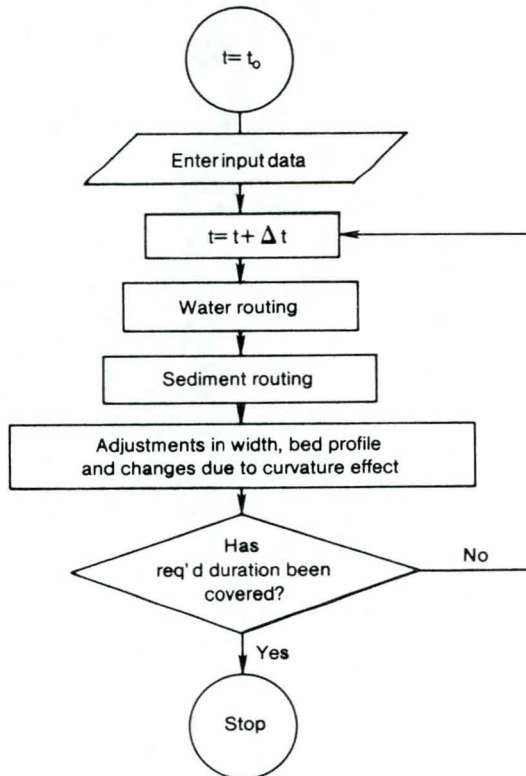


Fig. 2 Flow chart showing major steps of computation for FLUVIAL model

VI. WATER ROUTING

Water routing provides temporal and spatial variations of the stage, discharge, energy gradient and other hydraulic parameters in the channel. The water routing component has the following two major features: (1) Numerical solution of the continuity and momentum equation for longitudinal flow, (2) evaluation of flow resistance due to longitudinal and transverse flows, and (3) upstream and downstream boundary conditions. The continuity and momentum equations in the longitudinal direction are

$$\frac{\partial A}{\partial t} + \frac{\partial Q}{\partial s} - q = 0 \quad (1)$$

$$\frac{1}{A} \frac{\partial Q}{\partial t} + g \frac{\partial H}{\partial s} + \frac{1}{A} \frac{\partial}{\partial s} \left(\frac{Q^2}{A} \right) + gS - \frac{Q}{A^2} q = 0 \quad (2)$$

where Q is the discharge, A is the cross-sectional area of flow, t is the time, s is the curvilinear coordinate along discharge centerline measured from the upstream entrance, q is lateral inflow rate per unit length, H is the stage or water-surface elevation, and S is the energy gradient. The upstream boundary condition for water routing is the inflow hydrographs and the downstream condition is the stage-discharge relation or the base-level variation. Techniques for numerical solution of Eqs. 1 and 2 are described in Chen (1973) and Fread (1971, 1974), among others.

In a curved channel, the total energy gradient, S , in Eq. 2 is partitioned into the longitudinal energy gradient, S' , and the transverse energy gradient, S'' , due to secondary currents, i.e.

$$S = S' + S'' \quad (3)$$

The longitudinal energy gradient can be evaluated using any valid flow resistance relationship. If Manning's formula is employed, the roughness coefficient n must be selected by the modeler. However, if a formula for alluvial bed roughness, e.g., Brownlie's formula (1983), is used, the roughness coefficient is predicted by the formula.

Method for evaluating the transverse energy gradient by Chang (1983) is used in the model. Because of the streamwise changing curvature, the transverse energy loss varies with the growth and decay of secondary currents along the channel. Analytical relationships pertaining to curved channels are often based upon the mean channel radius, r_c . Under the streamwise changing curvature, the application of such relationships is limited to fully-developed transverse flow for which the curvature is defined. Streamwise variation of transverse flow, over much of the channel length, is characterized by its growth and decay. In order to describe this spatial variation, the mean flow curvature defined as the flow curvature along the discharge centerline is employed. It is assumed that analytical relationships for developed transverse flows are applicable for developing

transverse flows when the mean channel curvature, r_c , is replaced by the mean flow curvature, r_f . Upon entering a bend, the mean flow curvature increases with the growth in transverse circulation. In a bend, the transverse flow becomes fully developed if the flow curvature approaches the channel curvature. In the case of exiting from a bend to the downstream tangent in which the channel curvature is zero, the flow curvature decreases with the decay of transverse circulation.

The reason that the flow curvature lags behind the channel curvature during circulation growth and decay is attributed to the internal turbulent shear that the flow has to overcome in transforming from parallel flow into the spiral pattern and vice versa. From the dynamic equation for the transverse velocity, an equation governing the streamwise variation in transverse surface velocity, \tilde{v} , was derived (Chang, 1984). In finite difference form, the change in \tilde{v} over the distance Δs is given by

$$\tilde{v}_{i+1} = \left[\tilde{v}_i + F_1(f) \frac{U}{r_c} \exp(F_2(f) \Delta s) \Delta s \right] \exp[-F_2(f) \Delta s] \quad (4)$$

where \tilde{v} is the transverse surface velocity along discharge centerline, U is the average velocity of a cross section, i and $i+1$ are s -coordinate indices, F_1 and F_2 are functions of f (friction factor), and the overbar denotes averaging over the incremental distance between i and $i+1$. Eq. 4 provides the spatial variation in \tilde{v} , from which the mean flow curvature may be obtained using the transverse velocity profile. From the transverse velocity profile by Kikkawa, et al. (1976), the mean flow curvature, r_f , is related to the transverse surface velocity as

$$r_f = \frac{D_c}{\kappa} \frac{U}{\tilde{v}} \left(\frac{10}{3} - \frac{1}{\kappa} \frac{5}{9} \sqrt{\frac{f}{2}} \right) \quad (5)$$

where D_c is the flow depth at discharge centerline (thalweg) and κ is the Karman constant. At each time step, the mean flow curvature at each cross section is obtained using Eqs. 4 and 5. Accuracy of computation for the finite difference equation (Eq. 4) is maintained if the step size $\Delta s \leq 2D_c$. For this reason, the distance between two adjacent cross sections is divided into smaller increments if necessary. Flow parameters for these increments are interpolated from values known at adjacent cross sections.

If the temporal terms in Eqs. 1 and 2 are ignored, water routing may be simplified by computing water-surface profiles at successive time steps. This option is available in the model. Computation of the water-surface profile at each time step is based upon the standard-step method (see Chow, 1957) using techniques similar to the HEC-2 computer model (1982). For many cases, spatial variation in discharge due to channel storage is small and this technique produces closely similar results as the unsteady routing.

VII. SEDIMENT ROUTING

The sediment routing component for the FLUVIAL model has the following major features: (1) Computation of sediment transport capacity using a suitable formula for the physical conditions, (2) determination of actual sediment discharge by making corrections for sorting and diffusion, (3) upstream conditions for sediment inflow, and (4) numerical solution of the continuity equation for sediment. These features are evaluated at each time step, the results so obtained are used in determining the changes in channel configuration.

Determination of Sediment Discharge

To treat the time-dependent and non-equilibrium sediment transport, the bed material at each section is divided into several, say five, size fractions and the size for each fraction is represented by its geometric mean. For each size fraction, sediment transport capacity is first computed using a sediment transport formula. The FLUVIAL model currently provides the choices of the following five sediment formulas: (1) Engelund-Hansen formula (1967), (2) Yang's unit stream power formula (1972, 1986), (3) Graf's formula (1970), (4) Ackers-White formula, and (5) Parker, et al. formula for gravel (1982). The actual sediment rate is obtained by considering sediment material of all size fractions already in the flow and the exchange of sediment load with the bed using the method by Borah, et al. (1982). If the stream carries a load in excess of its capacity, it will deposit the excess material on the bed. In the case of erosion, any size fraction available for entrainment at the bed surface will be removed by the

flow and added to the sediment already in transport. During sediment removal, the exchange between the flow and the bed is assumed to take place in the active layer at the surface. Thickness of the active layer is based upon the relation defined by Borah, et al. This thickness is not only a function of the material size and composition, but also reflects the flow condition. During degradation, several of these layers may be scoured away, resulting in the coarsening of the bed material and formation of an armor coat. However, new active layers may be deposited on the bed in the process of aggradation. Materials eroded from the channel banks, excluding that portion in the wash load size range, are included in the accounting. Bed armoring develops if bed shear stress is too low to transport any available size.

The non-equilibrium sediment transport is also affected by diffusion, particularly for finer sediments. Because of diffusion, the deposition or entrainment of sediment is a gradual process and it takes certain travel time or distance to reach the transport capacity for a flow condition. Therefore, the actual sediment discharge at a section depends not only on the transport capacity at the section but also on the supply from upstream and its gradual adjustment toward the flow conditions of this section. In the model, the sediment discharge is corrected for the diffusion effects on deposition and entrainment using the method by Zhang, et al. (1983). The procedures for computing sediment transport rate, sediment sorting and diffusion are applied to the longitudinal and transverse directions. They are also coupled with bed-profile evolution described later in this section.

Sediment discharge may be limited by availability, as exemplified by the flow over a grade-control structure or bed rock. The very high transport capacity at such a section, associated with the high velocity, is limited by the supply rate from upstream; that is, the sediment discharge at such a section is under upstream control.

Upstream Boundary Conditions for Sediment Inflow

The rate of sediment inflow into the study reach is provided by the upstream boundary condition for sediment. If this rate is known, it may be

included as a part of the input and used in the simulation. Unfortunately, sediment rating data are rarely very reliable or simply not available. For such cases, it is assumed that the river channel remains unchanged above the study reach and sediment inflow rate is computed at the upstream section at each time step just like they are computed at other cross sections. For this reason, the study reach should extend far enough upstream so that the channel beyond may be considered basically stable. Factors that may induce river channel changes must be included in the study reach.

Numerical Solution of Continuity Equation for Sediment

Changes in cross-sectional area, due to longitudinal and transverse imbalances in sediment discharge, are obtained based upon numerical solution of continuity equations for sediment in the respective directions. First, the continuity equation for sediment in the longitudinal direction is

$$(1 - \lambda) \frac{\partial A_b}{\partial t} + \frac{\partial Q_s}{\partial s} - q_s = 0 \quad (6)$$

where λ is the porosity of bed material, A_b is the cross-sectional area of channel bed within some arbitrary frame, Q_s is the bed-material discharge, and q_s is the lateral inflow rate of sediment per unit length. According to this equation, the time change of cross-sectional area $\partial A_b / \partial t$ is related to the longitudinal gradient in sediment discharge $\partial Q_s / \partial s$ and lateral sediment inflow q_s . In the absence of q_s , longitudinal imbalance in Q_s is absorbed by channel adjustments toward establishing uniformity in Q_s .

The change in cross-sectional area ΔA_b for each section at each time step is obtained through numerical solution of Eq. 6. This area change will be applied to the bed and banks following correction techniques for channel width and channel-bed profile.

From Eq. 6, the correction in cross-sectional area of channel bed for a time increment can be written as

$$\Delta A_b = - \frac{\Delta t}{1 - \lambda} \left(\frac{\partial Q_s}{\partial s} - q_s \right) \quad (7)$$

At a section i , the lateral sediment inflow may be written as

$$q_{s_i} = \frac{1}{2} (q_{s_i}^j + q_{s_i}^{j+1}) \quad (8)$$

where superscripts j and $j+1$ are the times at t and $t + \Delta t$, respectively. This model employs an upstream difference in s and a centered difference in t for the partial derivative, $\partial Q_s / \partial s$, in Eq. 6, i.e.

$$\left(\frac{\partial Q_s}{\partial s} \right)_i = \frac{2}{\Delta s_i + \Delta s_{i-1}} \left(\frac{Q_{s_i}^j + Q_{s_i}^{j+1}}{2} - \frac{Q_{s_{i-1}}^j + Q_{s_{i-1}}^{j+1}}{2} \right) \quad (9)$$

where Δs_i is the distance between sections i and $i+1$, Δs_{i-1} is the distance between $i-1$ and i . With this upstream difference for $\partial Q_s / \partial s$, the change in bed area at a section i depends on sediment rates at this section and its upstream section $i-1$; it is independent of the sediment rate at the downstream section. In other words, it is under upstream control. Contrary to this, the stage at a section in subcritical flow depends on the downstream stage and is independent of the upstream stage, i.e., the stage is under downstream control in a subcritical flow.

VIII. SIMULATION OF CHANGES IN CHANNEL WIDTH

The change in cross-sectional area ΔA_b obtained in sediment routing represents the correction for a time increment t that needs to be applied to the bed and banks. With ΔA_b being the total correction, it is possible for both the bed and banks to have deposition or erosion; it is also possible to have deposition along the banks but erosion in the bed and vice versa. The direction of width adjustment is determined following the stream power approach and the rate of change is based upon bank erodibility and sediment transport described in the following.

Direction of Width Adjustment

For a time step, width corrections at all cross sections are such that the stream power for the reach moves toward uniformity; these corrections are subject to the physical constraint of rigid banks and limited by the

amount of sediment removal or deposition along the banks within the time step. A river channel undergoing changes usually has nonuniform spatial distribution in power expenditure or γQS . Usually the spatial variation in Q is small but that in S is pronounced. An adjustment in width reflects the river's adjustment in flow resistance; that is, in power expenditure. A reduction in width at a cross section is usually associated with a decrease in energy gradient for the section whereas an increase in width is accompanied by an increase in energy gradient. To determine the direction of width change at a section i , the energy gradient at this section, S_i , is compared with the weighted average of its adjacent sections, \bar{S}_i . Here

$$\bar{S}_i = \frac{S_{i+1}\Delta s_i + S_{i-1}\Delta s_{i+1}}{\Delta s_i + \Delta s_{i+1}} \quad (10)$$

If the energy gradient S_i is greater than \bar{S}_i , channel width at this section is reduced so as to decrease the energy gradient. On the other hand, if S_i is lower, channel width is increased in order to raise the energy gradient. These changes are subject to the rate of width adjustment and physical constraints.

Width changes in alluvial rivers are characterized by widening during channel-bed aggradation (or fill) and reduction in width at the time of degradation (or scour). Such river channel changes represent the river's adjustments in resistance to seek equal power expenditure along its course. A degrading reach usually has a higher channel-bed elevation and energy gradient than its adjacent sections. Formation of a narrower and deeper channel at the degrading reach decreases its energy gradient due to reduced boundary resistance. On the other hand, an aggrading reach is usually lower in channel-bed elevation and energy gradient. Widening at the aggrading reach increases its energy gradient due to increasing boundary resistance. These adjustments in channel width reduce the spatial variation in energy gradient and total power expenditure of the channel.

Rate of Width Adjustment

For a time increment, the amount of width change depends on the sediment rate, bank configuration and bank erodibility. The slope of an

erodible bank is limited by the angle of repose of the material. The rate of width change depends on the rate at which sediment material is removed or deposited along the banks. For the same sediment rate, width adjustment at a tall bank is not as rapid as that at a low bank. The rates of width adjustment for cases of width increase and decrease are somewhat different as described below separately.

An increase in width at a channel section depends on sediment removal along the banks. The maximum rate of widening occurs when sediment inflow from the upstream section does not reach the banks of this section while bank material at this section is being removed. River banks have different degrees of resistance to erosion; therefore, the rate of sediment removal along a bank needs to be modified by a coefficient. For this purpose, bank erodibility factor is introduced as an index for the erosion of bank material and the four bank types reflecting the variation in erodibility are classified as follows

- (1) Non-erodible banks,
- (2) erosion-resistant banks, characterized by highly cohesive material or substantial vegetation, or both,
- (3) moderately erodible banks having medium bank cohesion, and
- (4) easily erodible banks with noncohesive material.

Values of bank erodibility factor varies from 0 for the first type to 1 for the last type of banks. The values of 0.2 and 0.5 have been empirically determined for the second and third types, respectively, based upon test and calibration of the model using field data from rivers in the western U. S. However, bank erodibility factor should still be calibrated whenever data on width changes are available.

A decrease in channel width is accomplished by sediment deposition along the banks or a decrease in stage, or both. For practical reasons, deposition does not exceed the stage in the model. The maximum amount of width reduction at a section occurs when sediment inflow from the upstream section is spread out at this section and the sediment removal from the bank areas at this section is zero.

Within the limit of width adjustment, changes in width are made at all

cross sections in the study reach toward establishing uniformity in power expenditure.

IX. SIMULATION OF CHANGES IN CHANNEL-BED PROFILE

After the banks are adjusted, the remaining correction for A_b is applied to the bed. Distributions of erosion and deposition, or fill and scour, at a cross section are usually not uniform. Generally speaking, deposition tends to start from the low point and it is more uniformly distributed because it tends to build up the channel bed in nearly horizontal layers. This process of deposition is often accompanied by channel widening. On the other hand, channel-bed erosion tends to be more confined with greater erosion in the thalweg. This process is usually associated with a reduction in width as the banks slip back into the channel. Such characteristic channel adjustments are effective in reducing the streamwise variation in stream power as the river seeks to establish a new equilibrium. In the model, the allocation of scour and fill across a section during each time step is assumed to be a power function of the effective tractive force $\tau_0 - \tau_c$, i.e.

$$\Delta z = \frac{(\tau_0 - \tau_c)^n}{\sum_B (\tau_0 - \tau_c)^n \Delta y} \Delta A_b \quad (11)$$

where Δz is the local correction in channel-bed elevation, τ_0 (given by VDS) is the local tractive force, τ_c is the critical tractive force, n is an exponent, and y is the horizontal coordinate, and B is the channel width. The value of τ_c is zero in the case of fill.

The n value in Eq. 11 is generally between 0 and 1; it affects the pattern of scour-fill allocation. For the schematic cross section shown in Fig. 3, a small value of n , say 0.1, would mean a fairly uniform distribution of Δz across the section; a larger value, say 1, will give a less uniform distribution of Δz and the local change will vary with the local tractive force or roughly the depth. The value of n is determined at each time step such that the correction in channel-bed profile will result in the most rapid movement toward uniformity in power expenditure, or linear water-

surface profile, along the channel.

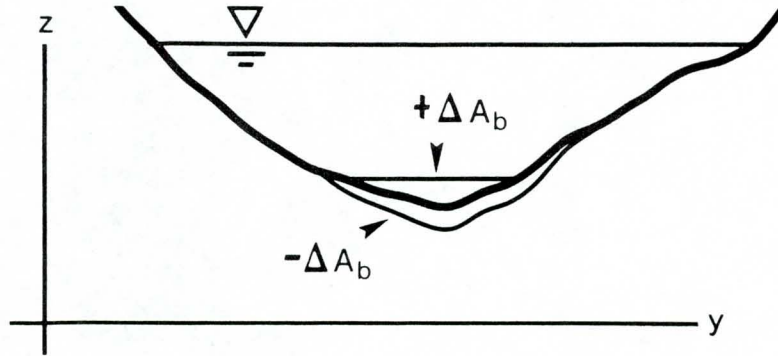


Fig. 3 Corrections of bed profile for aggradation and degradation. They are made in such ways that water-surface profile or power expenditure moves toward uniformity.

Eq. 11 may only be used in the absence of channel curvature. The change in bed area at a cross section in a curved reach is

$$\Delta A_b = \frac{1}{r_f} \int r \Delta z \, dr \quad (12)$$

where r_f is the radius of curvature at the discharge centerline or thalweg. Because of the curvature, adjacent cross sections are not parallel and the spacing Δs between them varies across the width. Therefore, the distribution of Δz given in Eq. 11 needs to be weighted according to the r -coordinate with respect to the thalweg radius, r_f/r , i.e.

$$\Delta z = \frac{(\tau_o - \tau_c)^{n/r}}{\sum_B (\tau_o - \tau_c)^{n/r} \Delta r} \Delta A_b \quad (13)$$

X. SIMULATION OF CHANGES DUE TO CURVATURE EFFECT

Simulation of curvature-induced scour and deposition is based upon the flow curvature for which the streamwise variation is given by Eq. 4. The major features of transverse sediment transport and changes in bed topography are described below.

Sediment transport, in the presence of transverse flow, has a component in that direction. Sediment movement in the transverse direction contributes to the adjustment of transverse bed profile. In an unsteady flow, the transverse bed profile varies with time, and it is constantly adjusted toward equilibrium through scour and deposition. The transverse bed load per unit channel length q_b' can be related to the streamwise transport q_b . Such a relationship by Ikeda (1982) can be written in parametric form as

$$\frac{q_b'}{q_b} = F \left(\tan \delta, \frac{\partial z}{\partial r} \right) \quad (14)$$

where δ is the angle of deviation of bottom currents from the streamwise direction. The near-bed transverse velocity is a function of the curvature, and it is computed using the flow curvature.

Eq. 14 relates the direction of bed-load movement to the direction of near-bed velocity and transverse bed slope $\partial z/\partial r$. As transverse velocity starts to move sediment away from the concave bank, it creates a transverse bed slope that counters the transverse sediment movement. An equilibrium is reached, i.e., $q_b' = 0$, when the effects of these opposing tendencies are in balance. Transverse bed-profile evolution is related to the variation in bed-material load. Ikeda and Nishimura (1986) developed a method for estimating transport and diffusion of fine sediments in the transverse direction by vertical integration of suspended load over the depth. Their model for predicting the transverse bed slope is also employed.

Changes in channel-bed elevation at a point due to transverse sediment movement are computed using the transverse continuity equation for sediment

$$\frac{\partial z}{\partial t} + \frac{1}{1-\lambda} \frac{1}{r} \frac{\partial}{\partial r} (r q_s') = 0 \quad (15)$$

Written in finite difference form with a forward difference for q_s' , this equation becomes

$$\Delta z_k = \frac{\Delta t}{1-\lambda} \frac{2}{r_k} \frac{r_{k+1} q_{s,k+1}' - r_k q_{s,k}'}{r_{k+1} - r_{k-1}} \quad (16)$$

where k is the radial (transverse) coordinate index measured from the center

of radius. Eq. 16 provides the changes in channel-bed elevation for a time step due to transverse sediment movement. These transverse changes, as well as the longitudinal changes, are applied to the stream bed at each time step. Bed-profile evolution is simulated by repeated iteration along successive time steps.

XI. TEST AND CALIBRATION OF MATHEMATICAL MODEL

The accuracy of a mathematical model depends on the physical foundation, numerical techniques, and physical relations for momentum, flow resistance and sediment transport. Test and calibration are important steps to be taken for more effective use of a model. Because of the difference in sensitivity of simulated results to each relation or empirical coefficient, more attention needs to be paid to those that generate sensitive results. Major items that require calibration include the roughness coefficient, sediment transport equation, bank erodibility factor, bed erodibility factor, etc.

To determine the sensitivity of flow, sediment transport and channel changes caused by the variation of each variable, different values of the variable need to be used in simulation runs and the results so obtained are compared. Generally speaking, the rate of channel changes is more sensitive to the sediment rate computed from a sediment equation but the equilibrium channel configuration is less sensitive. For example, the constriction scour at a bridge crossing, or the equilibrium local scour at a bridge pier, is found to be more or less independent of the sediment equation, or sediment size, since both inflow and outflow rates of sediment are affected by about the same proportion. It may also be stated that the rate of widening is sensitive to the bank erodibility factor but the equilibrium width is not nearly as sensitive.

Field data are generally required for test and calibration of a model. Generally, the channel configuration before and after the changes, flow record, sediment characteristics are required. Data sets with more complete information are also more useful. Several data sets that are useful for test and calibration are included in Appendix E.

APPENDIX A. REFERENCES

- Ackers, P., and White, W. R., "Sediment Transport: A New Approach and Analysis," Journal of the Hydraulics Division, ASCE, Vol. 99, No. HY11, November, 1973, pp. 2041-2060.
- Andrews, E. D., "Bank Stability and Channel Width Adjustment, East Fork River, Wyoming," Water Resources Research, Vol. 18, No. 4, August, 1982, pp. 1184-1192.
- Borah, D. K., Alonso, C. V., and Prasad, S. N., "Routing Graded Sediments in Streams: Formulations," Journal of the Hydraulics Division, ASCE, Vol. 108, No. HY12, December, 1982, pp. 1486-1503.
- Brownlie, W. R., "Flow Depth in Sand-Bed Channels," Journal of Hydraulic Engineering, ASCE, Vol. 109, No. 7, July, 1983, pp. 959-990.
- Chang, H. H., "Energy Expenditure in Curved Open Channels," Journal of Hydraulic Engineering, ASCE, Vol. 109, No. 7, July, 1983.
- Chang, H. H., "Variation of Flow Resistance through Curved channels," Journal of Hydraulic Engineering, ASCE, Vol. 110, No. 12, December, 1984, pp. 1772-1782.
- Chang, H. H., "Water and Sediment Routing through Curved Channels", Journal of Hydraulic Engineering, ASCE, Vol. 111, No. 4, April, 1985, pp. 644-658.
- Chen, Y-H., "Mathematical Modeling of Water and Sediment Routing in Natural Channels," Ph.D. Thesis, Department of Civil Engineering, Colorado State University, Ft. Collins, Colorado, March, 1973.
- Chow, V. T., Open Channel Hydraulics, McGraw-Hill Book Co., 1957.
- Engelund, F., and Hansen, E., "A Monograph on Sediment Transport in Alluvial Streams," Teknisk Forlag, Copenhagen, Denmark, 1967.
- Fread, D. L., "Discussion on Implicit Flood Routing in Natural Channels by M. Amein and C. S. Fang (December, 1970)," Journal of the Hydraulics Division, ASCE, Vol. 97, No. HY7, July, 1971, pp. 1156-1159.
- Fread, D. L., "Numerical Properties of Implicit Four-Point Finite difference Equations of Unsteady Flow," National Weather Service, NOAA, Technical Memorandum NWS Hydro-18, March, 1974.
- Graf, W. H. Hydraulics of Sediment Transport, McGraw-Hill Book Co., 1970.
- Ikeda, S., "Lateral Bed Load Transport on Side Slopes," Journal of the Hydraulics Division, ASCE, Vol. 108, No. HY11, November, 1982, pp. 1369-1373.

Ikeda, S., and Nishimura, T., "Flow and Bed Profile in Meandering Sand-Silt Rivers," Journal of Hydraulic Engineering, ASCE, Vol. 112, No. 7, July, 1986, pp. 562-579.

Kikkawa, H., Ikeda, S., and Kitagawa, A., "Flow and Bed Topography in Curved Open Channels," Journal of the Hydraulics Division, ASCE, Vol. 102, No. HY9, September, 1976, pp. 1327-42.

National Academy of Sciences, "An Evaluation of Flood-Level Prediction Using Alluvial River Models," Committee on Hydrodynamic Computer Models for Flood Insurance Studies, Advisory Board on the Built Environment, National Research Council, National Academy Press, Washington, D.C., 1983.

Parker, G., Klingeman, P. C., and McLean, D. G., "Bed Load and Size Distribution in Paved Gravel-Bed Streams," Journal of the Hydraulics Division, ASCE, Vol. 108, No. HY4, April, 1982, pp. 544-571.

U. S. Bureau of Reclamation, "Aggradation and Degradation in the Vicinity of Milburn Diversion Dam," Sedimentation Section, 1963.

Yang, C. T. "Unit Stream Power and Sediment Transport," Journal of the Hydraulics Division, ASCE, Vol.18, No. HY10, October 1972, pp. 1805-1826.

Yang, C. T., "Unit Stream Power Equation for Gravel," Journal of Hydraulic Engineering, ASCE, Vol. 110, No. HY12, December 1984, pp. 1783-1798.

Zhang, Q, Zhang, Z., Yue, J., Duan, Z., and Dai, M., "A Mathematical Model for the Prediction of the Sedimentation Process in Rivers," Proceedings of the 2nd Intern. Sympo. on River Sedimentation, Nanjing, China, 1983.

APPENDIX B. INPUT/OUTPUT INSTRUCTIONS FOR THE FLUVIAL MODEL

I. INPUT DESCRIPTION

The HEC-2 format for input data is used in all versions of the FLUVIAL model. Data records for HEC-2 pertaining to cross-sectional geometry (X1 and GR), job title (T1, T2, and T3), and end of job (EJ), are used in the FLUVIAL model. If a HEC-2 data file is available, it is not necessary to delete the unused records except that the information they contain are not used in the computation. For the purpose of water- and sediment-routing, additional data pertaining to sediment characteristics, flood hydrograph, etc., are required and supplied by other data records. Sequential arrangement of data records are shown in the following.

<u>Records</u>	<u>Description of Record Type</u>
T1, T2, T3	Title Records
G1	General Use Record
G2	General Use Records for Hydrographs
G3	General Use Record
G4	General Use Record for Plotting Selected Cross Sections
G5	General Use Record
GS	General Use Records for Initial Sediment Compositions
GB	General Use Records for Base-Level Variation
X1	Cross-Sectional Record
XF	Record for Specifying Special Features of a Cross Section
GR	Record for Ground Profile of a Cross Section
EJ	End of Job Record

Variable locations for each input record are shown by the field number. Each record has an input format of (A2, F6.0, 9F8.0). Field 0 occupying columns 1 and 2 is reserved for the required record identification characters. Field 1 occupies columns 3 to 8; Fields 2 to 10 occupy 8 columns each. The data records are tabulated and described in the following.

T1, T2, T3 Records

These three records are title records that are required for each job.

<u>Field</u>	<u>Variable</u>	<u>Value</u>	<u>Description</u>
0	IA	T1	Record identification characters
1-10	None		Numbers and alphameric characters for title

G1 Record

This record is required for each job, used to enter the general parameters listed below.

<u>Field</u>	<u>Variable</u>	<u>Value</u>	<u>Description</u>
0	IA	G1	Record identification characters
1	TYME	+	Starting time of computation on the hydrograph, in hours
2	ETIME	+	Ending time of computation on the hydrograph, in hours
3	DTMAX	+	Maximum time increment Δt allowed, in seconds
4	ISED	1	Select Graf's sediment transport equation.
		2	Select Yang's unit stream power equation. The sediment size is between 0.063 and 10 mm.
		3	Select Engelund-Hansen sediment equation.
		4	Select Parker gravel equation.
		5	Select Ackers-White sediment equation.
5	BEF	+	Bank erodibility factor for the study reach. This value is used for each section unless otherwise specified in Field 9 of the XF record. Use 1 for highly erodible banks; use 0.5 for moderately erodible banks; and 0.2 for erosion-resistant banks. Any value between 0 and 1 may be used.
6	IUC	0	English units are used in input and output.
		1	Metric units are used in input and output.
7	CNN	+	Manning's "n" value for the study reach. This value is used for a section unless otherwise spe-

cified in Field 4 of the XF record. If bed roughness is computed based upon alluvial bedforms as specified in Field 5 of the G3 record, only an approximate n value needs to be entered here.

8	PTIME1	+	First time point on the hydrograph at which complete cross-sectional output is requested. It is usually the peak time, but it may be left blank if no output is requested.
9	PTIME2	+	Second time point on the hydrograph at which complete cross-sectional output is requested. It is not the end of the hydrograph because complete cross-sectional output is automatically printed at the end of each simulation. This field may be left blank if no output is requested.
10	KPF	+	Frequency of printing the summary output, in number of time steps

G2 Record

These records are required for each job, used to define the flow hydrograph(s) in the channel reach. The first G2 record is used to define the spatial variation in water discharge along the reach; the succeeding ones are employed to define the time variation(s) of the discharge. Up to five hydrographs, with a maximum of 20 points for each, are currently dimensioned. This size may be expanded if required.

<u>Field</u>	<u>Variable</u>	<u>Value</u>	<u>Description</u>
First G2			
0	IA	G2	Record identification characters
1	IHP1	+	Number of last cross section using the first hydrograph. The number of section is counted from downstream to upstream with the downstream section being number one.
2	NP1	+	Number of points connected by straight segments used to approximate the first hydrograph.
3	IHP2	+	Number of last section using the second hydrograph if any. Otherwise leave it blank.
4	NP2	+	Number of points used to approximate the second hydrograph

- 5 IHP3 + Number of last section using the third hydrograph if any. Otherwise leave it blank.
- 6 NP3 + Number of points used to approximate the third hydrograph

Succeeding G2 Record(s)

- 1 Q11, Q21 + Discharge coordinate of point 1 for each hydrograph, in ft³/sec or m³/sec
Q31
- 2 TM11, TM21 + Time coordinate of point 1 for each hydrograph, in
TM23 hours
- 3 Q12, Q22 + Discharge coordinate of point 2 for each hydrograph,
Q32 in cfs or cms
- 4 TM12, TM22 + Time coordinate of point 2 for each hydrograph, in
TM23 hours

Continue with additional discharge and time coordinates.

G3 Record

This record is used to define required and optional river channel features for a job as listed below.

<u>Field</u>	<u>Variable</u>	<u>Value</u>	<u>Description</u>
0	IA	G3	Record identification characters
1	S11	+	Slope of the downstream section. Required for a job
2	BSP	0 +	One-on-one slope for rigid bank or bank protection Slope of bank protection in BSP horizontal units on 1 vertical unit. In the case of vertical bank, use 0.05 for BSP. This value is used for all cross sections unless otherwise specified in Field 8 of the XF record for a section.
3	DSOP	0 1	Downstream slope is allowed to vary during flow. Downstream slope is fixed at S11 given in Field 1.
4	TEMP	0 +	Water temperature is 15°C. Water temperature in degrees Celsius

5	ICNN	0	Manning's n defined in Field 7 of the G1 record or Field 4 of the XF record are used.
		1	Brownlie's formula for alluvial bed roughness is used and Manning's n is simulated in the model.
6	TDZAMA	0	Erodible bed layer is 100 ft (30.5 m) thick.
		+	Thickness of erodible bed layer in ft or m. This value is applied to the entire channel reach but it may be redefined for a section using Field 10 of the XF record.
8	RLMN	0	Lateral migration of channel is not considered.
		+	Maximum rate of lateral migration in feet (or meter) per day at average discharge. Enter average discharge in cfs (or cms) in Field 9 of G3.
10	RWD	+	Width of rigid bank zone, in ft or m. It is used to specify the width of bank protection of small channel in a flood plain. Channel and flood plain areas outside this zone remain erodible.

G4 Record

This is an optional record used to select certain cross sections for output at each summary output. Up to 4 cross sections may be selected. Each cross section is identified by its number which is counted from the downstream section.

<u>Field</u>	<u>Variable</u>	<u>Value</u>	<u>Description</u>
0	IA	G4	Record identification characters
1	IPLT1	+	Number of cross section
2	IPLT2	+	Number of cross section
3	IPLT3	+	Number of cross section
4	IPLT4	+	Number of cross section

G5 Record

This is an optional record used to specify certain selections for the job.

<u>Field</u>	<u>Variable</u>	<u>Value</u>	<u>Description</u>
--------------	-----------------	--------------	--------------------

0	IA	G5	Record identification characters
1	DT	0 +	The first time step is 50 seconds. Size of the first time step in seconds.
2	IROUT	0 1	Unsteady water routing is not used; water-surface profiles are computed using standard-step method. Unsteady water-routing based upon the dynamic wave is used to compute stages and water discharges at all cross sections for each time step.

GS Record

Two GS records are required for each job, used to specify initial bed-material compositions in the channel at the downstream and upstream cross sections. The first GS record is for the downstream section and the second is for the upstream section. From upstream to downstream, exponential decay in sediment size is assumed for the initial distribution. Sediment composition at each section is represented by five size fractions.

<u>Field</u>	<u>Variable</u>	<u>Value</u>	<u>Description</u>
0	IA	GS	Record identification characters
1	DFF	+	Geometric mean diameter of the smallest size fraction in mm
2	PC	+	Fraction of bed material in this size range

Continue with other DFF's and PC's.

GB Records

These optional records are used to define the time variation of base-level for rivers that discharge into a lake, reservoir or ocean. The GB input data, if included, will supersede other methods for determining the downstream water-surface elevation.

<u>Field</u>	<u>Variable</u>	<u>Value</u>	<u>Description</u>
First GB Record			
0	IA	GB	Record identification characters
1	KBL	+	Number of points used to define base-level changes

Succeeding GB Record(s)

0	IA	GB	Record identification characters
1	BSLL(1)	+	Base level of point 1, in ft or m
2	TMBL(1)	+	Time coordinate of point 1, in hours
3	BSLL(2)	+	Base level of point 2, in ft or m
4	TMBL(2)	+	Time coordinate of point 2, in hours

Continue with additional elevation and time coordinates.

X1 Record

This record is required for each cross section (100 cross sections can be used for the study reach); it is used to specify the cross-sectional geometry and program options applicable to that cross-section. Cross sections are arranged in sequential order starting from downstream.

<u>Field</u>	<u>Variable</u>	<u>Value</u>	<u>Description</u>
0	IA	X1	Record identification characters
1	SECNO	+	Original section number from the map
2	NP	+	Total number of stations or points on the next GR records for current cross section
7	DX	+	Length of reach between current cross section and next downstream section along the thalweg, in feet or meters
8	YFAC	0	Cross-section stations are not modified by the factor YFAC.
		+	Factor by which all cross-section stations are multiplied to increase or decrease area. It also multiplies YC1, YC2 and CPC in the XF record.

XF Record

This is an optional record used to specify special features of a cross section.

<u>Field</u>	<u>Variable</u>	<u>Value</u>	<u>Description</u>
--------------	-----------------	--------------	--------------------

0	IA	XF	Record identification characters
1	YC1	0 +	Regular erodible left bank Station of rigid left bank in ft or m, to the left of which channel is nonerodible.
2	YC2	0 +	Regular erodible right bank Station of rigid right bank, to the right of which channel is nonerodible
3	RAD	0 + -	Straight channel with zero curvature Radius of curvature at channel centerline in ft or m. Center of radius is on same side of channel where the station (Y-coordinate) starts. Radius of curvature at channel centerline in ft or m. Center of radius is on opposite side of zero station.
4	CN	0 +	Roughness of this section is the same as that given in Field 7 of G1 record. Manning's "n" value for this section
5	CPC	0 +	Center of thalweg coincides with channel invert at this section. Station (Y-coordinate) of the thalweg in ft or m
6	IRC	0 1	Regular erodible cross section Rigid or nonerodible cross section such as drop structure or road crossing. Up to 10 such sections are allowed in the study reach.
8	BSP	0 + 5	Slope of bank protection is the same as that given in Field 2 of G3 record. Slope of bank protection at this section in BSP horizontal units on 1 vertical unit. Use 0.05 for vertical bank. Slope of rigid bank is defined by the GR coordinates.
9	BEFX	0 >0.01	Bank erodibility factor is defined in Field 5 of the G1 record Bank erodibility factor at this section.
10	TDZAM	0 +	Erodible bed layer at this section is defined by TDZAMA in Field 6 of the G3 record. Thickness of erodible bed layer in ft or m.

GR Record

This record specifies the elevation and station of each point for a digitized cross section; it is required for each X1 record.

<u>Field</u>	<u>Variable</u>	<u>Value</u>	<u>Description</u>
0	IA	GR	Record identification characters
1	Z1	<u>+</u>	Elevation of point 1, in ft or m. May be positive or negative.
2	Y1	<u>+</u>	Station of point 1, in ft or m
3	Z2	<u>+</u>	Elevation of point 2, in ft or m
4	Y2	<u>+</u>	Station of point 2, in ft or m

Continue with additional GR records using up to 47 points to describe the cross section. Stations should be in increasing order.

EJ Record

This record is required following the last cross section for each job. Each group of records beginning with the T1 record is considered as a job.

<u>Field</u>	<u>Variable</u>	<u>Value</u>	<u>Description</u>
0	IA	EJ	Record identification characters
1-10			Not used

II. OUTPUT DESCRIPTION

Output of the model include initial bed-material compositions, time and spatial variations of the water-surface profile, channel width, flow depth, water discharge, velocity, energy gradient, median sediment size, and bed-material discharge. In addition, cross-sectional profiles are printed at different time intervals.

Symbols used in the output are generally descriptive, some of them are

defined below:

SEC NO	Number of a cross-section
TIME	Time on the hydrograph
DT	Size of the time step or Δt in sec
W.S.ELEV	Water-surface elevation in ft or m
WIDTH	Surface width of channel flow in ft or m
DEPTH	Depth of flow measured from channel invert to the water-surface in ft or m
Q	Discharge of flow in cfs or cms
V	Mean velocity of a cross-section in fps or mps
SLOPE	Energy gradient
D50	Median size or d_{50} of sediment load in mm
QS	Bed-material discharge for all size fractions in cfs or cms
FR	Froude number at a cross section
N	Manning's roughness coefficient
SED. YIELD	Bulk volume of sediment having passed a cross section since beginning of simulation, in cubic yards or cubic meters
WSEL	Water-surface elevation, in ft or m
Z	Vertical coordinate (elevation) of a point on channel boundary of a cross-section, in ft or m
Y	Horizontal coordinate (station) of a point on channel boundary of a cross-section, in ft or m
DZ	Change in elevation during the current time step, in ft or m
TDZ	Total or accumulated change in elevation, in ft or m

III. IMPORTANT MESSAGES FOR INPUT PREPARATION

1. The computing time of this program is sensitive to the reach length between two adjacent cross sections, DX . Very small reach lengths which may result in excessive computing time should be avoided. In HEC-2, a downstream section and an upstream section are usually used at each bridge crossing, but these two sections should be combined into one, if possible, for the FLUVIAL application.

2. The GR points used to define the ground profile should be selected to provide an accurate definition of the initial profile. As such, sufficient points should be used for each cross section. Also, large spacing between adjacent points should be avoided even if there is no difference in initial elevation. Detailed results rely upon the adequate number of points used.

3. The number of GR points used in defining the ground profile also affects the computing time because these points are executed a great number of times for each job. Points that are definitely outside the flow boundary level should be deleted during initial editing. However, because of the possibility for bank erosion, there should be sufficient points to cover any such potential changes.

4. Ineffective flow areas should be specified, either by excluding them from the GR points or by raising the GR elevations above the water level.

5. Very fine sediments with a grain size less than 0.0625 mm constitute the wash load and should be excluded from the size-fraction data on GS records.

6. The bank erodibility factor, BEF, in Field 5 of Record G1, is a control for the rate of channel widening. A small value slows down widening. This value should be calibrated against field data whenever possible.

7. The radius of curvature, RAD, in Field 3 of the XF record may be specified only if the station of the concave bank is specified in Field 1 or 2 of the XF record. Under this situation, lateral migration is controlled by RLMN in the G3 record. In using this option, the GR stations should be approximately equally spaced in the erodible part of channel.

8. The radius of curvature r_c (or RAD) along a reach between two adjacent cross sections is computed by interpolating those defined at the cross

sections. Since r_C has infinite value at a straight section, its adjacent reaches also have infinite r_C . For this reason, a curved reach must be between cross sections with finite r_C values.

9. The device codes for running this program are as follows: 1 for READ, 3 for WRITE into an output file, and 5 for WRITE at the terminal.

PLACED AT INSIDE COVER

Sample Input/Output of the FLUVIAL Model

* FLUVIAL-12 SIMULATION OF RIVER HYDRAULICS, *
 * SEDIMENT TRANSPORT AND RIVER CHANNEL CHANGES *

XX

THIS PROGRAM IS DEVELOPED AND FURNISHED BY HOWARD H. CHANG AND IS ACCEPTED AND USED BY THE RECIPIENT UPON THE EXPRESS UNDERSTANDING THAT THE DEVELOPER MAKES NO WARRANTIES, EXPRESS OR IMPLIED, CONCERNING THE ACCURACY, COMPLETENESS, RELIABILITY, USABILITY, OR SUITABILITY FOR ANY PARTICULAR PURPOSE OF THE INFORMATION AND DATA CONTAINED IN THIS PROGRAM OR FURNISHED IN CONNECTION THEREWITH, AND THE DEVELOPER SHALL BE UNDER NO LIABILITY WHATSOEVER TO ANY PERSON BY REASON OF ANY USE MADE THEREOF.

T1 SANTA CRUZ RIVER

T2 EXISTING CONDITIONS WITH CAP

T3 100-YEAR FLOOD

G1	4.10	30.00	600.00	2.00	0.50	0.00	0.03	18.00	0.00	24.00
G2	70.00	9.00	0.00	0.00	0.00	0.00	0.00	0.00	0.00	0.00
G2	4000.00	3.00	27000.00	7.20	70000.00	15.00	80000.00	17.80	80000.00	18.20
G2	60000.00	21.50	30000.00	25.00	3000.00	37.00	1000.00	50.00		
G3	0.00	0.00	0.00	0.00	0.00	0.00	0.00	0.00	0.00	25.00
G4	3.00	26.00	27.00	0.00	0.00	0.00	0.00	0.00	0.00	0.00
GS	0.14	0.15	0.37	0.20	0.74	0.20	1.50	0.20	5.30	0.25
GS	0.14	0.15	0.37	0.20	0.74	0.20	1.50	0.20	5.30	0.25
J1	-10.00	7.00	0.00	0.00	0.00	0.00	0.00	0.00	1973.00	0.00
J2	-1.00	0.00	-1.00	0.00	0.00	0.00	-1.00	0.00	0.00	0.00
J3	38.00	43.00	53.00	21.00	55.00	26.00	56.00	22.00	54.00	4.00
J3	1.00	50.00	0.00	0.00	0.00	0.00	0.00	0.00	0.00	0.00
NC	0.04	0.04	0.03	0.10	0.30	0.00	0.00	0.00	0.00	0.00
QT	6.00	33000.00	38200.00	40000.00	65000.00	70000.00	80000.00	0.00	0.00	0.00
X1	9.97	21.00	19820.00	20528.00	0.00	0.00	0.00	0.00	0.00	0.00
X3	10.00	0.00	0.00	0.00	0.00	0.00	0.00	0.00	0.00	0.00
GR	1983.90	18478.00	1974.00	18538.00	1975.50	18572.00	1971.50	18785.00	1969.00	18881.00
GR	1970.80	19157.00	1969.00	19405.00	1970.10	19495.00	1968.10	19567.00	1970.60	19794.00
GR	1970.60	19820.00	1962.70	19842.00	1962.50	20000.00	1962.70	20054.00	1968.10	20092.00
GR	1969.70	20248.00	1967.50	20274.00	1967.70	20410.00	1978.30	20528.00	1976.90	20833.00
GR	1975.80	21316.00								
X1	10.09	15.00	19458.00	20267.00	600.00	650.00	640.00	0.00	0.00	0.00
X3	10.00	0.00	0.00	0.00	0.00	0.00	0.00	0.00	0.00	0.00
GR	1984.30	17390.00	1986.10	18493.00	1973.50	18616.00	1972.20	19037.00	1973.30	19458.00
GR	1964.10	19738.00	1964.10	19931.00	1966.60	20000.00	1965.70	20039.00	1970.80	20084.00
GR	1970.80	20180.00	1981.20	20267.00	1981.20	20350.00	1981.00	20466.00	1978.70	20701.00

X1	11.08	25.00	17783.00	20599.00	600.00	950.00	950.00	0.00	0.00	0.00
X3	10.00	0.00	0.00	0.00	0.00	0.00	0.00	0.00	0.00	0.00
GR	1996.50	17099.00	1996.00	17783.00	1990.60	17953.00	1983.10	18586.00	1983.10	18664.00
GR	1987.90	18767.00	1987.90	18854.00	1989.20	19000.00	1986.70	19184.00	1987.90	19238.00
GR	1983.10	19399.00	1985.40	19473.00	1982.90	19697.00	1984.50	19983.00	1982.90	20000.00
GR	1981.10	20256.00	1985.60	20271.00	1984.90	20355.00	1983.10	20410.00	1981.80	20539.00
GR	1988.50	20599.00	1989.70	21140.00	1991.00	22147.00	1989.40	22969.00	1993.30	23164.00
X1	11.27	25.00	17764.00	20568.00	1300.00	750.00	980.00	0.00	0.00	0.00
X3	10.00	0.00	0.00	0.00	0.00	0.00	0.00	0.00	0.00	0.00
GR	2012.70	15120.00	2010.60	15851.00	2010.40	16094.00	1998.90	16532.00	1998.50	17250.00
GR	1991.70	17425.00	1994.90	17764.00	1993.10	17965.00	1986.10	18316.00	1986.30	18450.00
GR	1990.10	18474.00	1990.80	18814.00	1989.00	19250.00	1989.90	19606.00	1986.30	19786.00
GR	1987.20	20000.00	1984.70	20156.00	1985.20	20283.00	1988.50	20303.00	1986.10	20466.00
GR	1989.40	20520.00	1994.40	20568.00	1996.00	21469.00	1995.30	22865.00	1994.60	24026.00
X1	11.39	30.00	18345.00	20382.00	800.00	450.00	660.00	0.00	0.00	0.00
X3	10.00	0.00	0.00	0.00	0.00	0.00	0.00	0.00	0.00	0.00
GR	2009.50	16143.00	2003.40	16536.00	2000.70	17025.00	2001.20	17516.00	1994.90	17697.00
GR	1992.80	18126.00	1992.80	18345.00	1988.30	18363.00	1988.30	18479.00	1993.00	18501.00
GR	1992.10	18850.00	1992.40	19160.00	1993.00	19453.00	1990.30	19532.00	1993.00	19636.00
GR	1990.10	19785.00	1992.10	19837.00	1989.90	19887.00	1990.80	19962.00	1987.40	19978.00
GR	1987.20	20001.00	1986.30	20262.00	1992.10	20278.00	1993.30	20382.00	1991.20	20419.00
GR	1992.40	20740.00	1998.90	20795.00	1997.80	21951.00	1996.60	23333.00	1994.80	24638.00
X1	11.51	30.00	18435.00	20471.00	600.00	610.00	610.00	0.00	0.00	0.00
X3	10.00	0.00	0.00	0.00	0.00	0.00	0.00	0.00	0.00	0.00
GR	2016.50	15304.00	2015.10	15898.00	2014.50	16299.00	2000.30	16778.00	1999.80	17389.00
GR	1994.20	17949.00	1994.60	18435.00	1988.80	18475.00	1988.80	18530.00	1989.90	18574.00
GR	1994.40	18608.00	1993.70	19081.00	1994.40	19484.00	1992.80	19530.00	1994.40	19564.00
GR	1991.70	19592.00	1992.80	19658.00	1994.20	19720.00	1991.90	19814.00	1995.10	19914.00
GR	1989.40	19929.00	1989.40	20000.00	1989.40	20181.00	1992.60	20191.00	1991.20	20267.00
GR	1994.40	20356.00	1993.30	20434.00	1995.50	20471.00	1993.90	20735.00	2000.90	20766.00
X1	11.62	25.00	18633.00	20190.00	590.00	590.00	590.00	0.00	0.00	0.00
X3	10.00	0.00	0.00	0.00	0.00	0.00	0.00	0.00	0.00	0.00
GR	2016.90	15495.00	2015.40	16069.00	2011.30	16443.00	1999.10	17787.00	1996.40	18008.00
GR	1994.80	18326.00	1994.80	18633.00	1989.90	18649.00	1989.90	18727.00	1994.20	18762.00
GR	1996.00	19060.00	1997.10	19347.00	1997.80	19520.00	1994.40	19616.00	1995.70	19714.00
GR	1994.20	19797.00	1989.20	19806.00	1989.20	19974.00	1993.50	20000.00	1996.20	20190.00
GR	1995.70	20674.00	2002.00	20706.00	1999.80	21769.00	1999.30	22747.00	2000.50	23670.00
X1	11.73	20.00	18749.00	20150.00	600.00	600.00	600.00	0.00	0.00	0.00
X3	10.00	0.00	0.00	0.00	0.00	0.00	0.00	0.00	0.00	0.00
GR	2007.20	17621.00	2002.70	17782.00	2003.40	18000.00	1998.40	18147.00	1996.20	18403.00
GR	1996.90	18749.00	1995.50	18910.00	1991.20	18923.00	1991.50	18986.00	1995.30	19014.00
GR	1998.40	19238.00	1999.80	19522.00	1997.30	19627.00	1990.60	19639.00	1991.50	19828.00

TIME = 11.03 HRS DT = 600 SECS TIME STEP = 48

SEC. NO.	W.S.ELEV. FEET	WIDTH FEET	DEPTH FEET	Q CFS	V FPS	SLOPE	D50 MM	QS CFS	FR	SED. YIELD C. Y.
9.97	1973.06	1767.94	10.56	48088.0	6.15	0.00273	1.01	50.11	0.52	0.4039E+05
10.09	1974.78	1610.79	11.26	48088.0	6.40	0.00276	1.19	46.85	0.52	0.3955E+05
10.21	1976.74	2058.60	12.29	48088.0	5.70	0.00261	1.55	37.33	0.50	0.3061E+05
10.32	1978.01	2281.61	10.75	48088.0	4.73	0.00161	0.92	28.93	0.40	0.2108E+05
10.52	1979.49	2568.60	8.82	48088.0	3.96	0.00103	0.46	23.77	0.32	0.1749E+05
10.72	1981.11	2456.87	9.37	48088.0	5.46	0.00285	1.03	61.51	0.51	0.6380E+05
10.90	1984.14	2109.79	9.40	48088.0	6.25	0.00365	0.78	80.31	0.58	0.6399E+05
11.08	1987.72	2009.23	7.91	48088.0	6.57	0.00403	1.26	69.76	0.61	0.7272E+05
11.27	1991.67	2498.26	7.22	48088.0	5.84	0.00365	1.13	63.48	0.57	0.6109E+05
11.39	1994.25	2877.34	9.13	48088.0	5.73	0.00412	1.46	64.48	0.59	0.5684E+05
11.51	1996.55	3046.37	7.14	48088.0	5.13	0.00308	0.86	59.14	0.52	0.4496E+05
11.62	1998.35	2848.63	8.52	48088.0	5.25	0.00305	0.89	59.45	0.52	0.4636E+05
11.73	2000.16	2830.48	8.61	48088.0	5.20	0.00293	0.84	60.80	0.51	0.4682E+05
11.85	2001.92	2818.54	7.29	48088.0	5.22	0.00294	0.87	63.35	0.51	0.5053E+05
11.96	2003.89	2175.83	9.32	48088.0	6.56	0.00447	1.38	66.68	0.63	0.6021E+05
12.07	2006.57	1906.62	10.89	48088.0	7.06	0.00477	1.66	64.39	0.66	0.5638E+05
12.19	2009.30	2807.93	11.04	48088.0	5.31	0.00310	0.92	50.14	0.52	0.4081E+05
12.30	2011.04	2917.76	11.48	48088.0	4.88	0.00246	0.87	40.82	0.47	0.3804E+05
12.42	2012.58	3033.69	10.26	48088.0	4.88	0.00259	0.94	36.52	0.48	0.3983E+05
12.53	2014.10	2943.47	12.30	48088.0	4.88	0.00250	1.19	36.33	0.47	0.4503E+05
12.64	2015.63	3514.99	10.73	48088.0	4.49	0.00239	1.31	33.30	0.45	0.4099E+05
12.76	2017.30	2675.16	11.72	48088.0	5.83	0.00396	2.01	34.89	0.58	0.3853E+05
12.87	2019.64	3755.56	12.19	48088.0	4.69	0.00302	1.88	24.40	0.50	0.2029E+05
12.99	2020.85	3482.93	13.12	48088.0	3.41	0.00095	0.61	14.76	0.30	0.5545E+04
13.07	2021.32	2398.74	14.20	48088.0	5.30	0.00251	0.89	37.22	0.48	0.2697E+05
13.26	2024.00	743.80	12.57	48088.0	10.39	0.00496	2.93	22.37	0.73	0.3134E+05
13.39	2027.61	4502.14	17.43	48088.0	2.55	0.00051	0.34	5.70	0.22	0.3762E+04
13.51	2028.29	6211.99	14.75	48088.0	3.81	0.00295	1.99	35.20	0.47	0.6303E+05
13.62	2030.34	7194.86	11.16	48088.0	3.89	0.00385	1.24	54.48	0.52	0.4648E+05
13.74	2032.48	7788.40	10.44	48088.0	3.43	0.00280	0.79	47.28	0.45	0.3674E+05
13.85	2034.14	7385.69	10.96	48088.0	3.48	0.00276	0.79	47.62	0.45	0.3850E+05
13.96	2035.66	5381.92	9.89	48088.0	3.88	0.00260	0.76	50.99	0.45	0.3977E+05
14.07	2037.38	6228.43	11.09	48088.0	3.96	0.00338	1.11	53.24	0.50	0.4528E+05
14.19	2039.32	6282.13	10.49	48088.0	3.72	0.00277	0.80	49.89	0.46	0.3972E+05
14.31	2041.00	5525.00	9.75	48088.0	3.96	0.00288	0.80	54.98	0.47	0.4261E+05

TIME = 18.03 HRS DT = 600 SECS TIME STEP = 90

SEC. NO.	W.S.ELEV. FEET	WIDTH FEET	DEPTH FEET	Q CFS	V FPS	SLOPE	D50 MM	QS CFS	FR	SED. YIELD C. Y.
9.97	1975.11	1931.37	12.61	80000.0	6.90	0.00229	1.21	82.18	0.50	0.1463E+06
10.09	1976.49	1643.27	13.63	80000.0	7.40	0.00233	1.69	78.20	0.51	0.1391E+06
10.21	1978.18	2029.60	15.17	80000.0	6.65	0.00218	1.80	71.80	0.48	0.1174E+06
10.32	1979.42	2457.88	11.86	80000.0	5.86	0.00184	0.96	70.38	0.44	0.9992E+05
10.52	1981.25	2703.86	10.34	80000.0	5.22	0.00142	0.54	69.64	0.39	0.8941E+05
10.72	1983.02	2547.44	9.94	80000.0	6.25	0.00237	0.84	107.68	0.49	0.1934E+06
10.90	1985.52	2148.96	11.64	80000.0	7.29	0.00316	0.93	124.39	0.57	0.2217E+06
11.08	1988.97	2484.11	10.65	80000.0	7.49	0.00421	1.56	124.39	0.64	0.2243E+06
11.27	1993.01	2844.85	7.97	80000.0	6.81	0.00367	1.23	118.59	0.59	0.1982E+06
11.39	1995.42	3025.67	10.94	80000.0	6.67	0.00371	1.33	116.74	0.59	0.1908E+06
11.51	1997.63	3169.98	6.42	80000.0	6.29	0.00325	0.99	114.95	0.55	0.1784E+06
11.62	1999.70	3741.13	9.16	80000.0	5.96	0.00338	1.03	114.84	0.55	0.1792E+06
11.73	2001.48	2879.13	8.00	80000.0	6.18	0.00269	0.97	106.78	0.51	0.1785E+06
11.85	2003.15	2932.05	6.47	80000.0	6.33	0.00300	1.06	108.81	0.54	0.1832E+06
11.96	2005.04	2371.07	11.24	80000.0	7.61	0.00417	1.84	111.29	0.64	0.1950E+06
12.07	2007.21	1661.26	13.77	80000.0	8.45	0.00367	2.07	103.67	0.62	0.1842E+06
12.19	2010.00	3135.59	11.36	80000.0	6.67	0.00389	1.37	103.37	0.60	0.1535E+06
12.30	2012.10	3139.07	12.08	80000.0	5.91	0.00261	1.05	80.89	0.50	0.1306E+06
12.42	2013.93	4781.08	12.50	80000.0	5.14	0.00288	1.04	68.68	0.50	0.1209E+06
12.53	2015.62	5029.66	13.32	80000.0	4.89	0.00260	1.36	67.79	0.48	0.1209E+06
12.64	2017.26	6769.78	11.73	80000.0	4.30	0.00252	1.35	63.46	0.46	0.1103E+06
12.76	2018.88	4550.76	14.06	80000.0	5.57	0.00351	2.33	68.98	0.55	0.1121E+06
12.87	2020.86	4486.27	13.77	80000.0	5.17	0.00268	1.93	62.99	0.49	0.8287E+05
12.99	2022.28	4830.06	14.31	80000.0	4.29	0.00159	0.73	58.20	0.38	0.6025E+05
13.07	2023.05	4193.44	16.41	80000.0	5.48	0.00299	1.53	60.20	0.52	0.9734E+05
13.26	2026.90	3674.71	17.85	80000.0	6.99	0.00564	3.04	53.01	0.70	0.8499E+05
13.39	2029.13	4893.08	17.87	80000.0	3.42	0.00076	0.23	31.51	0.28	0.2583E+05
13.51	2029.86	8430.53	15.00	80000.0	3.60	0.00187	0.46	75.69	0.39	0.1408E+06
13.62	2031.21	8252.57	12.22	80000.0	4.17	0.00295	0.92	106.48	0.48	0.1691E+06
13.74	2033.08	8089.32	10.77	80000.0	4.26	0.00308	0.76	119.83	0.49	0.1619E+06
13.85	2034.87	7806.27	11.29	80000.0	4.23	0.00287	0.70	122.45	0.48	0.1642E+06
13.96	2036.44	5448.32	9.38	80000.0	4.84	0.00278	0.72	128.25	0.49	0.1730E+06
14.07	2038.19	6716.11	11.96	80000.0	4.61	0.00313	0.93	129.93	0.50	0.1799E+06
14.19	2040.12	6849.74	10.00	80000.0	4.52	0.00301	0.73	135.13	0.49	0.1778E+06
14.31	2041.94	6995.04	9.36	80000.0	4.48	0.00301	0.74	137.92	0.49	0.1874E+06
14.42	2043.69	5915.87	10.18	80000.0	4.82	0.00306	0.85	140.46	0.51	0.1983E+06

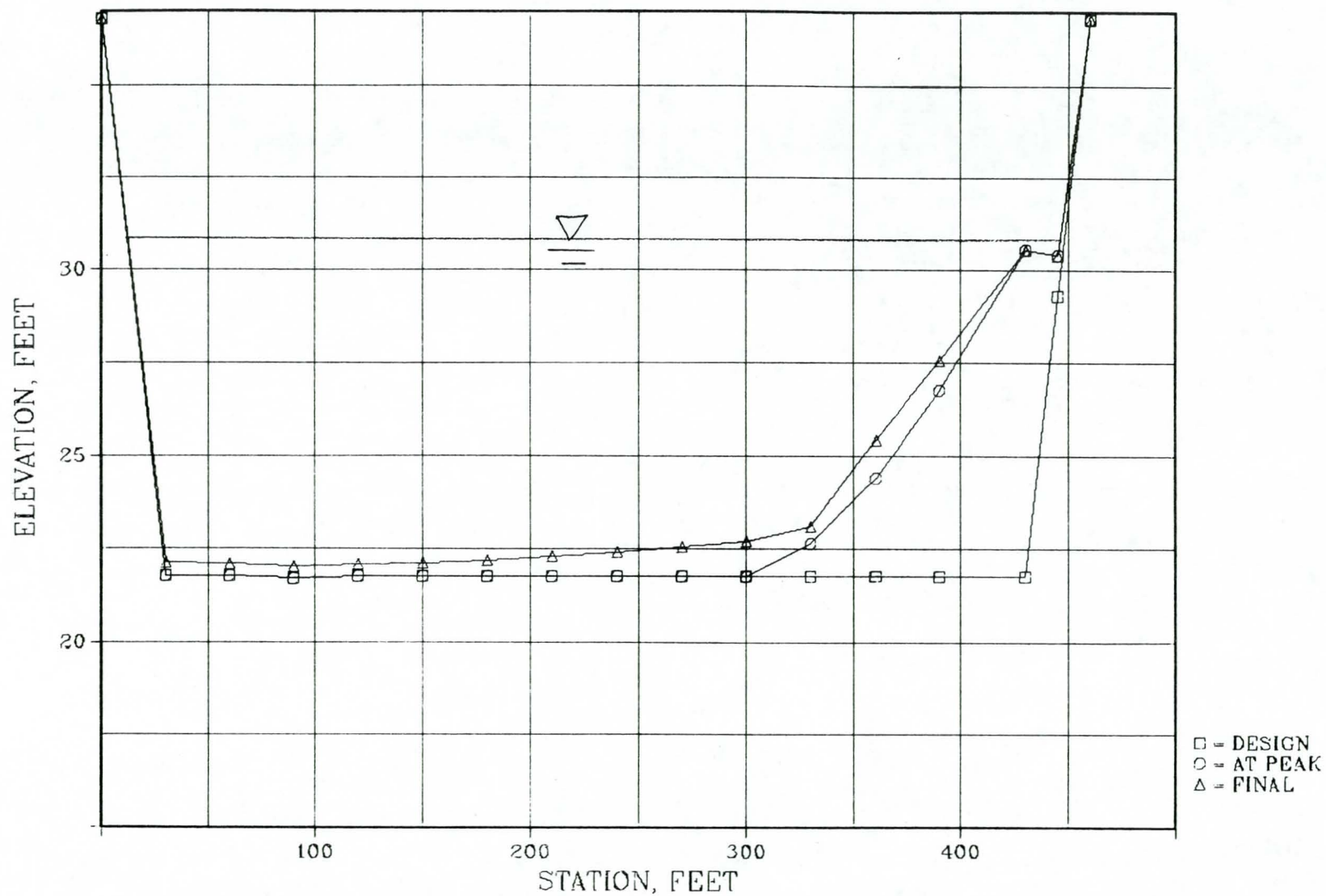
14.53	2045.72	5543.09	12.07	80000.0	5.37	0.00404	1.51	142.57	0.58	0.2117E+06
14.64	2047.98	4709.25	12.06	80000.0	5.51	0.00353	1.19	143.79	0.55	0.1938E+06
14.76	2050.00	5831.58	10.64	80000.0	4.67	0.00272	0.67	137.45	0.48	0.1787E+06
14.88	2051.89	6113.82	12.71	80000.0	4.82	0.00322	1.08	141.08	0.52	0.1928E+06
14.99	2053.77	5099.29	10.89	80000.0	5.25	0.00336	0.82	145.89	0.54	0.1885E+06
15.10	2055.77	5065.73	13.18	80000.0	5.29	0.00340	1.19	141.04	0.54	0.1923E+06
15.22	2057.72	5039.85	13.90	80000.0	5.08	0.00296	0.98	140.92	0.51	0.1778E+06
15.33	2059.41	4641.35	13.89	80000.0	5.08	0.00265	0.75	137.67	0.49	0.1741E+06
15.44	2060.91	4500.86	11.17	80000.0	4.90	0.00225	0.52	139.73	0.45	0.1713E+06
15.56	2062.09	2616.10	14.48	80000.0	6.17	0.00236	0.85	145.88	0.49	0.1840E+06
15.67	2063.51	3047.03	9.58	80000.0	5.45	0.00191	0.45	138.31	0.44	0.1788E+06
15.78	2064.65	2486.67	11.70	80000.0	6.32	0.00239	1.02	147.26	0.49	0.2150E+06
15.88	2066.06	3022.04	13.29	80000.0	6.08	0.00273	1.00	152.03	0.51	0.2123E+06
16.02	2067.95	2657.88	12.70	80000.0	6.24	0.00251	0.85	149.04	0.50	0.1994E+06
16.17	2069.85	2485.35	12.22	80000.0	6.16	0.00219	0.70	147.52	0.47	0.1962E+06
16.28	2071.05	2600.55	10.55	80000.0	5.80	0.00190	0.45	145.74	0.44	0.1936E+06
16.37	2072.06	2857.38	11.19	80000.0	5.51	0.00182	0.35	147.21	0.43	0.1970E+06
16.50	2073.23	2656.30	11.37	80000.0	5.70	0.00185	0.35	153.73	0.44	0.2097E+06
16.61	2074.54	3890.80	10.23	80000.0	5.11	0.00213	0.35	164.84	0.45	0.2279E+06
16.73	2075.91	3697.61	12.30	80000.0	5.61	0.00273	0.49	199.94	0.50	0.3215E+06
16.89	2078.47	2566.01	13.67	80000.0	7.12	0.00370	0.88	243.47	0.60	0.3953E+06

ID

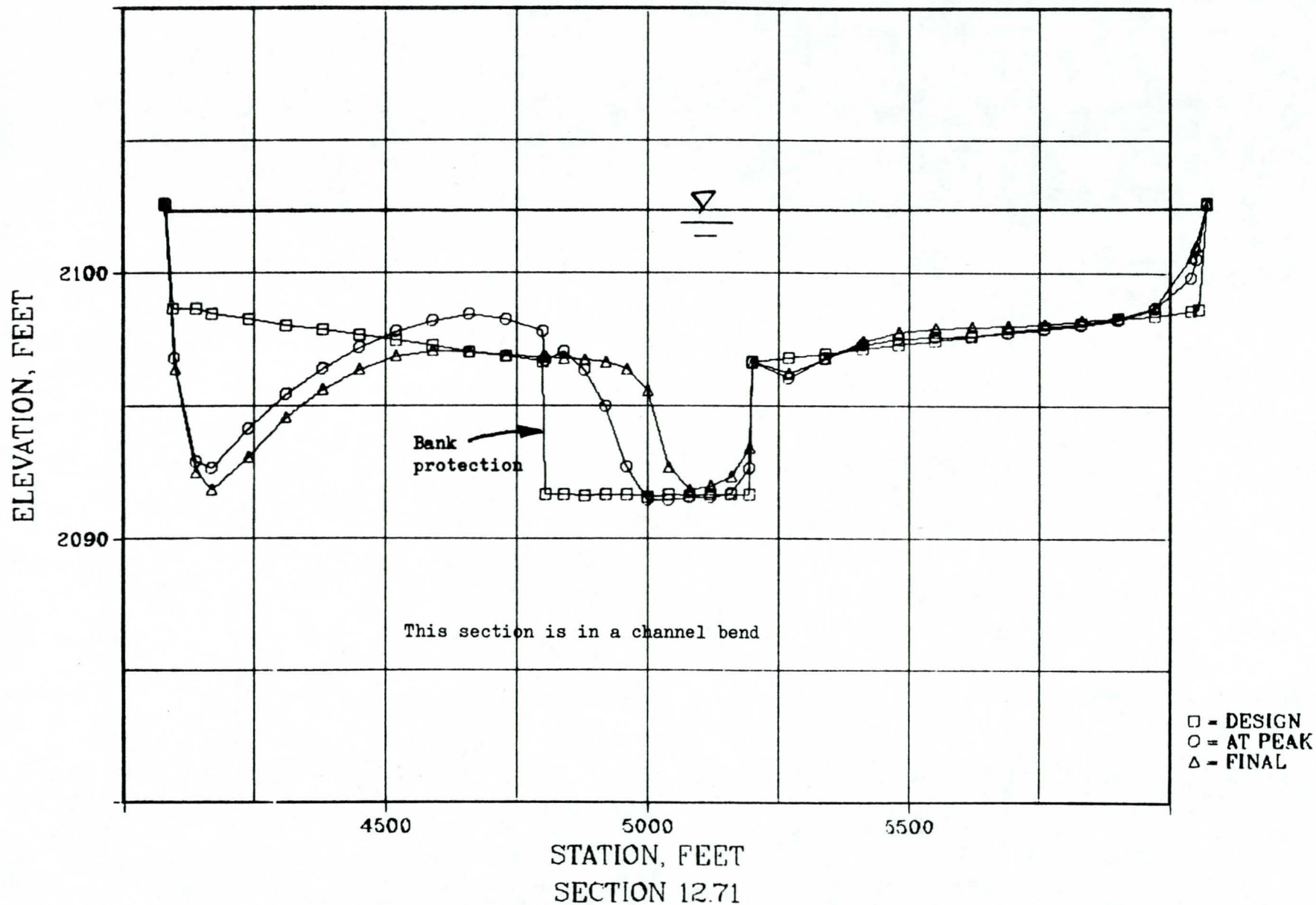
56 SEC NO 16.73 TIME = 18.03 HRS WSEL =2075.91 WIDTH = 3697.61

Z	DZ	TDZ	Y	Z	DZ	TDZ	Y	Z	DZ	TDZ	Y
2089.60	0.00	0.00	16450.0	2078.60	0.00	0.00	16677.0	2078.10	0.00	0.00	17020.0
2079.20	0.00	0.00	17428.0	2075.48	0.01	0.08	17452.0	2078.60	0.00	0.00	17469.0
2075.16	0.01	0.16	17958.0	2073.83	0.01	0.43	18035.0	2075.90	0.00	0.00	18107.0
2079.20	0.00	0.00	18357.0	2071.99	0.01	0.59	18435.0	2072.46	0.01	0.55	18588.0
2072.45	0.01	0.55	18878.0	2072.45	0.01	0.55	19046.0	2072.45	0.01	0.55	19154.0
2072.45	0.01	0.55	19486.0	2072.36	0.01	0.56	19601.0	2064.77	0.02	1.47	19625.0
2063.63	0.02	1.53	19898.0	2071.55	0.01	0.65	19970.0	2072.17	0.01	0.57	20000.0
2070.42	0.02	0.82	20209.0	2070.42	0.02	0.82	20427.0	2069.25	0.02	1.05	20466.0
2072.36	0.01	0.56	20498.0	2073.01	0.01	0.51	20723.0	2073.83	0.01	0.43	20995.0
2071.56	0.01	0.66	21105.0	2073.38	0.01	0.48	21128.0	2073.65	0.01	0.45	21344.0
2074.76	0.01	0.26	21822.0	2077.90	0.00	0.00	21836.0				

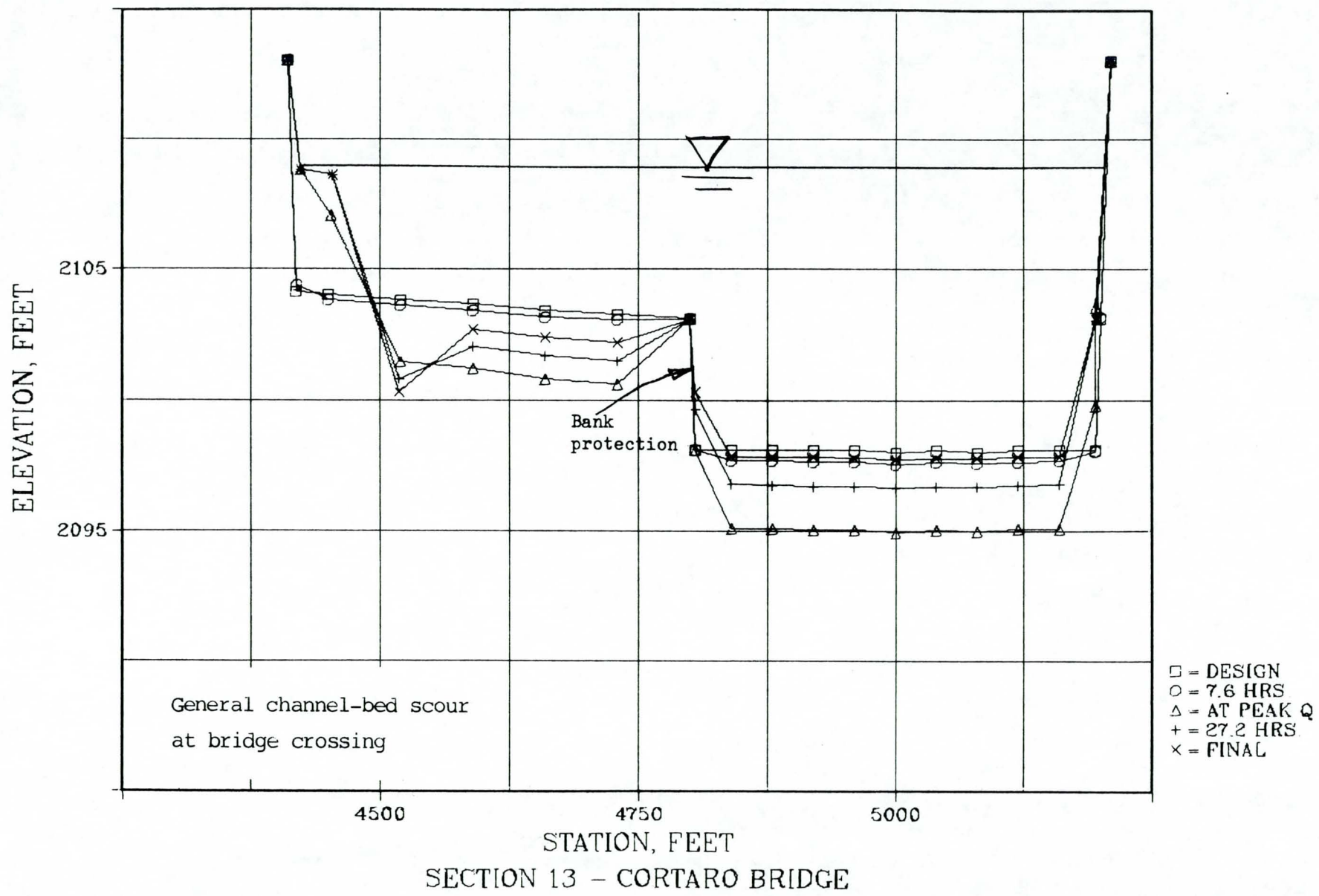
CROSS-SECTIONAL CHANGES
CURVED CONCRETE CHANNEL WITH DEPOSITION
RADIUS OF BEND = -2,000 FT



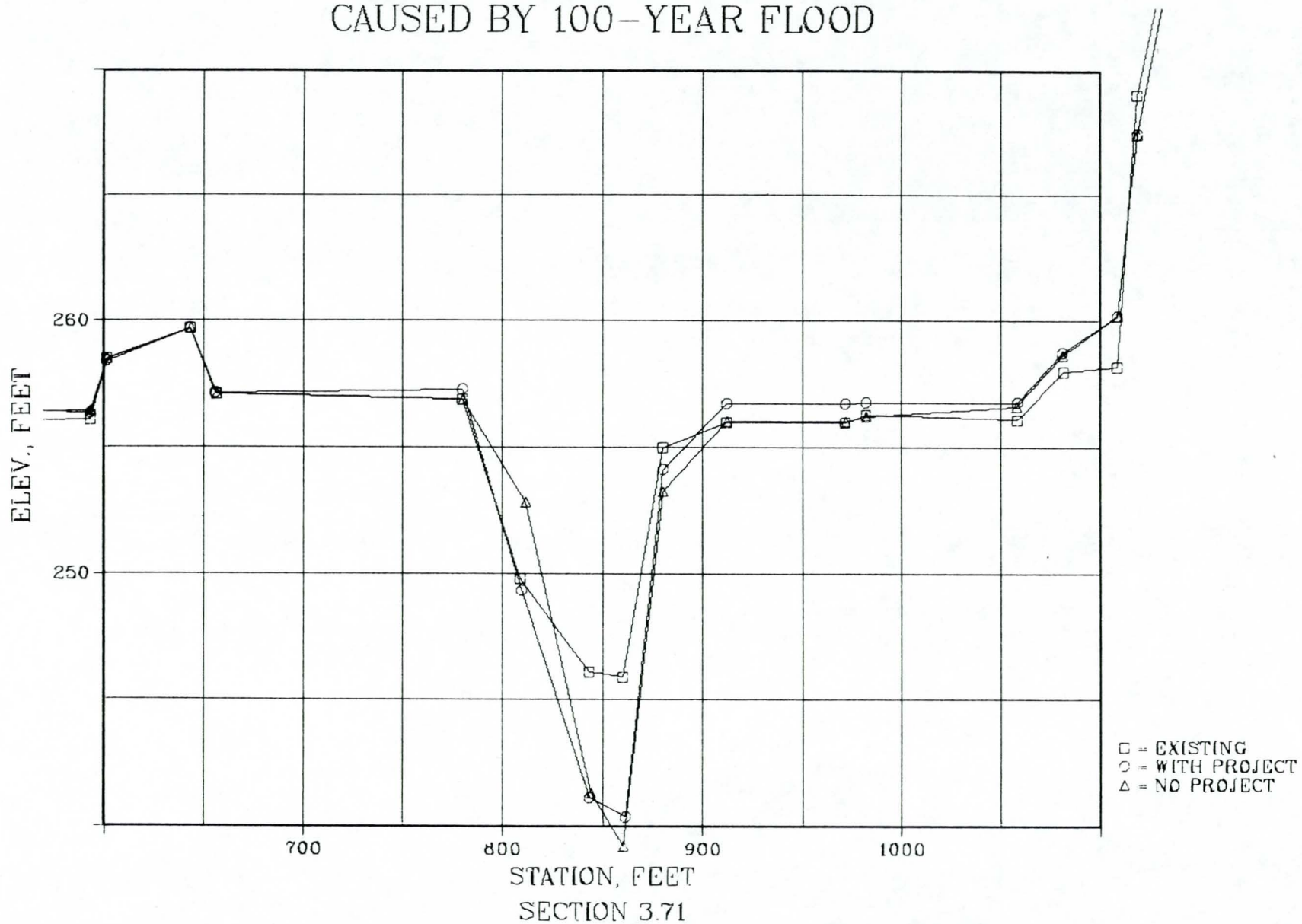
CROSS-SECTIONAL PROFILES DURING 100-YEAR FLOOD SANTA CRUZ RIVER



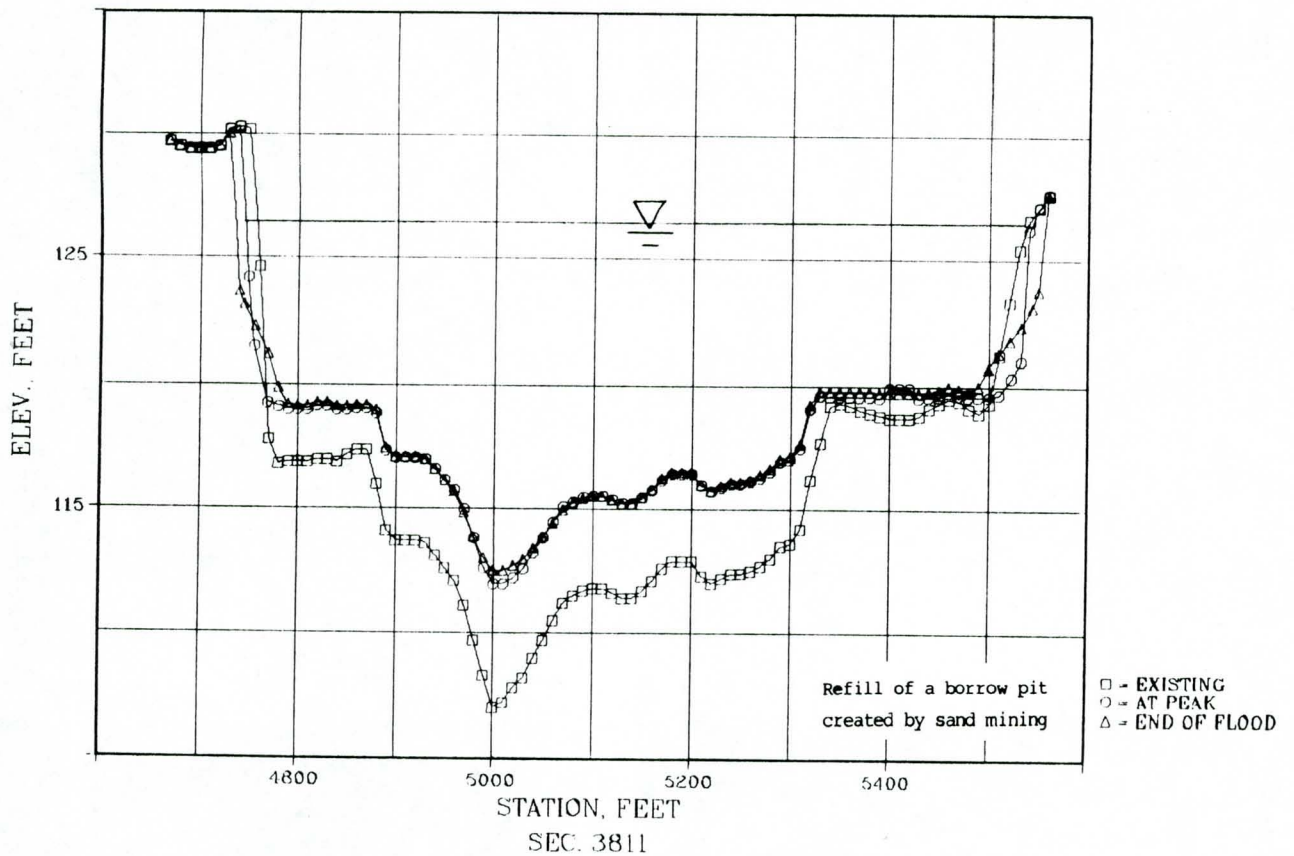
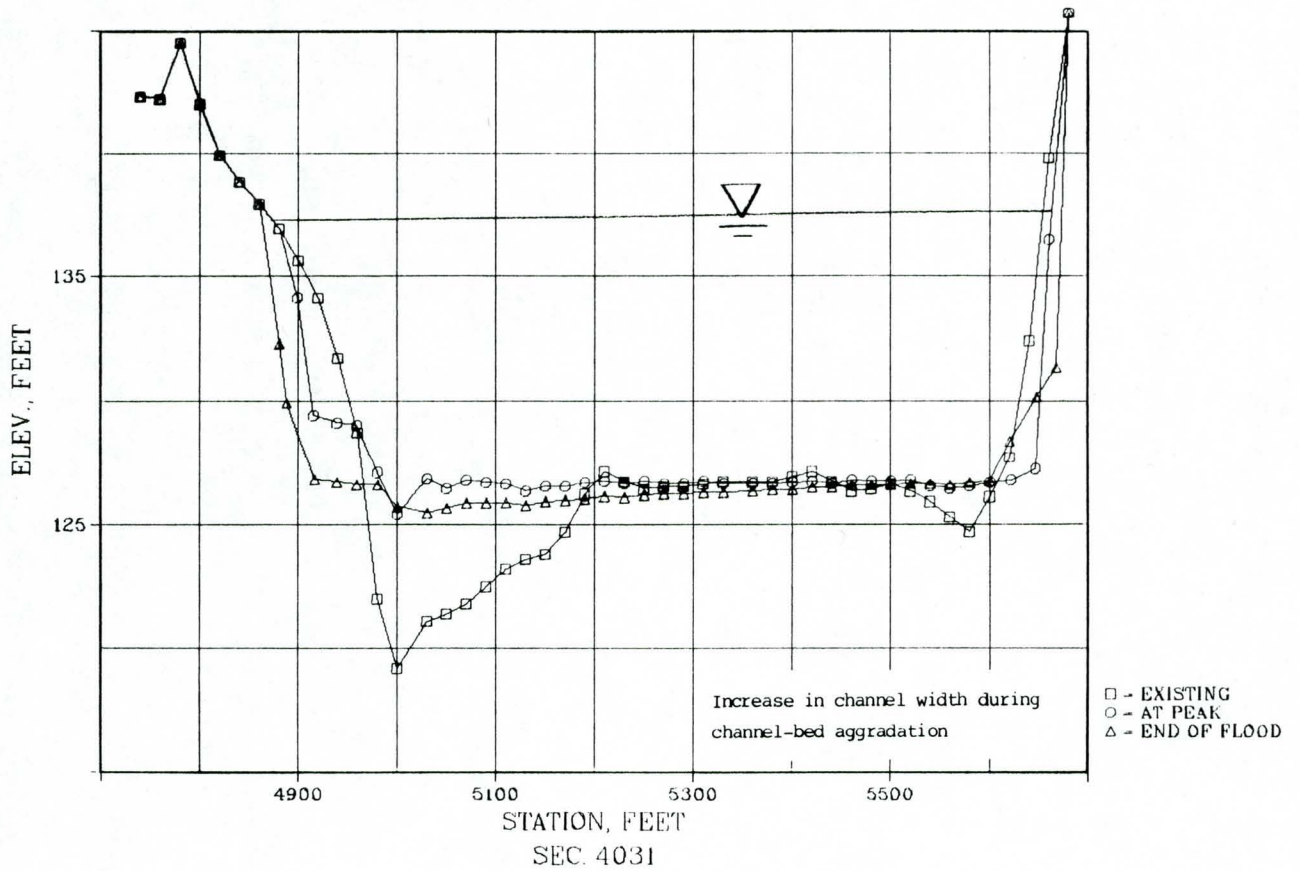
CROSS-SECTIONAL CHANGES SANTA CRUZ RIVER DESIGN CONCEPT 4-1

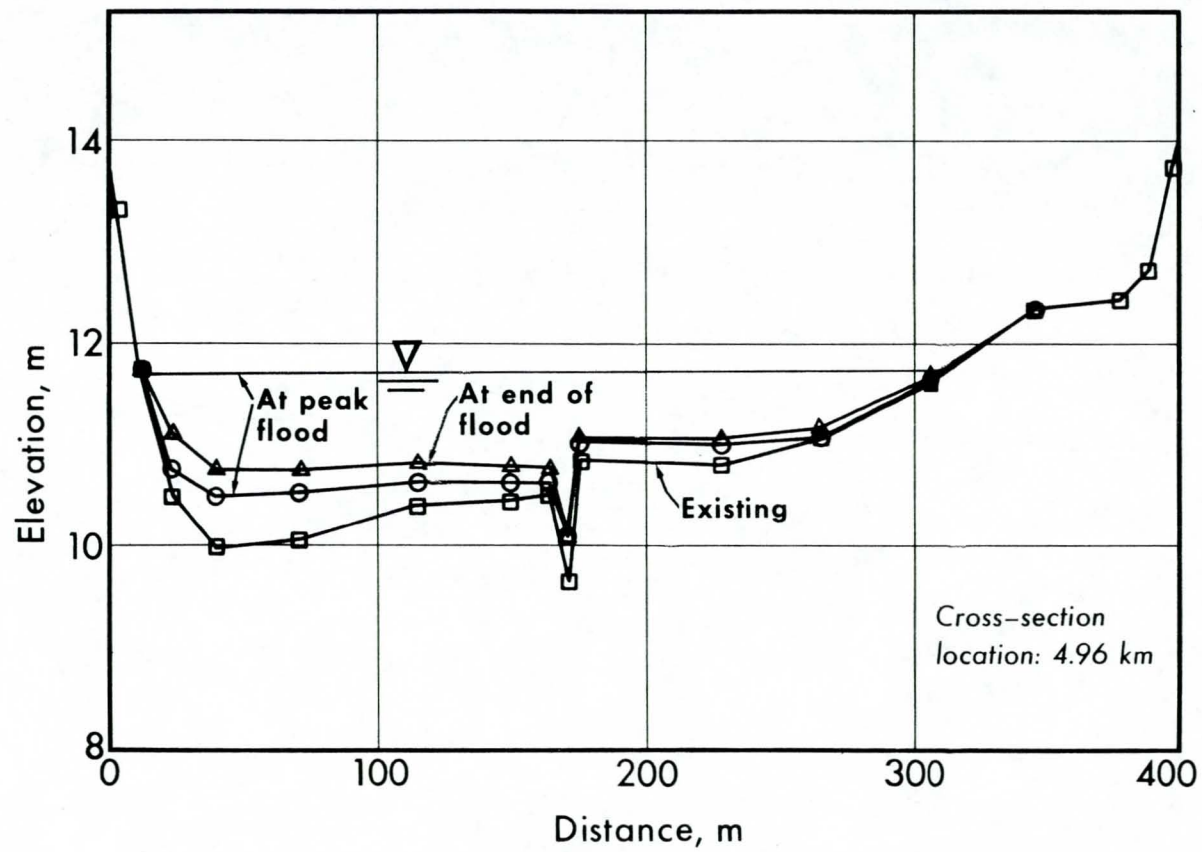


CROSS-SECTIONAL CHANGES CAUSED BY 100-YEAR FLOOD

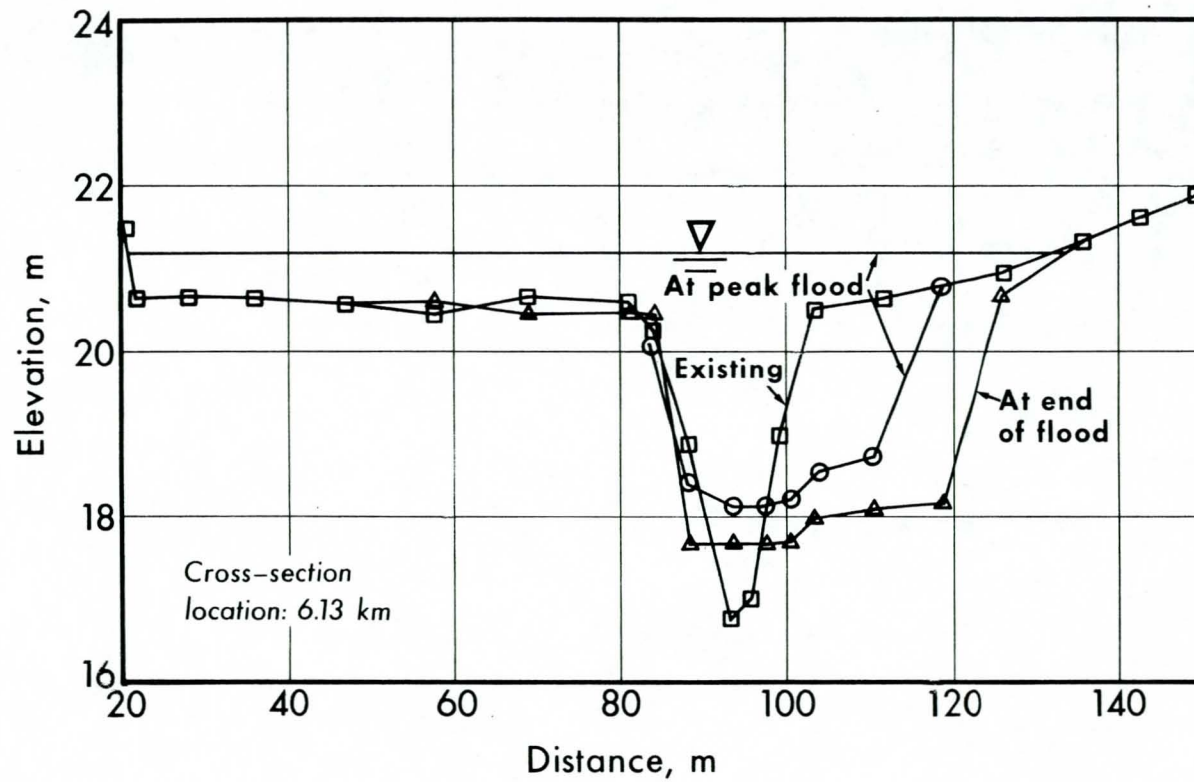


SAN LUIS REY RIVER CROSS-SECTIONAL CHANGES DURING 100-YEAR FLOOD



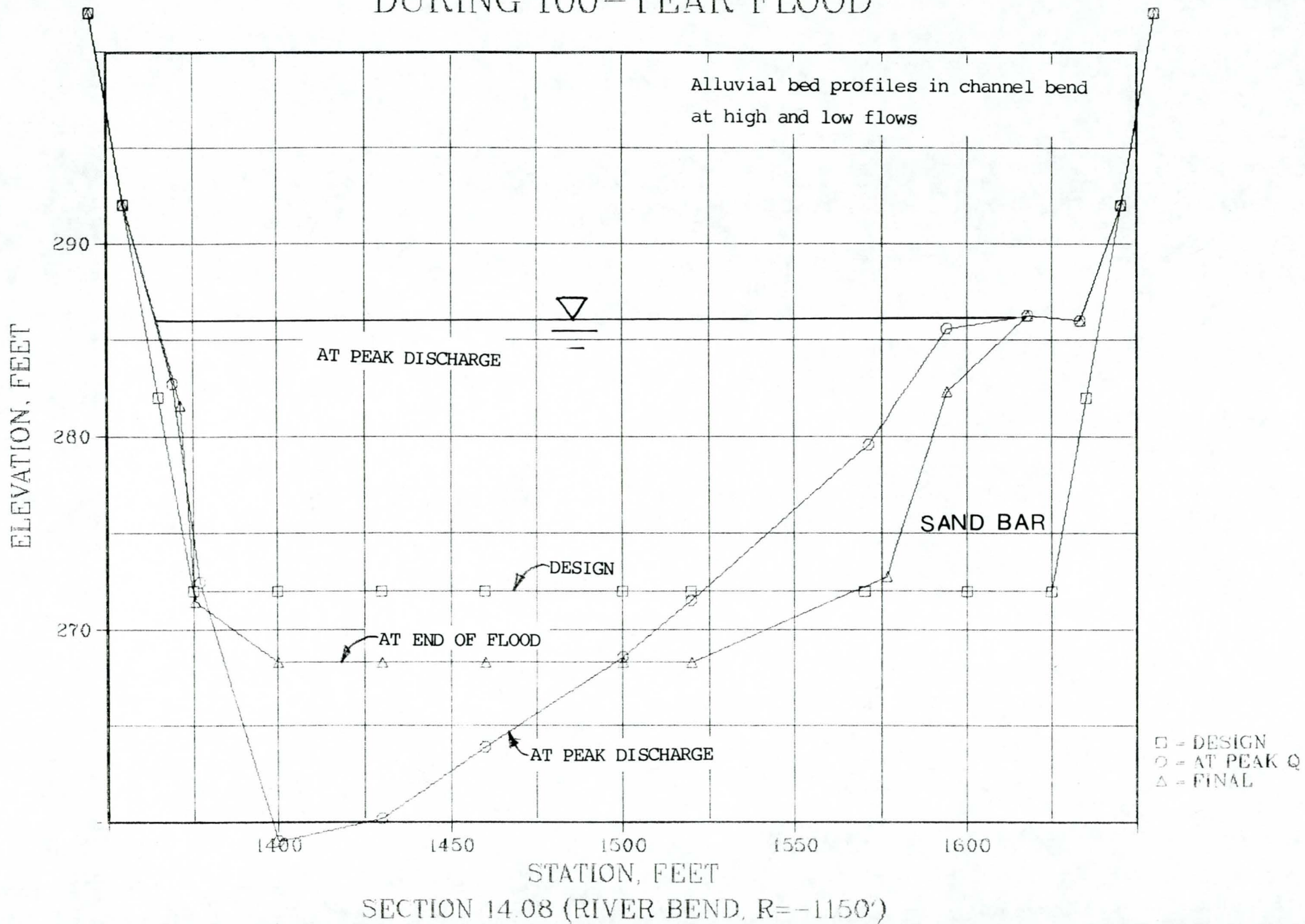


Simulated changes in cross section during 100-year flood showing deposition

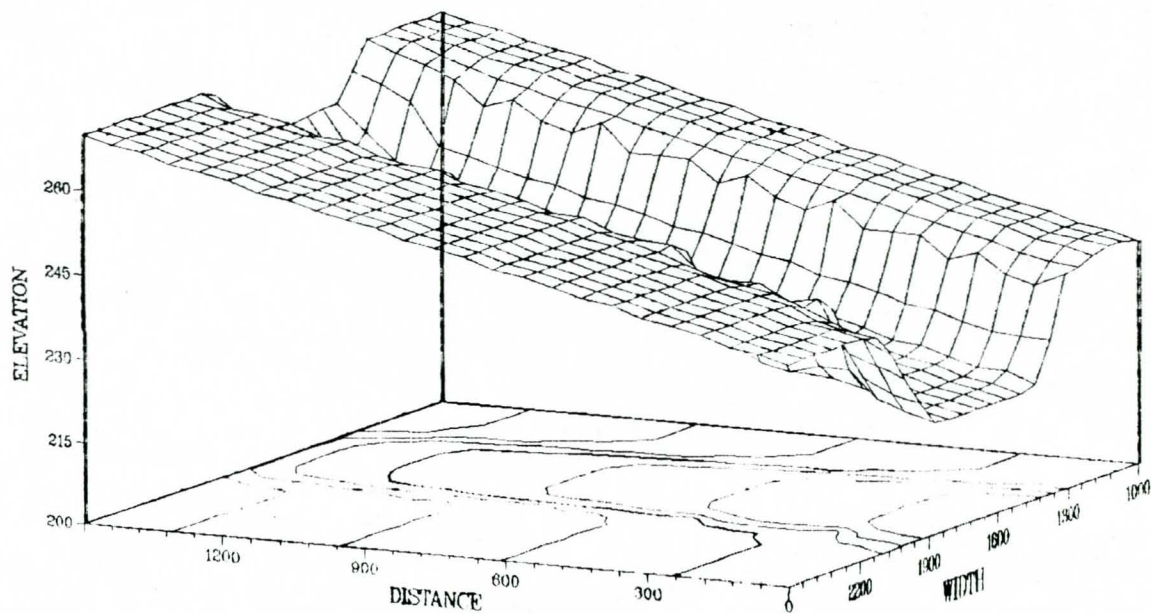


Simulated changes in cross section during 100-year flood showing widening of main channel

CROSS-SECTIONAL CHANGES SANTA CRUZ RIVER DURING 100-YEAR FLOOD



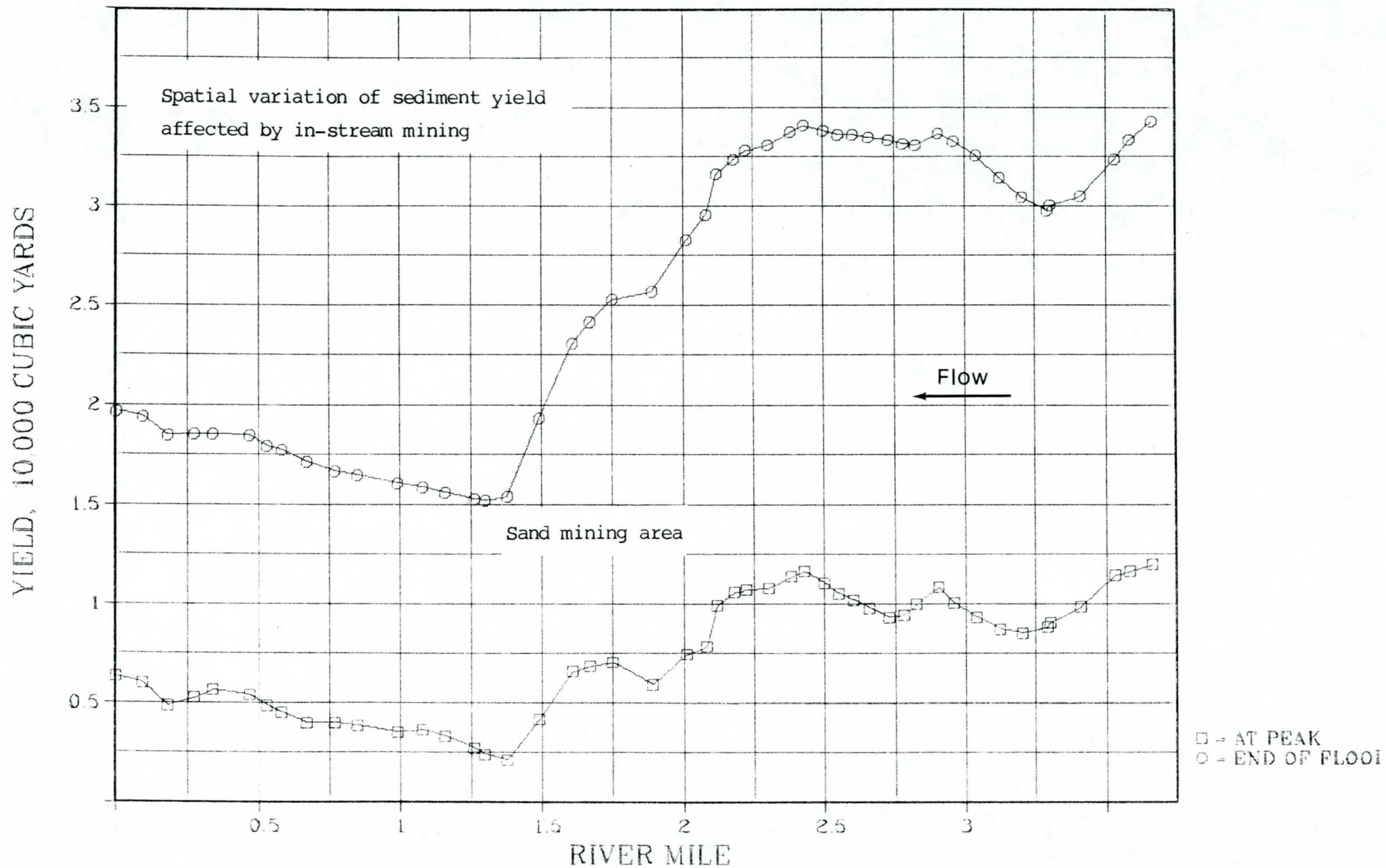
C3SUR BED FORM
V-PLOTTER 25 0-1500



-500,1000,200

SAN LUIS REY RIVER

TIME AND SPATIAL VARIATIONS IN SEDIMENT YIELD DURING 100-YEAR FLOOD



MODELING OF RIVER CHANNEL CHANGES

By Howard H. Chang,¹ M. ASCE

ABSTRACT: A computer-based flood- and sediment-routing model which simulates river channel changes is described together with its application in the case study of a disturbed river. Simulated results of this study are supported by field observations and measurements. This model incorporates the interrelated changes in channel bed profile, width, and lateral migration in channel bends. These changes reflect, in part, a river's adjustments in power expenditure. The interrelation of changes in channel bed profile and width is illustrated by a physical example and explained by the river's tendency to establish equal power expenditure along the channel. Such power transformation associated with river channel evolution tends to restore the dynamic equilibrium in sediment transport, that is, equal sediment load along the channel. The case study demonstrates that in the case of severely disturbed rivers, flood-level computation using a fixed-bed model may be quite inaccurate and improved accuracy can be provided by an erodible-bed model.

INTRODUCTION

River channel changes generally include channel-bed aggradation and degradation, width variation, and lateral migration in channel bends. These changes may occur naturally or as a result of a change in the environment. Man is also regarded as a geomorphic agent with certain activities such as sand and gravel mining, bridge construction, river control schemes, etc., having contributed to river channel changes. Langbein and Leopold (12) maintained that the equilibrium channel represents a state of balance with a minimum rate of energy expenditure or an equal rate of energy expenditure along the channel. Changes induced by nature or man's activities distort the channel equilibrium and therefore result in river channel changes.

The three types of river channel changes in channel-bed elevation, channel width, and lateral migration are closely interrelated to each other and may occur concurrently. Changes in channel-bed elevation are often inseparable from width variation because a channel tends to become narrower during degradation, and it tends to widen during aggradation. Earlier versions of the FLUVIAL model have considered channel-bed aggradation and degradation (3,4,5) and width variation (4,5). The current version FLUVIAL-11 which simulates all three types of changes has been formulated, developed and applied in a case study. This paper describes this model and its application in the case study. Special attention is given to the nature of energy (or power) transformation in alluvial rivers associated with river channel evolution.

ANALYTICAL BACKGROUND

This mathematical model has five major components: (1) Water routing; (2) sediment routing; (3) changes in channel width; (4) changes in channel-bed profile; and (5) lateral migration of the channel. This model

¹Prof. of Civ. Engrg., San Diego State Univ., San Diego, Calif.

Note.—Discussion open until July 1, 1984. To extend the closing date one month, a written request must be filed with the ASCE Manager of Technical and Professional Publications. The manuscript for this paper was submitted for review and possible publication on November 2, 1982. This paper is part of the *Journal of Hydraulic Engineering*, Vol. 110, No. 2, February, 1984. ©ASCE, ISSN 0733-9429/84/0002-0157/\$01.00. Paper No. 18578.

employs a space-time domain in which the space domain is represented by the discrete cross sections along the river reach and the time domain is represented by discrete time steps. In water routing, the time and spatial variations of the discharge, stage, velocity, energy gradient, etc., along the reach are obtained by an iterative procedure. At each time step, sediment discharge at each cross section is computed; changes in channel width, channel-bed profile and lateral migration are obtained and applied to each cross section. The bed-material composition is updated at each time step. Water routing is assumed to be uncoupled from the sediment processes. The five components are described.

Water Routing.—Basic equations for water routing include the continuity and momentum equation of flow, these are

$$\frac{\partial Q}{\partial x} + \frac{\partial A}{\partial t} - q = 0 \dots\dots\dots (1)$$

$$g \frac{\partial H}{\partial x} + \frac{1}{A} \frac{\partial Q}{\partial t} + \frac{1}{A} \frac{\partial}{\partial x} \left(\frac{Q^2}{A} \right) + gS - \frac{Q}{A^2} q = 0 \dots\dots\dots (2)$$

in which Q = flow discharge; x = distance in the longitudinal or flow direction; A = cross-sectional area of flow; t = time; q = lateral inflow rate per unit channel length; g = gravitational acceleration; H = stage or water surface elevation; and S = energy gradient. Eqs. 1 and 2 constitute a system of partial differential equations; they may be written in finite difference form in the space-time domain. With the prescribed initial and boundary conditions, time and spatial variations of Q and H along the reach may be obtained by an iterative procedure. This technique for water routing can be found elsewhere (6).

If the temporal terms in Eqs. 1 and 2 are ignored, water routing may be simplified by computing water-surface profiles at successive time steps. This option is available in the model. Computation of the water-surface profile at each time step is based upon the standard-step method using techniques similar to the HEC-2 computer model (9). For many cases, spatial variation in discharge due to channel storage is small and this technique produces closely similar results as the previous one.

Sediment Routing.—The sediment routing component has three major features: (1) Numerical solution of the continuity equation for sediment in the longitudinal direction; (2) computation of bed-material load using a formula suitable for the physical conditions; and (3) accounting of bed-material composition.

The continuity equation for sediment in the longitudinal direction is

$$(1 - \lambda) \frac{\partial A_c}{\partial t} + \frac{\partial Q_s}{\partial x} - q_s = 0 \dots\dots\dots (3)$$

in which λ = porosity of bed material; A_c = cross-sectional area of channel bed within some arbitrary frame; Q_s = volumetric sediment rate; and q_s = lateral inflow rate of sediment per unit length. The change in cross-sectional area ΔA_c for each section at each time step is obtained through numerical solution of Eq. 3. Techniques for numerical solution can be found in the literature (3,4). The area change ΔA_c is applied to the bed and banks following the techniques of corrections of channel-bed profile

and channel width described in the following sections.

Sediment rate is computed separately for cases of erosion and deposition using different size fractions of the bed material. For a particular size, transport capacity is obtained from a sediment equation. In the case of deposition, sediment rate is controlled by the transport capacity but, in the case of erosion, sediment rate is availability controlled. Simulation of sediment transport and accounting of bed-material composition by tracking river channel evolution are similar to those developed by Bennett and Nordin (2). Materials eroded from the channel banks, excluding that portion in the wash load size range, are included in the accounting. Bed armouring develops if bed shear stress is too low to transport any available size.

Changes in Channel Width.—Simulation of width variation is based upon the concept of minimum stream power. At a time step, width corrections for all cross sections are such that the total stream power (or rate of energy expenditure) for the reach is minimized; these corrections are subject to the physical constraint of rigid banks and limited by the amount of sediment removal or deposition along the banks within the time step. Total stream power of a channel reach is

$$P = \int_L \gamma Q S dx \dots\dots\dots (4)$$

in which P = total stream power of the reach; L = length of the reach; and γ = specific weight of water and sediment mixture. Written in finite difference form, this equation becomes

$$P = \sum_{i=1}^{N-1} \frac{1}{2} \gamma (Q_i S_i + Q_{i+1} S_{i+1}) \Delta x_i \dots\dots\dots (5)$$

in which N = total number of cross-sections for the reach; i = cross section index counted from upstream to downstream; and Δx_i = distance between Sections i and $i + 1$. Previous studies (5,12,13) have established that minimum stream power for an alluvial river is equivalent to equal power expenditure per unit channel length, that is, constant γQS along the reach. A river channel undergoing changes usually has uneven spatial distribution in power expenditure or γQS . Usually the spatial variation in Q is small but that in S is pronounced. Total stream power of a reach decreases with the reduction in spatial variation in QS (or S if Q is nearly uniform) along the reach. Adjustments in channel widths are made in such a way that the spatial variation of QS is minimized subject to the constraints and limitations aforementioned. An adjustment in width reflects the river's adjustment in flow resistance, that is, in power expenditure. A reduction in width at a cross section is usually associated with a decrease in energy gradient for the section whereas an increase in width is accompanied by an increase in energy gradient. Using these guidelines, a technique for width correction has been developed as described in a previous publication (5).

Width changes in alluvial rivers are characterized by the formation of small widths at degrading reaches and widening at aggrading reaches (4,5,11,13,15). This type of width formation represents the river's ad-

justment in resistance to seek equal power expenditure along its course. A degrading reach usually has a higher channel-bed elevation and energy gradient than its adjacent reaches. Formation of a narrower and deeper channel at the degrading reach decreases its energy gradient due to reduced boundary resistance and lower bed elevation. On the other hand, an aggrading reach is usually lower in channel-bed elevation and energy gradient. Widening at the aggrading reach increases its energy gradient due to increased boundary resistance and higher bed elevation. These adjustments in channel width reduce the spatial variation in energy gradient and total power expenditure of the channel. Since sediment rate is directly proportional to γQS (1), these adjustments also favor the establishment of channel's equilibrium in sediment load, that is, equal sediment rate along the reach.

Changes in Channel-Bed Profile.—After the banks are adjusted, the remaining correction for ΔA_c obtained in sediment routing is applied to the bed. Erosion and deposition at a cross section have different patterns. Generally speaking, deposition tends to be more uniformly distributed in that it tends to build up the channel bed in horizontal layers. This process of deposition is often accompanied by channel widening. On the other hand, channel-bed erosion tends to be more confined with greater erosion in the thalweg. This process is usually associated with a reduction in width. These channel adjustments reduce the spatial variation in power expenditure as the river seeks to establish a new equilibrium. In the model, deposition at an aggrading section starts at the lowest point, and it builds up the channel bed in horizontal layers. For a degrading section, the change in area is distributed in proportion to the effective tractive force, $\tau - \tau_{cr}$, along the bed, where τ is the local tractive force and τ_{cr} is the critical tractive force.

Lateral Migration.—In a river bend, erosion on the concave bank and deposition on the convex bank results in lateral migration of the channel. This river channel change is attributed to the transverse currents in the river bend. In the present model, the mechanism for lateral migration is provided by transverse currents, transverse sediment movement and the continuity equation for sediment in the transverse direction. Bottom filaments of stream current in a bend have a component in the transverse direction toward the convex bank. The role of transverse velocity consists in moving the bottom layers of the stream away from the concave bank. Erosion of the concave bank occurs under the action of the transverse velocity which, being directed down the slope and added to the gravitational force, scours particles of the material on the concave bank. As particles are scoured from the concave bank, they tend to be deposited on the convex bank, resulting in a shift in channel course. Rozovskii (14) studied the angle of deviation of bottom filaments from the direction tangent to the centerline of a bend. Kikkawa, et al. (10, p. 1332) developed an analytical relationship for the angle of deviation β of mean particle path from the tangential direction. In the relationship, β is expressed as a function of the flow direction of bottom filaments, transverse bed slope, and flow and sediment characteristics. With this relationship, the transverse sediment rate is related to the longitudinal sediment rate as

$$q'_s = \tan \beta q_s \dots \dots \dots (6)$$

in which q'_s = transverse sediment rate per unit channel length; and q_s = longitudinal sediment rate per unit width. Erosion of the concave bank is simulated by the removal of sediment and bank collapse due to the combined effects of velocity and gravitational force. Because bank stability depends on a large number of factors including bank height, slope angle, drainage state, cohesion, etc. (17), the rate of bank erosion given by Eq. 6 is multiplied by a coefficient of bank erosion which is determined based upon river data. The change in channel-bed elevation at a point along a section is obtained from the continuity for sediment in the transverse direction, or

$$(1 - \lambda) \frac{\partial z}{\partial t} + \frac{1}{r} \frac{\partial}{\partial r} (r q'_s) = 0 \dots \dots \dots (7)$$

in which z = channel-bed elevation at a point; and r = radial or transverse coordinate. With a forward difference in r for the spatial derivative as suggested by Chang and Hill (3), the change in channel-bed elevation Δz for a time step Δt due to transverse sediment movement is

$$\Delta z_k = \frac{\Delta t}{1 - \lambda} \frac{2}{r_k + r_{k+1}} \frac{r_{k+1} q'_{sk+1} - r_k q'_{sk}}{r_{k+1} - r_k} \dots \dots \dots (8)$$

in which k = radial coordinate index counted from the convex bank toward the concave bank.

MODEL DESCRIPTION

The mathematical model FLUVIAL-11 has been developed; its input data, computing procedures and output parameters are described.

Input Data.—Input to the model include the initial cross sections, channel roughness, initial bed-material composition, inflow hydrograph and physical constraints such as check dams, rigid banks, bedrock outcrops, etc. The input data follow the HEC-2 (9) format.

Computing Procedures.—Major steps of computation in the model include the following:

1. Enter input data.
2. Compute water-surface elevations and sediment loads at all cross sections.
3. Set $t = t + \Delta t$.
4. Determine changes in channel cross-sectional area using techniques for sediment routing.
5. Compute and apply changes in channel width.
6. Obtain new channel-bed profiles.
7. Compute and make changes in cross-sectional profile due to lateral migration for those sections in channel bends.
8. Update bed-material compositions.

After step 8, the computation returns to Step 2 for another time step. The iteration continues until the required time period is covered.

Output Description.—Output of the model include initial bed-material compositions, time and spatial variations of the water-surface profile, channel width, flow depth, flood discharge, velocity, energy gradient, roughness coefficient, median sediment size, and bed-material load. In addition, cross-sectional profiles are printed at different time intervals.

CASE HISTORY OF RIVER CHANNEL CHANGES

The San Dieguito River at Rancho Santa Fe, California, went through significant changes in a two-mile reach (see Fig. 1) during recent floods. Measurements of river channel changes and flood hydrographs were made by the County of San Diego (7,16), providing a valuable set of field data for river studies.

Physical Conditions.—The study reach is about four miles from the ocean and about five miles below Lake Hodges Dam. The channel has a wide and flat natural configuration; the natural slope and bed-material size decrease significantly in the downstream direction. Bed material of the study reach varies from coarse sand ($d_{50} = 0.85$ mm) at the upstream end to fine sand ($d_{50} = 0.24$ mm) downstream.

The natural channel configuration was distorted prior to recent flood events by man's activities including sand mining and construction of the Via de Santa Fe Road and bridge as shown in Fig. 1. As a result of sand mining, several large borrow pits with a depth as great as 25 ft were created. The natural wide channel was encroached upon by the road embankment on each side of the bridge (Section 51). While the river channel has an erodible bed and banks, the banks, however, are constrained by the hills at the south bank of Section 51 and along the north

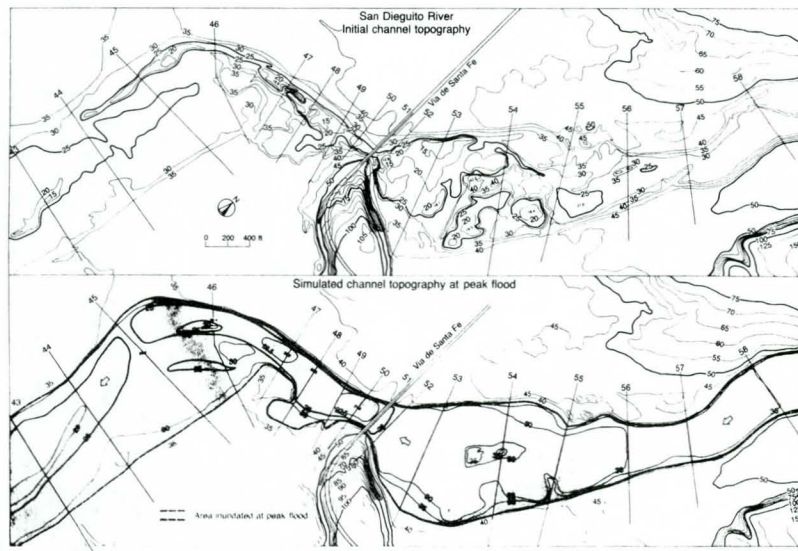


FIG. 1.—Topographies and Cross Section Locations

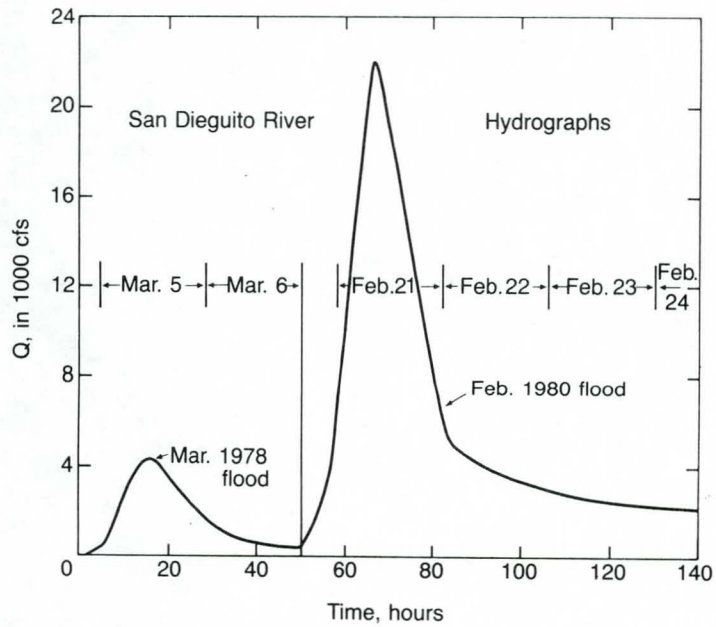


FIG. 2.—Flood Hydrographs

banks of Section 60–63 and by bank protections at the north banks of Sections 51 and 58.

Two floods passed through the river, one in March, 1978 (peak flow = 4,400 cfs), and another in February, 1980 (peak flow = 22,000 cfs),

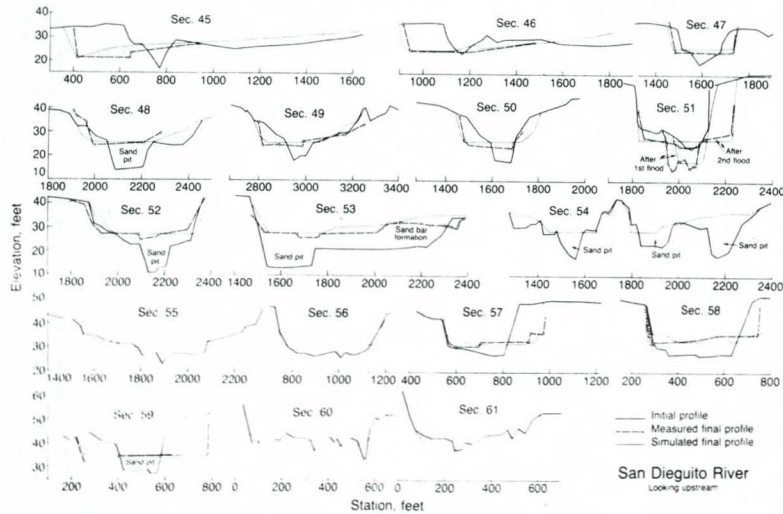


FIG. 3.—Simulated and Measured Cross-Sectional Changes

when Lake Hodges spilled. Hydrographs of these floods are shown in Fig. 2. Prior to these events, Lake Hodges had not spilled for 26 yr.

River Channel Changes.—Significant changes in the river channel were observed after the March, 1978, flood. Channel-bed scour occurred near borrow pits and notably at the bridge crossing where measurements were made as shown in Fig. 3 for Section 51. Deposition was observed in the borrow pits. With limited flood discharge and duration, these borrow pits were only partially refilled.

Major changes in the river channel occurred during the greater February, 1980, flood. These changes included channel-bed aggradation and degradation, width variation, and lateral migration of the channel as described below. These changes were recorded by photographs taken during the flood, by a high water mark at Section 52, and by channel-bed measurements at selected cross sections after the flood as shown in Fig. 3.

Major aggradation occurred in the borrow pits as they were largely refilled after the flood. Major degradation occurred near the borrow pits and at the bridge crossing during the flood. Failure of several bridge piers as shown in Fig. 4 was caused by channel-bed scour, high velocity, and debris accumulation on the piers.

Channel-bed aggradation and degradation were accompanied by changes in channel width. The initial channel width was highly uneven along the reach primarily due to width encroachment by road embankments at the bridge crossing. Sand mining also contributed to the initial uneven width variation. As shown in Fig. 3, changes in channel width that occurred during the flood consisted of widening at the bridge crossing (Section 51) and other initially narrow sections (Sections 47, 49, 50, 57, 58, 59) and reductions in width at initially wide sections, notably at

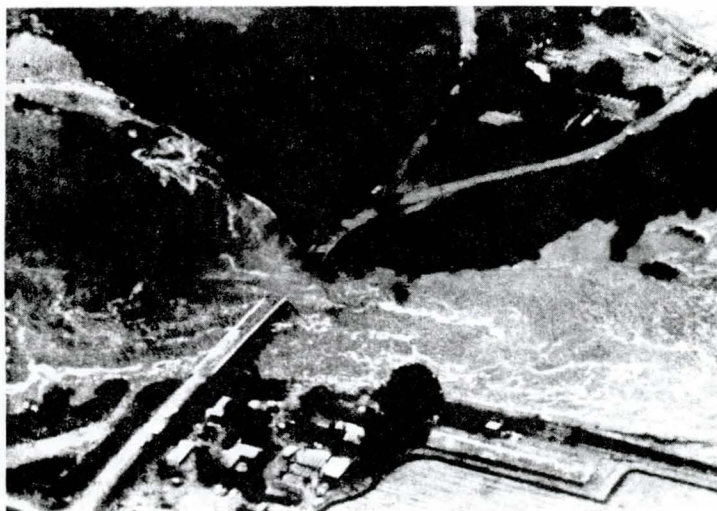


FIG. 4.—San Dieguito River Near Via de Santa Fe Road on February 21, 1980 (Looking Toward South)

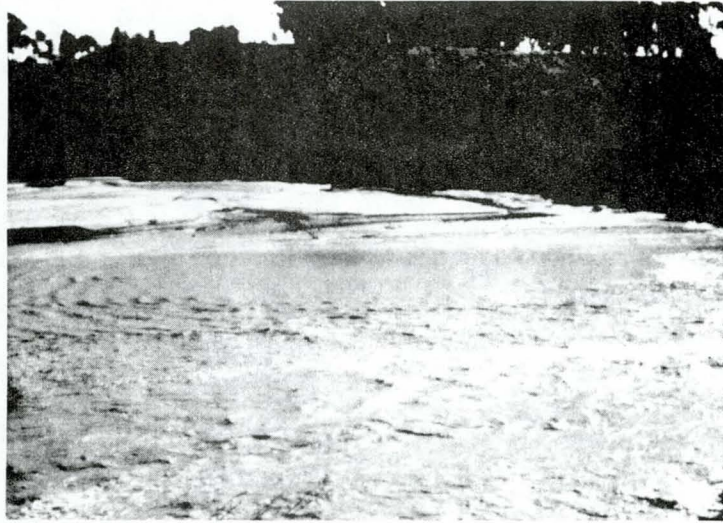


FIG. 5.—Sand Bar Formation Near Section 53 (Looking Toward South)

Sections 53 and 54. Widening was accomplished by erosion of the channel banks subject to the physical constraints; reduction in width was due to sediment deposition along the banks in the form of sand bars. At Section 53, where the width showed a substantial reduction, the sand bar formed along the south bank at the end of the flood (see Figs. 3 and 5) had a width of about 400 ft or one-half of the initial channel width. The initial highly uneven spatial variation in channel width was gradually reduced during the flood.

Lateral migration of the river channel was pronounced along the channel bend from Section 44 to 46 where the concave bank was on erodible



FIG. 6.—Channel Bank Scour Near Sections 45 and 46 (Looking Toward North)

farm land. The channel shifted laterally toward the concave bank for as much as 200 ft, putting this part of the farm land into the river channel. A picture of the new concave channel bank taken after the flood is shown in Fig. 6.

SIMULATION AND RESULTS

The mathematical model FLUVIAL-11 was used to simulate river channel changes in the San Dieguito River during the 1978 and 1980 floods. Graf's equation (8) for bed-material load was used in computing the sediment movement. Channel roughness in terms of Manning's n was selected to be 0.035 in consideration of the channel irregularity and minor vegetation growth; it was estimated to be 0.04 at the bridge crossing. The combined duration of 140 hr for these two floods was computed using 2,000 time steps.

Simulated results as presented in Figs. 1, 3, and 7-10 are described.

Changes in River Channel Configuration.—River channel changes, including those in channel-bed profile, channel width, and lateral migration, as simulated by the computer model, are described herein. Changes in the longitudinal channel-bed profile (see Fig. 7) are characterized by aggradation in the borrow pits, erosion at higher grounds, and the gradual formation of a more or less smooth channel-bed profile at the end of the flood. In that process, considerable variation in the longitudinal channel-bed elevation through the downstream portion of the river reach is predicted at the peak flood as shown in Figs. 1 and 7. The higher channel-bed elevations at Sections 45, 46, and 48 are asso-

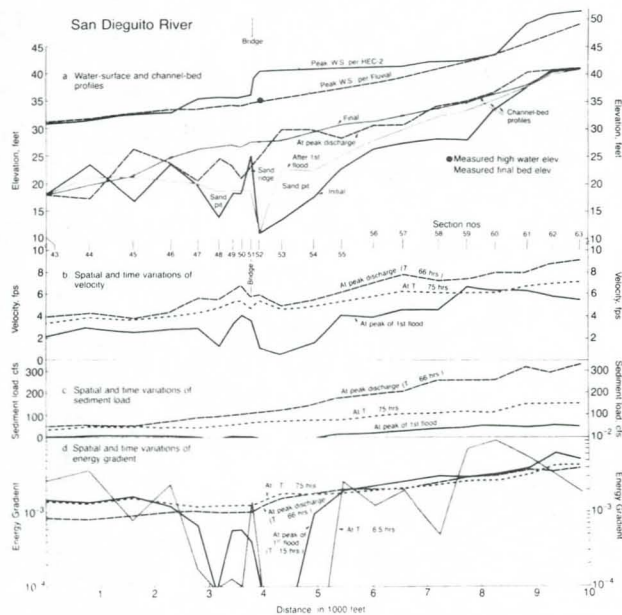


FIG. 7.—Simulated and Measured Results

ciated with large channel widths while the lower elevations at Sections 47 and 50 are due to their small widths.

Changes in channel width which occur concurrently with variations in channel-bed elevation and lateral migration are simulated. Width changes are characterized by the gradual widening at those initially narrow sections, notably at Sections 47, 49, 50, 51, 57, 58 and 59 and reductions in width at initially wide sections, notably at Sections 53 and 54. Initial and simulated final cross-sectional profiles of these sections are shown in Fig. 3 together with some measured profiles. Simulated channel width at the peak flood (shown in Fig. 1) is highly uneven in its spatial variation along the river. This variation is gradually reduced during the flood as reflected by the simulated final cross-sectional profiles in Fig. 3. By comparing the initial and final channel-bed profiles, one finds that widening at a section is through bank erosion and that the reduction in width is usually through sand-bar formation along the bank(s). Simulated time variation of the cross-sectional profile for Section 53 shown in Fig. 8 shows the sand-bar formation and the associated reduction in channel width. A picture of this sand bar taken at the end of the flood is shown in Fig. 5.

That changes in channel width and channel-bed elevation are closely related may be illustrated by the simulated time variation of the cross-sectional profile at Section 51 (see Fig. 9). Initially Section 51 is on a sand ridge with borrow pits existing on both sides. Gully erosion through this sand ridge during the first flood is simulated, followed by gradual widening and lessening of the gully depth during the second flood. The maximum scour depth is predicted to occur in the initial gully. The simulated results correlate well with measurements at this section shown in Fig. 3, in which the uneven final channel-bed profile as measured is related to the removal of several piers during the flood.

Lateral migration of the channel at Sections 44, 45, and 46 in the river bend as simulated is illustrated by the time variation of the cross-sectional profile at Section 46 (see Fig. 10). Lateral migration is through gradual erosion of the concave bank and deposition on the convex bank.

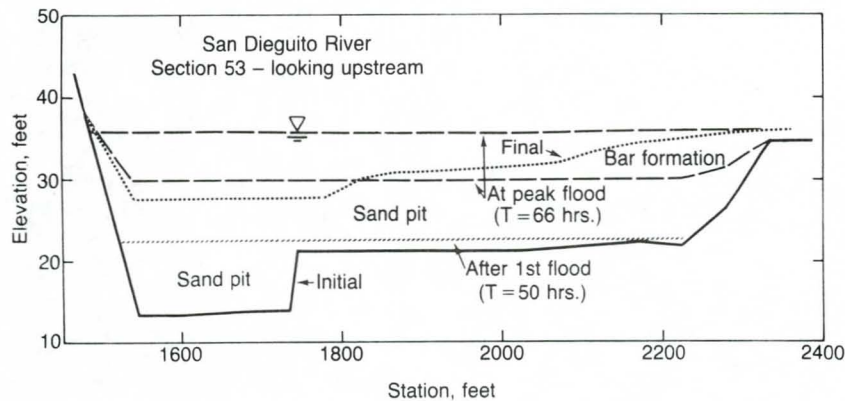


FIG. 8.—Simulated Cross-Sectional Changes at Section 53

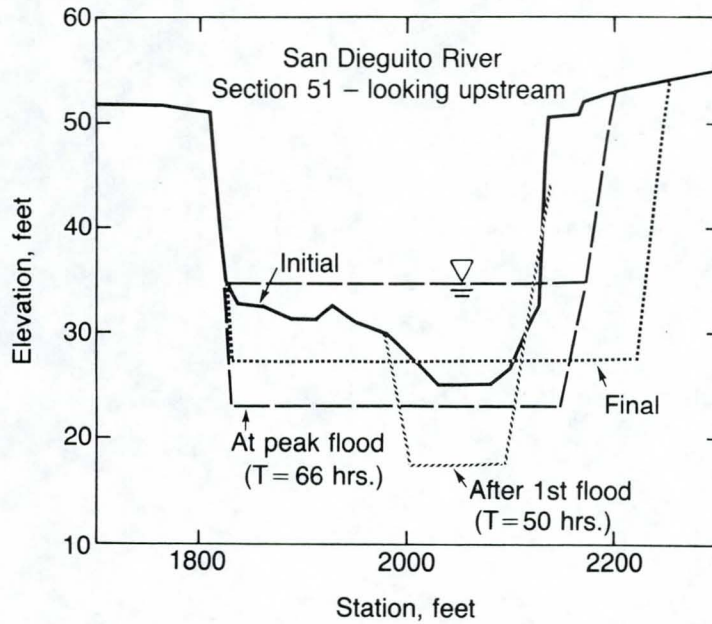


FIG. 9.—Simulated Cross-Sectional Changes at Via de Santa Fe Bridge

A picture of the eroded concave bank is shown in Fig. 6.

River Channel Changes in Relation to Power Expenditure.—Changes in river-channel configuration are accompanied by changes in flow resistance and hence the rate of energy (or power) expenditure. The γQS product represents the rate of energy expenditure per unit channel length. Since the spatial variation of Q is small, the spatial variation of γQS may be represented by the spatial variation of the energy gradient S shown in Fig. 7.

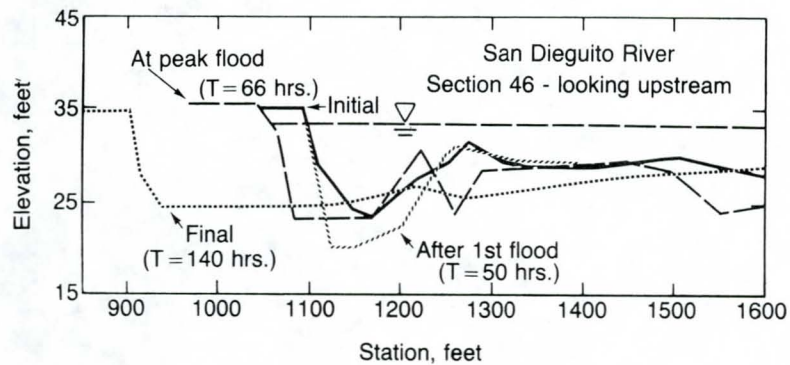


FIG. 10.—Simulated Cross-Sectional Changes at Section 46 Showing Lateral Migration Toward the Concave Bank

Simulated river channel changes are associated with the gradual reduction of the spatial variation of energy gradient along the channel subject to the physical constraint of rigid banks. That the adjustment in river-channel configuration is closely related to the change in power expenditure can be illustrated by the sequential changes of cross-sectional profile at Section 51 as shown in Fig. 9. Because it is an initial sand ridge (see Fig. 7), the energy gradient at this section is initially much greater than those of its adjacent sections. This pronounced spatial variation in energy gradient is reduced through gully erosion at this section and deposition at the adjacent sections. The gully which is small in width and has a low channel-bed elevation provides the least possible flow resistance and therefore lowest energy gradient at this section; it also reduces the back-water effect on the upstream section where the energy gradient is therefore increased. At subsequent time intervals, the energy gradient at Section 51 becomes less than its adjacent sections. Cross-sectional changes at this section then include widening in channel width and aggradation in the gully. These changes are accompanied by increases in boundary resistance and energy gradient at this section, favoring the establishment of equal energy gradient along the reach. This pattern of river channel changes, characterized by the formation of narrow channel width during channel-bed degradation and widening during aggradation, is evident in nature and has been reported in the literature (4,5,11,13,15).

Changes in Sediment and Hydraulic Parameters.—That flood- and sediment-routing in erodible channels is closely related to river-channel changes may be illustrated by the time and spatial variations of the velocity and sediment load shown in Fig. 7 at the peaks of the first and the second flood. The pronounced spatial variations in velocity and sediment load at the first peak flood are associated with the uneven river channel configuration dotted with borrow pits within which velocities and sediment loads are substantially lower. Changes in the river channel are such that they provide the mechanism to establish the dynamic equilibrium of sediment transport, that is, equal sediment load along the river reach. As shown, the spatial variation of sediment load is gradually reduced during the second flood. The same general trend may also be stated for the spatial variations in velocity and energy gradient. The slightly lower velocity at the bridge crossing is due to the additional flow resistance of bridge piers.

Variations of sediment size due to hydraulic sorting as simulated are not pronounced for this river reach. Certain trends can still be recognized, including coarsening of the material during scour and reduction in size during deposition. Channel widening through bank erosion brings finer bank materials into the channel and hence contributes to a reduction in sediment size.

Water-Surface Profiles.—The water-surface profile at the peak flood obtained using the FLUVIAL-11 model is compared with that obtained using the fixed-bed model HEC-2 in Fig. 7. The HEC-2 profile which is based upon the initial river-channel configuration indicates critical flow at Sections 46, 51, and 60, and subcritical flow at remaining sections, while the FLUVIAL-11 model predicts subcritical flow for the entire reach. The HEC-2 water-surface profile is highly uneven; the higher water-sur-

face elevations immediately upstream of the bridge crossing are primarily due to the higher bed elevation of the sand ridge and channel constriction at the bridge crossing. The FLUVIAL-11 water-surface profile is more uniform and its elevation at Section 52 is substantiated by the measured high water mark.

SUMMARY AND CONCLUSIONS

The mathematical model FLUVIAL-11 has been formulated and developed; it has been employed to simulate flood- and sediment-routing and associated river channel changes in the San Dieguito River near the Via de Santa Fe bridge. Simulated results using this model are supported by field observations and measurements.

An alluvial river is the author of its own geometry; therefore it will respond to any change imposed upon by nature or by men through self adjustments. River channel changes may include channel-bed aggradation and degradation, width variation, and lateral migration in channel bends. These changes are interrelated as they may occur concurrently. therefore, a mathematical model for erodible channels must include these variables.

River channel changes in the San Dieguito River are characterized by the trend toward a more uniform configuration from the initially distorted configuration. In this process, the river channel tends to become narrower during channel-bed degradation and it tends to widen during aggradation. This pattern of adjustments reflects the river's tendency to seek equal power expenditure along the channel. River channel changes also provide a mechanism with which the river seeks to establish the dynamic equilibrium in sediment transport, that is equal sediment load along the reach.

In severely disturbed rivers, flood-level computation using a fixed-bed model can be quite inaccurate. Improved accuracy for flood-level determination in such channels may be provided by an erodible-bed model.

ACKNOWLEDGMENT

The San Dieguito River study was made for the Committee on Hydrodynamic Models, National Research Council, National Academy of Sciences. This river was selected by the Committee as a test case for the study of computer-based flood and sediment routing models. This study was conducted for the Federal Emergency Management Agency by the Academy. The writer wishes to thank the staff of the County of San Dieguito for data collection. Suggestions on the manuscripts by Richard M. Fragaszy, Joseph C. Hill and V. Miguel Ponce are greatly appreciated.

APPENDIX I.—REFERENCES

1. Bagnold, R. A., "An Approach to Sediment Transport Problem from General Physics," U.S. Geological Survey Professional Paper 422-I, Washington, D.C., 1966, 137 pp.
2. Bennett, J. S., and Nordin, C. F., "Simulation of Sediment Transport and Armouring," *Hydrological Sciences Bulletin*, XXII, 4, Dec., 1977, pp. 555-569.

3. Chang, H. H., and Hill, J. C., "Computer Modeling of Erodible Flood Channels and Deltas," *Journal of the Hydraulics Division*, ASCE, Vol. 102, No. HY10, Oct., 1976, pp. 1461-1475.
4. Chang, H. H., and Hill, J. C., "Minimum Stream Power for Rivers and Deltas," *Journal of the Hydraulics Division*, ASCE, Vol. 103, No. HY12, Dec., 1977, pp. 1375-1389.
5. Chang, H. H., "Mathematical Model for Erodible Channels," *Journal of the Hydraulics Division*, ASCE, Vol. 108, No. HY5, May, 1982, pp. 678-689.
6. Fread, D. L., "Numerical Properties of Implicit Four-Point Finite Difference Equations of Unsteady Flow," National Weather Service, NOAA, Technical Memorandum NWS Hydro-18, Mar., 1974.
7. "Flood Plain Changes During Major Floods," Department of Sanitation and Flood Control, Community Services Agency, County of San Diego, Calif., 1979.
8. Graf, W. H., *Hydraulics of Sediment Transport*, McGraw-Hill Book Co., New York, N.Y., 1971, 509 pp.
9. "HEC-2 Water Surface Profiles, Users Manual," Hydrologic Engineering Center, U.S. Army, Corps of Engineers, Nov., 1976.
10. Kikkawa, H., Ikeda, S., and Kitagawa, A., "Flow and Bed Topography in Curved Open Channels," *Journal of the Hydraulics Division*, ASCE, Vol. 102, No. HY9, Sept., 1976, pp. 1327-1342.
11. Lane, E. W., "A Study of the Shape of Channels Formed by Natural Streams Flowing in Erodible Material," *Missouri River Division Sediment Series No. 9*, U.S. Army Engineer Division, Missouri River, Corps of Engineers, Omaha, Neb., 1957.
12. Langbein, W. B., and Leopold, L. B., "River Meanders, Theory of Minimum Variance," U.S. Geol. Survey Prof. Paper 282-B, 1957.
13. Leopold, L. B., Wolman, M. G., and Miller, J. P., *Fluvial Processes in Geomorphology*, W. H. Freeman and Co., San Francisco, Calif., 1964, 522 pp.
14. Rozovskii, I. L., "Flow of Water in Bends of Open Channels," Israel Program for Scientific Translations, Jerusalem, Israel, 1961 (available from Office of Technical Services, U.S. Department of Commerce, Washington, D.C., PST Catalog No. 363, OTS 60-51133).
15. Schumm, S. A., *The Fluvial System*, John Wiley and Sons, New York, N.Y., 1977, 338 pp.
16. "Storm Report, February 1980," San Diego County Flood Control District, San Diego, Calif., 1980, 26 pp.
17. Thorne, C. R., "Processes and Mechanisms of River Bank Erosion," *Gravel-Bed Rivers*, R. D. Hey, J. C. Bathurst, and C. R. Thorne, eds., John Wiley and Sons, New York, N.Y., 1982, pp. 227-271.

APPENDIX II.—NOTATION

The following symbols are used in this paper:

- A = cross-sectional area of flow;
- A_c = channel cross-sectional area within references frame;
- D = average flow depth;
- d_{50} = median size of sediment;
- g = gravitational acceleration;
- H = stage or water-surface elevation;
- i = cross-section index counted from upstream to downstream;
- k = radial (transverse) coordinate index;
- L = length of stream reach;
- N = total number of cross-sections for stream reach;
- n = Manning's roughness coefficient;
- P = total stream power of river reach;
- Q = flow discharge;

Q_s = sediment discharge;
 q = discharge of lateral inflow per unit channel length;
 q_s = lateral inflow of sediment per unit channel length or longitudinal sediment rate per unit width;
 q'_s = transverse sediment rate per unit channel length;
 r = radial or transverse coordinate;
 S = energy gradient;
 t = time;
 x = distance along longitudinal (flow) direction;
 β = angle of deviation from direction tangent to centerline of channel;
 γ = specific weight of water and sediment mixture;
 λ = porosity;
 τ = tractive force; and
 τ_{cr} = critical tractive force.

WATER AND SEDIMENT ROUTING THROUGH CURVED CHANNELS

By Howard H. Chang,¹ M. ASCE

ABSTRACT: A mathematical model for water and sediment routing through curved alluvial channels is developed and applied in a case study. This model, which is for alluvial streams with nonerodible banks, may be employed to simulate stream bed changes during a given flow, thereby providing the necessary information for the design of dikes, levees, or other bank protection. This model incorporates the major effects of transverse circulation, inherent in curved channels, on the flow and sediment processes. In the simulation of the evolution in stream bed profile, the effect of transverse flow is tied in with the aggradation and degradation development. River flow through curved channels is characterized by the changing curvature, to which variations of flow pattern and bed topography are closely related. Simulation of these changing features is based upon the fluid dynamics governing the growth and decay of transverse circulation along the channel.

INTRODUCTION

An important factor that affects the hydraulics of flow, sediment transport, and bed topography through curved alluvial channels is the spiral motion or transverse circulation. Greater depths and higher velocities near concave banks produced by the transverse circulation, in addition to aggradation and degradation, are necessary considerations for levee or dike design. The importance of transverse circulation was stressed in a recent evaluation of mobile bed mathematical models by the National Academy of Sciences (3). In this connection, research effort toward improved incorporation of the effect of transverse flow in modeling was recommended.

A mathematical model for water and sediment routing through curved alluvial channels is described herein. This model simulates time and spatial variations in water level, sediment transport, and bed topography. In the prediction of stream bed profile changes, aggradation and degradation are tied in with the effect of transverse flow under the changing channel curvature. Application of this model is limited to alluvial channels with nonerodible banks, large width-depth ratio, and mild curvature, all characteristic of natural rivers with bank protection. A case study using this model on the San Lorenzo River in California during a flood event is presented.

Analyses of flow and bed topography in curved channels have been accomplished by Yen (26), Engelund (13), Kikkawa et al. (19), Zimmermann and Kennedy (28), Falcon Ascanio and Kennedy (14), and Odgaard (20), among others. Some of these analytical methods are used in the model. However, such methods are generally for curved channels with fully developed transverse flow. Because of the streamwise (lon-

¹Prof. of Civ. Engrg., San Diego State Univ., San Diego, Calif. 92182.

Note.—Discussion open until September 1, 1985. To extend the closing date one month, a written request must be filed with the ASCE Manager of Journals. The manuscript for this paper was submitted for review and possible publication on November 30, 1983. This paper is part of the *Journal of Hydraulic Engineering*, Vol. 111, No. 4, April, 1985. ©ASCE, ISSN 0733-9429/85/0004-0644/\$01.00. Paper No. 19656.

WATER AND SEDIMENT ROUTING THROUGH CURVED CHANNELS

By Howard H. Chang,¹ M. ASCE

ABSTRACT: A mathematical model for water and sediment routing through curved alluvial channels is developed and applied in a case study. This model, which is for alluvial streams with nonerodible banks, may be employed to simulate stream bed changes during a given flow, thereby providing the necessary information for the design of dikes, levees, or other bank protection. This model incorporates the major effects of transverse circulation, inherent in curved channels, on the flow and sediment processes. In the simulation of the evolution in stream bed profile, the effect of transverse flow is tied in with the aggradation and degradation development. River flow through curved channels is characterized by the changing curvature, to which variations of flow pattern and bed topography are closely related. Simulation of these changing features is based upon the fluid dynamics governing the growth and decay of transverse circulation along the channel.

INTRODUCTION

An important factor that affects the hydraulics of flow, sediment transport, and bed topography through curved alluvial channels is the spiral motion or transverse circulation. Greater depths and higher velocities near concave banks produced by the transverse circulation, in addition to aggradation and degradation, are necessary considerations for levee or dike design. The importance of transverse circulation was stressed in a recent evaluation of mobile bed mathematical models by the National Academy of Sciences (3). In this connection, research effort toward improved incorporation of the effect of transverse flow in modeling was recommended.

A mathematical model for water and sediment routing through curved alluvial channels is described herein. This model simulates time and spatial variations in water level, sediment transport, and bed topography. In the prediction of stream bed profile changes, aggradation and degradation are tied in with the effect of transverse flow under the changing channel curvature. Application of this model is limited to alluvial channels with nonerodible banks, large width-depth ratio, and mild curvature, all characteristic of natural rivers with bank protection. A case study using this model on the San Lorenzo River in California during a flood event is presented.

Analyses of flow and bed topography in curved channels have been accomplished by Yen (26), Engelund (13), Kikkawa et al. (19), Zimmermann and Kennedy (28), Falcon Ascanio and Kennedy (14), and Odgaard (20), among others. Some of these analytical methods are used in the model. However, such methods are generally for curved channels with fully developed transverse flow. Because of the streamwise (lon-

¹Prof. of Civ. Engrg., San Diego State Univ., San Diego, Calif. 92182.

Note.—Discussion open until September 1, 1985. To extend the closing date one month, a written request must be filed with the ASCE Manager of Journals. The manuscript for this paper was submitted for review and possible publication on November 30, 1983. This paper is part of the *Journal of Hydraulic Engineering*, Vol. 111, No. 4, April, 1985. ©ASCE, ISSN 0733-9429/85/0004-0644/\$01.00. Paper No. 19656.

gitudinal) changing curvature, the developed transverse flow generally occurs over short channel lengths. In addition, the transverse flow lags behind the channel curvature pattern. It is clear that this changing curvature and phase lag have important effects on the flow and sediment processes as pointed out by numerous researchers, e.g., Rozovskii (22), Yen and Yen (27), Hooke (16), Bridge and Jarvis (6), Parker et al. (21), and Dietrich and Smith (11). The changing curvature of flow is quantified herein using a recently developed relationship for the growth and decay of transverse flow (10).

ANALYTICAL DEVELOPMENT

The mathematical model, FLUVIAL-12, which utilizes analytical equations governing the flow and sediment processes, has the following four major interactive components: (1) Water routing; (2) evaluation of changing flow curvature; (3) computation of sediment transport and sorting; and (4) prediction of stream bed profile changes. It represents an extension of the existing model FLUVIAL-14 (8) by incorporating the effect of transverse flow on each of these components. Features common to these models are therefore only briefly described.

The model employs a space-time domain in which the space domain is represented by discrete cross sections, and the time domain is represented by discrete time steps. Temporal and spatial variations in flow, sediment transport, and stream bed profile are computed following an iterative procedure. Water routing, which is coupled with the changing curvature, is assumed to be uncoupled from the sediment processes. These four components of the model are described as follows.

Water Routing.—For an inflow hydrograph, water routing provides temporal and spatial variations of the stage, discharge, energy gradient, and other hydraulic parameters in the channel. The water routing component has the following two major features: (1) Numerical solution of the continuity and momentum equation for longitudinal flow; and (2) evaluation of flow resistance due to longitudinal and transverse flows. The continuity and momentum equations are

$$\frac{\partial A}{\partial t} + \frac{\partial Q}{\partial s} - q = 0 \dots\dots\dots (1)$$

$$\frac{1}{A} \frac{\partial Q}{\partial t} + g \frac{\partial H}{\partial s} + \frac{1}{A} \frac{\partial}{\partial s} \left(\frac{Q^2}{A} \right) + gS - \frac{Q}{A^2} q = 0 \dots\dots\dots (2)$$

in which A = cross-sectional area of flow; t = time; Q = water discharge; s = curvilinear coordinate along channel center line measured from the upstream entrance; q = lateral inflow rate per unit length; g = gravitational acceleration; H = stage or water surface elevation; and S = energy gradient. Techniques for numerical solution of Eqs. 1 and 2 have been developed by other researchers. This model employs the solution techniques and accuracy criteria developed by Fread (15) and by Amein and Chu (2).

In a curved channel, the total energy gradient, S , in Eq. 2 can be partitioned into the longitudinal energy gradient, S' , and the transverse energy gradient, S'' , i.e.

$$S = S' + S'' \dots \dots \dots (3)$$

The longitudinal energy gradient can be evaluated using any valid flow resistance relationship. This model employs the Manning formula for flow resistance. The transverse energy gradient is evaluated using the following equation for wide channels (9)

$$S'' = \left(\frac{2.86\sqrt{f} + 2.07f}{0.565 + \sqrt{f}} \right) \left(\frac{h_c}{r_c} \right)^2 F^2 \dots \dots \dots (4)$$

in which f = Darcy-Weisbach friction factor; h_c = flow depth at channel center line; r_c = mean channel radius; and F = Froude number.

Evaluation of Changing Flow Curvature.—Analytical relationships pertaining to curved channels are often based upon the mean channel radius, r_c . Because of the streamwise changing curvature, application of such relationships is limited to the fully developed transverse flow for which the curvature is defined. Streamwise variation of transverse flow, over much of the channel length, is characterized by its growth and decay. In order to describe this variation, the mean flow curvature defined as the flow curvature along channel center line is employed. It is assumed that analytical relationships for developed transverse flows are applicable for developing transverse flows when the mean channel curvature, r_c , is replaced by the mean flow curvature, r_f . Upon entering a bend, the mean flow curvature increases with the growth in transverse circulation. In a bend, the transverse flow becomes fully developed if the flow curvature approaches the channel curvature. In the case of exiting from a bend to the downstream tangent in which the channel curvature is zero, the flow curvature decreases with the decay of transverse circulation.

The reason that the flow curvature lags behind the channel curvature during circulation growth and decay is attributed to the internal turbulent shear that the flow has to overcome in transforming from parallel flow into the spiral pattern and vice versa (22). From the dynamic equation for the transverse velocity, the writer (10) has developed an equation governing the spatial variation in transverse surface velocity, v , along channel center line. Details of this development are given in Appendix I. In finite difference form, the change in v over the distance Δs is given by

$$v_{i+1} = \left[v_i + \sqrt{\frac{\bar{f}}{2}} \left(\frac{10}{3} - \frac{15}{\kappa 9} \sqrt{\frac{\bar{f}}{2}} \right) \frac{\bar{U}}{\bar{r}_c} \exp \left(\bar{F} \frac{\kappa}{h_c} \sqrt{\frac{\bar{f}}{2}} \Delta s \right) \Delta s \right] \exp \left(-\bar{F} \frac{\kappa}{h_c} \sqrt{\frac{\bar{f}}{2}} \Delta s \right) \dots \dots \dots (5)$$

in which v = transverse surface velocity along channel center line; κ = Karman's constant, which has the approximate value of 0.4; U = average velocity of a cross section; $i, i + 1$ = s -coordinate indices; F = a function of f and κ ; and the overbar denotes averaging over the distance between i and $i + 1$. Eq. 5 provides the spatial variation in v , from which the

mean flow curvature may be obtained using the transverse velocity profile. Similar transverse velocity profiles have been established by different researchers (19,22,25). From the velocity profile developed by Kikkawa et al. (19), the mean flow curvature, r_f , is related to the transverse surface velocity and other parameters, i.e.

$$r_f = \frac{h_c U}{\kappa v} \left(\frac{10}{3} - \frac{15}{\kappa 9} \sqrt{\frac{f}{2}} \right) \dots \dots \dots (6)$$

At each time step, the mean flow curvature at each cross section is obtained using Eqs. 5 and 6. Accuracy of computation for the finite difference equation (Eq. 5) is maintained if the step size $\Delta s \leq 2h_c$ (10). Following this criterion, the distance between two adjacent cross sections is divided into smaller increments if necessary. Flow parameters for these increments are interpolated from values known at adjacent cross sections.

Computation of Sediment Transport and Sorting.—Sediment transport, in the presence of transverse flow, can be considered as consisting of the longitudinal and transverse components. The longitudinal sediment load is computed using a shear-stress type formula, because of the transverse variation in stream bed configuration. For this purpose, the Engelund-Hanson formula (12) is included in the model, but it may be replaced by any other valid formula. The relation for the transverse variation in shear stress developed by Kikkawa et al. (19) has the form

$$\tau_o = \rho g n^2 h^{-1/3} \bar{u}^2 \dots \dots \dots (7)$$

in which τ_o = local longitudinal shear stress; ρ = density of fluid; n = Manning's coefficient; h = local depth; and \bar{u} = depth-averaged longitudinal velocity.

Other investigators have developed analytical relationships for the equilibrium transverse bed profile in alluvial channel bends (6,13,14,19,20,28). In an unsteady flow, the transverse bed profile varies with time, and it is constantly adjusted toward the equilibrium state through scour and deposition. Sediment movement in the transverse direction contributes to the adjustment of transverse bed profile. The transverse bed load can be related to the longitudinal bed load by the direction of near-bed sediment movement (17,19,21). Such a relationship developed by Kikkawa et al. (19), which is employed in the model, can be written in parametric form as

$$\tan \delta = \phi \left(\frac{v_b}{u_b} \right) - \psi \left(\frac{1}{\tau_*} \right) \frac{\partial z}{\partial r} \dots \dots \dots (8)$$

in which δ = angle of deviation of sediment particle path from the longitudinal (tangential) direction; ϕ , ψ = functions; v_b = near-bed transverse velocity; u_b = near-bed longitudinal velocity, τ_* = dimensionless shear stress acting on bed = $u_*^2 / (\rho_s - \rho)gd$; u_* = shear velocity; d = diameter of sediment, ρ_s = mass density of sediment; and z = local bed elevation. The near-bed transverse velocity, v_b , is a function of the curvature (19,22,25); it is computed using the mean flow curvature.

Eq. 8 relates the direction of bed load movement to the direction of near-bed velocity and transverse bed slope $\partial z/\partial r$. As transverse velocity starts to move sediment away from the concave bank, it creates a transverse bed slope that counters the transverse sediment movement. An equilibrium is reached when the effects of these counteractive factors are in balance. Under this situation, the angle of deviation becomes zero. In this model, transverse bed profile evolution is related to the transverse variation in bed material load. Since bed material load, excluding wash load, is usually concentrated near the bed, it is assumed to follow the direction given by Eq. 8, i.e.

$$q'_s = q_s \tan \delta \dots\dots\dots (9)$$

in which q'_s = transverse bed material load per unit channel length; and q_s = longitudinal bed material load per unit channel width.

Unsteady sediment transport is complicated by sediment sorting. Methods for estimating sediment rate by tracking variation in bed material composition and stream bed profile evolution have been developed by Bennett and Nordin (4), Alonso et al. (1), and Borah et al. (5), among others. To treat this time-dependent sediment transport, bed materials are divided into five size fractions, and the size for each fraction is represented by its geometric mean diameter. For each size fraction, sediment transport capacity is first computed using a sediment transport formula. Then the actual sediment rate is obtained by considering sediment material of all size fractions already in the flow and the exchange of sediment load with the bed using the method by Borah et al. (5). If the stream carries a load in excess of its capacity, it will deposit the excess material on the bed. In the case of erosion, any size fraction available for entrainment at the bed surface will be removed by the flow and added to the sediment already in transport. During sediment removal, the exchange between the flow and the bed is assumed to take place in the active layer at the surface. Thickness of the active layer is based upon the relation defined by Borah et al. (5). As a function of the material size and composition, this thickness also reflects the flow condition. During degradation, several of these layers may be scoured away, resulting in the coarsening of the bed material and formation of a armor coat. However, new active layers may be deposited on the bed in the process of aggradation. These procedures for computing sediment rate and sediment sorting are applied to the longitudinal and transverse direction. They are also coupled with stream bed profile changes described in the next section.

Prediction of Stream Bed Profile Changes.—Changes in stream bed profile, at each time step, due to longitudinal and transverse variations in sediment load are simulated. Changes along the longitudinal direction, i.e., aggradation or degradation, are computed using the continuity equation for sediment movement in the longitudinal direction. This is explained in Ref. 7.

Changes in channel bed elevation at a point due to transverse load are computed using the continuity equation

$$\frac{\partial z}{\partial t} + \frac{1}{1 - \lambda} \frac{1}{r} \frac{\partial}{\partial r} (rq'_s) = 0 \dots\dots\dots (10)$$

in which λ = porosity. Written in finite difference form with a forward difference for q'_s (7), Eq. 10 becomes

$$\Delta z_j = \frac{\Delta t}{1 - \lambda} \frac{2}{r_j + r_{j+1}} \frac{r_{j+1}q'_{s_{j+1}} - r_jq'_{s_j}}{r_{j+1} - r_j} \dots\dots\dots (11)$$

in which j = radial (transverse) coordinate index. Eq. 11 provides the changes in channel bed elevation for a time step, Δt , due to transverse sediment movement. These transverse changes, as well as the longitudinal changes, are applied to the stream bed at each time step. Stream bed profile evolution is simulated by repeated iteration along successive time steps.

SAN LORENZO RIVER STUDY

The FLUVIAL-12 model described herein was tested by simulating flow and bed profile changes in the San Lorenzo River (see Figs. 1 and 2), which drains into the Santa Cruz Harbor on the Pacific coast through the City of Santa Cruz, California. A field study, sponsored by the San Francisco District of the U.S. Army Corps of Engineers, was made during the February 1980 flood for the purpose of analyzing river bed scour-fill processes during the flood (23). This river reach, which has several channel bends near the mouth, is protected by riprap on its bank slopes.

The lower two-mile reach of the San Lorenzo River was simulated using the mathematical model for the February 1980 flood. Hydrographs for this flood event and tidal variation at the harbor used in the simulation are shown in Fig. 3. The 90-hr flood duration was computed using 800 time steps. Initial bed materials in the river varied from very coarse sand (median diameter = 1.05 mm) at the upstream end to coarse sand (median diameter = 0.64 mm) at the mouth. Sediment load consisted primarily of bed load during the flow period.

Selected results obtained from this simulation are shown in Figs. 4-6 for the curved reach where significant river bed changes are predicted. These results are compared with measurements made at the gaging stations (G2-G6 in Fig. 1) on February 19, 1980, around the time of 78.5 hr on the hydrograph. Simulated water surface profiles at the time of the peak flood and at the time of measurement (time = 78.5 hr) are shown in Fig. 4(b) with the simulated profile of minimum river bed elevation at the time of measurement. These results compare favorably with measurements. The simulated river bed profile is closely related to the streamwise variation in the mean flow curvature shown in Fig. 4(c), characterized by an increase in curvature as the flow enters a bend and a decrease in curvature after leaving the bend exit. Upon entering a bend, the rate of increase in flow curvature is more rapid initially and then it slows down gradually. In a long bend, the flow curvature will approach the channel curvature, and thus, the transverse circulation becomes fully developed. Such a condition is predicted at Sections 10, 11, 19 and 22. The transverse flow, as predicted, is not fully developed in other shorter bends where the flow curvature remains less than the channel curvature. Upon leaving a bend, the flow curvature decreases following an exponential decay curve, and it persists for a considerable distance downstream, consistent with the experimental findings by Ippen and

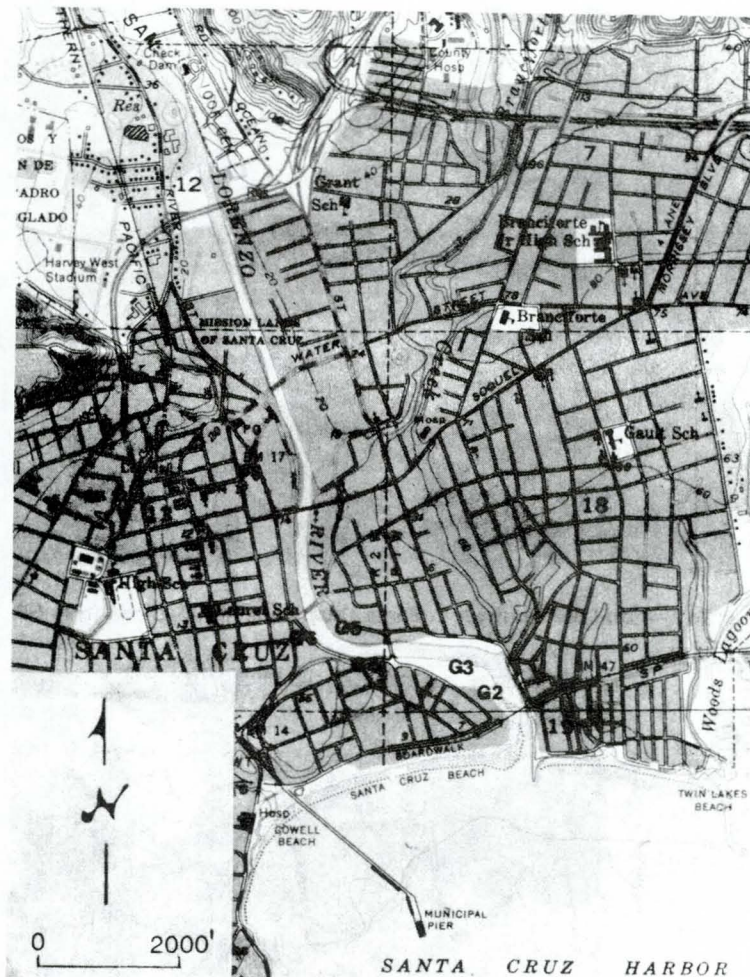


FIG. 1.—San Lorenzo River in Santa Cruz, California with Gaging Stations G2-G6

Drinker (18) and by Yen (24) on the decay of transverse circulation. Simulated results shown in Fig. 4 indicate that river bed scour is related to the flow curvature with the maximum scour occurring at the bend exit. These results are consistent with previous experimental findings by Rozovskii (22) and Yen (26). Simulated cross-sectional profiles at the five gaging stations are compared with measurements as shown in Fig. 5, which indicates that the maximum scour depth is attributed to the development of transverse bed profile. Simulated river bed topography through a bend is illustrated by the results from Sec. 9–Sec. 14 shown in Fig. 6. It shows increasing transverse bed slope and scour near the concave bank in the downstream direction consistent with the

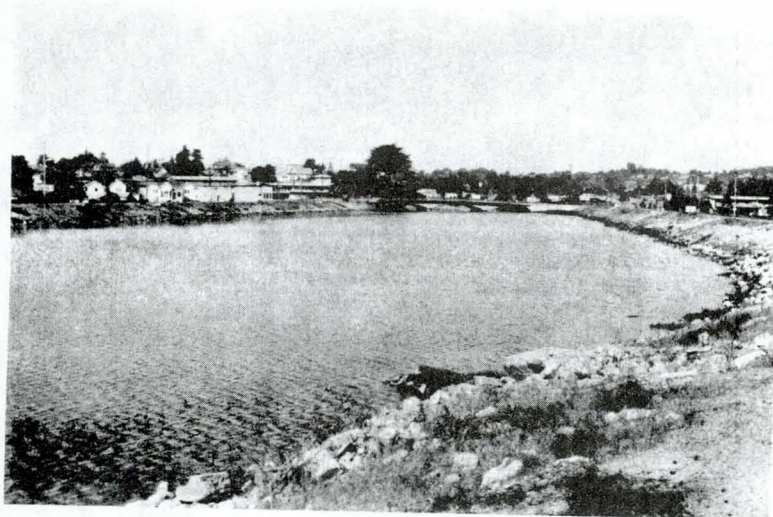


FIG. 2.—San Lorenzo River in Santa Cruz: Looking Upstream from G2

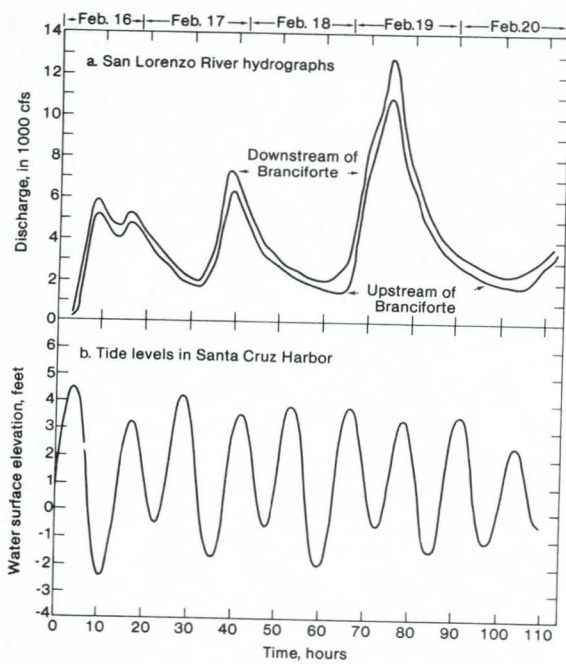


FIG. 3.—Hydrographs and Tidal Variation During the 1980 Flood

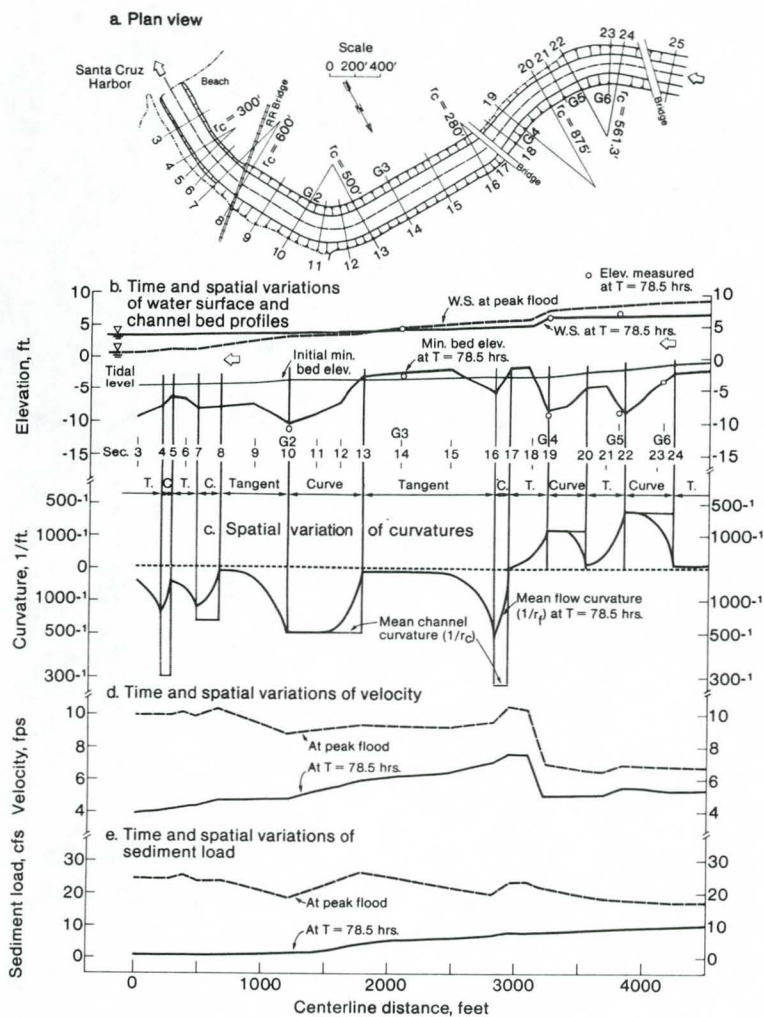


FIG. 4.—Simulated Results and Measured Elevations for Curved Reach of San Lorenzo River in Santa Cruz

growth in flow curvature. Maximum scour is reached at the bend exit, followed by a gradual decrease in transverse bed slope and scour depth with the decrease in flow curvature.

While the scour depth is found to be generally in direct relation to the flow curvature, river bed evolution is also affected by aggradation and degradation which result from the longitudinal imbalance in sediment load. For example, spatial variation in sediment load at the peak discharge shown in Fig. 4(e) has an increasing trend in the downstream direction associated with a low tide in the harbor. This indicates a general trend of river bed degradation at this point in time, as more sediment is removed from the reach than the amount supplied. At the time

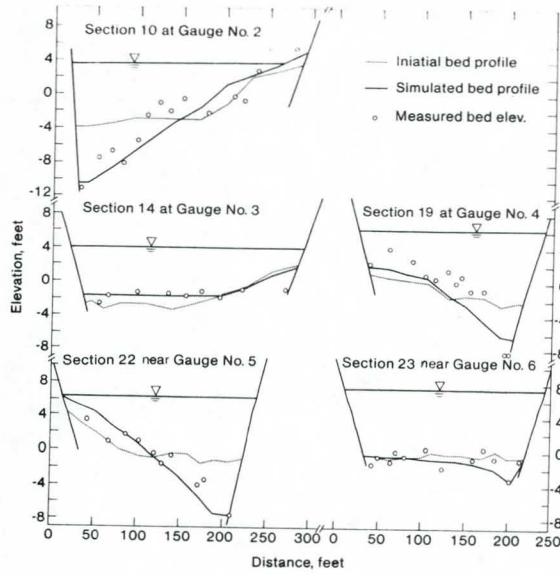


FIG. 5.—Simulated and Measured Bed Profiles at 78.5 hr

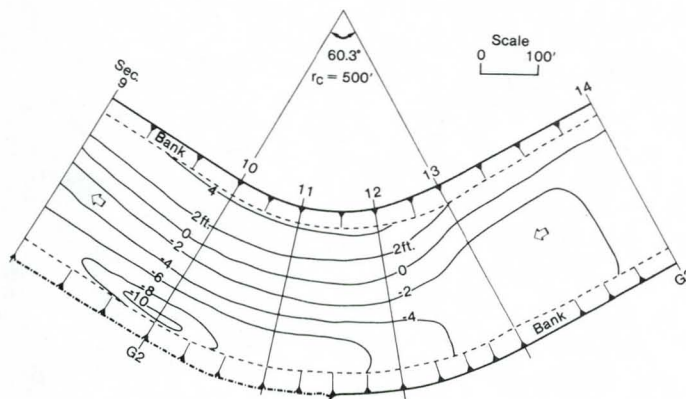


FIG. 6.—Simulated Bed Topography through River Bend at 78.5 hr

of 78.5 hr, on the other hand, the sediment load has a decreasing trend in the downstream direction associated with a high tide. River bed aggradation is predicted at this time as some sediment is stored in the reach. In view of these fluvial processes, modeling of river bed changes induced by transverse circulation also must be tied in with aggradation and degradation.

SUMMARY AND CONCLUSIONS

A mathematical model for water and sediment routing through curved alluvial channels is formulated, developed and tested with field data.

This model, which is applicable to alluvial streams with nonerodible banks, may be employed to simulate stream bed changes during a specified flow, thereby providing the necessary information for the design of dikes, levees, or other bank protection.

The model incorporates the major effects of transverse flow, inherent in curved channels, on the flow and sediment processes. In the simulation of stream bed profile evolution, the effect of transverse flow is tied in with aggradation and degradation.

River flow through curved channels is characterized by the changing curvature, to which variations of flow pattern and bed topography are closely related. These changing features are quantified using a relationship governing the growth and decay of transverse flow along the channel. This relationship also provides the phase shift between transverse flow development and the channel curvature pattern. In a bend, bed topography simulated by the model is characterized by a transverse bed slope with greater depth near the concave bank. The maximum depth is found to occur near the bend exit and relatively large depths persist for a considerable distance in the downstream direction. These analytical results are consistent with previous experimental findings.

ACKNOWLEDGMENT

The San Lorenzo River was selected by the Committee on Hydrodynamic models, National Research Council, National Academy of Sciences as a test case for the evaluation of computer-based flood and sediment routing models. The Committee was chaired by Dr. John F. Kennedy and assisted by Dr. T. Nakato.

APPENDIX I.—STREAMWISE VARIATION IN TRANSVERSE VELOCITY

The dynamic equation for transverse velocity has the form (22,24)

$$\bar{u} \frac{\partial \bar{v}}{\partial s} + \bar{v} \frac{\partial \bar{v}}{\partial r} + \bar{w} \frac{\partial \bar{v}}{\partial z} = \frac{\bar{u}^2}{r} - gS_r + \frac{\partial}{\partial z} \left(\epsilon \frac{\partial \bar{v}}{\partial z} \right) \dots \dots \dots (12)$$

in which \bar{u} = longitudinal velocity component; \bar{v} = transverse velocity component; \bar{w} = vertical velocity component; r = radius of curvature; z = vertical coordinate; S_r = transverse water surface slope; and ϵ = eddy viscosity. Since velocity components \bar{v} and \bar{w} are small in comparison to \bar{u} , the terms $\bar{v} \partial \bar{v} / \partial r$ and $\bar{w} \partial \bar{v} / \partial z$ are of the second order and are therefore neglected. The simplified equation relates the spatial variation in transverse velocity, $\partial \bar{v} / \partial s$, to the centrifugal acceleration, transverse water surface slope, and transverse turbulent shear. This equation will be evaluated along channel center line at the water surface. Since wall effects are not considered in this equation, it is limited to channels with a width depth ratio greater than about 5 (Ref. 22, p. 73).

By assuming that, in the process of circulation growth or decay, transverse velocity profiles remain similar, Rozovskii (22) has shown that the term for transverse turbulent shear in Eq. 12 evaluated at water surface can be approximated as a function of channel roughness, i.e.

$$\frac{\partial}{\partial z} \left(\epsilon \frac{\partial \bar{v}}{\partial z} \right) = -\kappa F(f, \kappa) \sqrt{\frac{f}{2}} \frac{uv}{h_c} \dots \dots \dots (13)$$

in which κ = Karman's constant, which has the approximate value of 0.4; F = a function of f and κ ; u = longitudinal surface velocity along channel center line; and v = transverse surface velocity along channel center line. After substituting Eq. 13 into Eq. 12, the following equation is obtained:

$$\frac{dv}{ds} = \frac{u}{r_c} - \frac{gS_r}{u} - \kappa F \sqrt{\frac{f}{2}} \frac{v}{h_c} \dots \dots \dots (14)$$

The longitudinal surface velocity u in this equation can be related to the mean velocity, U , as

$$\frac{u}{U} = \Phi(f) \dots \dots \dots (15)$$

in which Φ = a function of the friction factor, f (28). The transverse water surface slope is closely approximated by the following relationship (18,22,24)

$$S_r = \frac{U^2}{gr_c} \dots \dots \dots (16)$$

After substituting Eqs. 15 and 16 into Eq. 14 and rearranging terms, the following equation is obtained:

$$\frac{dv}{ds} + F \frac{\kappa}{h_c} \sqrt{\frac{f}{2}} v = \left(\Phi - \frac{1}{\Phi} \right) \frac{U}{r_c} \dots \dots \dots (17)$$

The parameter $\Phi - 1/\Phi$ is evaluated using the boundary condition of developed transverse flow as described below. Similar profiles for developed transverse flow have been established by various investigators (19,22,25). From the velocity profile developed by Kikkawa et al. (19), the following equation for transverse surface velocity is obtained

$$\frac{v}{U} = \frac{1}{\kappa} \frac{h_c}{r_c} \left(\frac{10}{3} - \frac{15}{\kappa 9} \sqrt{\frac{f}{2}} \right) \dots \dots \dots (18)$$

From this equation and Eq. 17 with $dv/ds = 0$ for developed transverse flow, the parameter $\Phi - 1/\Phi$ is evaluated. After substitution of $\Phi - 1/\Phi$, Eq. 17 becomes

$$\frac{dv}{ds} + F \frac{\kappa}{h_c} \sqrt{\frac{f}{2}} v = \sqrt{\frac{f}{2}} \left(\frac{10}{3} - \frac{15}{\kappa 9} \sqrt{\frac{f}{2}} \right) \frac{U}{r_c} \dots \dots \dots (19)$$

This equation, in which v = the dependent variable and the coefficients are functions of the independent variable, s , alone, is a linear differential equation of the first order. The general solution, which can be found in a standard text, has the form

$$v = \left[c + \int \sqrt{\frac{f}{2}} \left(\frac{10}{3} - \frac{15}{\kappa 9} \sqrt{\frac{f}{2}} \right) \frac{U}{r_c} \exp \left(\int F \frac{\kappa}{h_c} \sqrt{\frac{f}{2}} ds \right) ds \right] \exp \left(- \int F \frac{\kappa}{h_c} \sqrt{\frac{f}{2}} ds \right) \dots \dots \dots (20)$$

in which c = a constant. From the boundary condition at the initial upstream point where v = the initial transverse velocity, v_i , the value of c is obtained, i.e.

$$c = v_i \dots \dots \dots (21)$$

Eq. 20 provides the spatial variation of transverse velocity along channel center line.

APPENDIX II.—REFERENCES

1. Alonso, C. V., Borah, D. K., and Prasad, S. N., "Numerical Model for Routing Graded Sediments in Alluvial Channels," Appendix J, *Final Report to the U.S. Army Corps of Engineers*, Vicksburg District, U.S. Department of Agriculture Sedimentation Laboratory, Oxford, Miss., Apr., 1981.
2. Amein, M., and Chu, H. L., "Implicit Numerical Modeling for Unsteady Flows," *Journal of the Hydraulics Division*, ASCE, Vol. 101, No. HY6, June, 1975, pp. 717-732.
3. *An Evaluation of Flood-Level Prediction Using Alluvial River Models*, Committee on Hydrodynamic Computer Models for Flood Insurance Studies, Advisory Board on the Built Environment, National Research Council, National Academy Press, Washington, D.C., 1983.
4. Bennett, J. S., and Nordin, C. F., "Simulation of Sediment Transport and Armouring," *Hydrological Sciences Bulletin*, XXII, 4, Dec., 1977, pp. 555-569.
5. Borah, D. K., Alonso, C. V., and Prasad, S. N., "Routing Graded Sediments in Streams: Formulations," *Journal of the Hydraulics Division*, ASCE, Vol. 108, No. HY12, Dec., 1982, pp. 1486-1503.
6. Bridge, J. S., and Jarvis, J., "Velocity Profiles and Bed Shear Stress over Various Bed Configurations in a River Bend," *Earth Surface Processes*, Vol. 2, 1977, pp. 281-294.
7. Chang, H. H., and Hill, J. C., "Computer Modeling of Erodible Flood Channels and Deltas," *Journal of the Hydraulics Division*, ASCE, Vol. 102, No. HY10, Oct., 1976, pp. 1461-77.
8. Chang, H. H., "Mathematical Model for Erodible Channels," *Journal of the Hydraulics Division*, ASCE, Vol. 108, No. HY5, Proc. Paper 17062, May, 1982, pp. 678-689.
9. Chang, H. H., "Energy Expenditure in Curved Open Channels," *Journal of Hydraulic Engineering*, ASCE, Vol. 109, No. 7, July, 1983, pp. 1012-1022.
10. Chang, H. H., "Variation of Flow Resistance Through Curved Channels," *Journal of Hydraulic Engineering*, ASCE, Vol. 110, No. 12, Dec., 1984, pp. 1772-1782.
11. Dietrich, W. E., and Smith, J. D., "Influence of Point Bar on Flow Through Curved Channels," *Water Resources Research*, Vol. 19, No. 5, Oct., 1983, pp. 1173-1192.
12. Engelund, F., and Hansen, E., "A Monograph on Sediment Transport in Alluvial Streams," *Teknisk Forlag*, Copenhagen, Denmark, 1967.
13. Engelund, F., "Flow and Bed Topography in Channel Bends," *Journal of the Hydraulics Division*, ASCE, Vol. 100, No. HY11, Nov., 1974, pp. 1631-1648.
14. Falcon Ascanio, M., and Kennedy, J. F., "Flow in Alluvial River Curves," *Journal of Fluid Mechanics*, Vol. 133, 1983, pp. 1-16.

15. Fread, D. L., "Numerical Properties of Implicit Four-Point Finite Difference Equations of Unsteady Flow," National Weather Services, NOAA, *Technical Memorandum NWS Hydro-18*, Mar., 1974.
16. Hooke, R. LeB., "Distribution of Sediment and Shear Stress in a Meander Bend," *Journal of Geology*, Vol. 83, 1975, pp. 543-567.
17. Ikeda, S., "Lateral Bed Load Transport on Side Slopes," *Journal of the Hydraulics Division*, ASCE, Vol. 108, No. HY11, Nov., 1982, pp. 1369-1373.
18. Ippen, A. T., and Drinker, P. A., "Boundary Shear Stresses in Curved Trapezoidal Channels," *Journal of the Hydraulics Division*, ASCE, Vol. 88, No. HY5, Sept., 1962, pp. 143-179.
19. Kikkawa, H., Ikeda, S., and Kitagawa, A., "Flow and Bed Topography in Curved Open Channels," *Journal of the Hydraulics Division*, ASCE, Vol. 102, No. HY9, Sept., 1976, pp. 1327-1342.
20. Odgaard, A. J., "Bed Characteristics in Alluvial Channel Bends," *Journal of the Hydraulics Division*, ASCE, Vol. 108, No. HY11, Nov., 1982, pp. 1268-1281.
21. Parker, G., Sawai, K., and Ikeda, S., "Bend Theory of River Meanders. Part 2. Nonlinear Deformation of Finite Amplitude Bends," *Journal of Fluid Mechanics*, Vol. 112, 1981.
22. Rozovskii, I. L., "Flow of Water in Bends of Open Channels," Israel Program for Scientific Translations, Jerusalem, Israel, 1961 (available from Office of Technical Services, U.S. Department of Commerce, Washington, D.C., *PST Catalog No. 363*, OTS 60-51133).
23. *San Lorenzo River, Field and Simulation Studies*, prepared for Department of the Army, San Francisco District, Corps of Engineers, San Francisco, California, prepared by Jones-Tillson and Associates, Water Resources Engineers, and H. Esmaili and Associates, Sept., 1980.
24. Yen, B. C., *Characteristics of Subcritical Flow in a Meandering Channel*, Institute of Hydraulic Research, the University of Iowa, Iowa City, Iowa, 1965, 155 pp.
25. Yen, B. C., "Spiral Motion of Developed Flow in Wide Curved Open Channels," Chapter 22, *Sedimentation (Einstein)*, H. W. Shen, ed., P.O. Box 606, Ft. Collins, Colo., 1972.
26. Yen, C. L., "Bed Topography Effect on Flow in a Meander," *Journal of the Hydraulics Division*, ASCE, Vol. 96, No. HY1, Jan., 1970, pp. 57-73.
27. Yen, C. L., and Yen, B. C., "Water Surface Configuration in Channel Bends," *Journal of the Hydraulics Division*, ASCE, Vol. 97, No. HY2, Feb., 1971, pp. 303-321.
28. Zimmermann, C., and Kennedy, J. F., "Transverse Bed Slopes in Curved Alluvial Streams," *Journal of the Hydraulics Division*, ASCE, Vol. 104, No. HY1, Proc. Paper 13482, Jan., 1978, pp. 33-48.

APPENDIX III.—NOTATION

The following symbols are used in this paper:

- A = cross-sectional area of flow;
- c = constant;
- d = sediment diameter;
- F = function;
- F = Froude number;
- f = Darcy-Weisbach friction factor;
- g = gravitational acceleration;
- H = stage or water-surface elevation;
- h = flow depth;
- h_c = flow depth at channel center line;

n = Manning's coefficient;
 Q = discharge;
 q = lateral inflow discharge per unit channel length;
 q_s = longitudinal bed material load per unit channel width;
 q'_s = transverse bed material load per unit channel length;
 r = radius of curvature or radial coordinate;
 r_c = mean channel radius;
 r_f = mean flow radius;
 S = total energy gradient = $S' + S''$;
 S' = longitudinal energy gradient;
 S'' = transverse energy gradient;
 S_r = transverse water surface slope;
 s = curvilinear coordinate;
 t = time;
 U = mean flow velocity;
 u = longitudinal surface velocity along channel center line;
 \bar{u} = longitudinal velocity component;
 \bar{u} = depth-averaged longitudinal velocity;
 u_b = near-bed longitudinal velocity;
 u_* = shear velocity;
 v = transverse surface velocity along channel center line;
 \bar{v} = transverse velocity component;
 v_b = near-bed transverse velocity;
 v_i = initial transverse velocity;
 \bar{w} = vertical velocity component;
 z = vertical coordinate or channel bed elevation;
 δ = angle of deviation of sediment particle path from the longitudinal direction;
 ϵ = eddy viscosity;
 κ = Karman's constant;
 λ = porosity;
 ρ = mass density of fluid;
 ρ_s = mass density of sediment;
 τ_o = local longitudinal shear stress;
 τ_* = dimensionless shear stress; and
 ϕ, ψ = functions.

Subscripts

i = s -coordinate index; and
 j = r -coordinate index.

COMPUTER-BASED DESIGN OF RIVER BANK PROTECTION

By Howard H. Chang¹, Zbig Osmolski², and David Smutzer³

ABSTRACT

A study using the FLUVIAL-11 computer model was made for the Rillito River in order to determine the design configuration for the bank protection which must contain the design flood and extend below the potential channel-bed scour. The computer model simulates sediment transport and associated river channel changes which, in a curved reach, is also affected by the spiral motion or secondary currents. Because of the streamwise variation in spiral motion, uneven bed topography is usually produced, characterized by a lower bed elevation near the concave bank. Such non-uniformity in bed topography is more pronounced at high flow when the spiral motion is stronger; it becomes partially eliminated during the subsequent low flow. This explains why an observer of the post-flood channel may fail to recognize the uneven bed scour under the muddy water at high flow. The bank protection for the Rillito River was designed based upon the simulated pattern of channel-bed scour. Variable toe elevations for the banks were used to provide an effective protection.

INTRODUCTION

Natural rivers through urban regions usually need to be stabilized in order to prevent channel migration. A common, economical practice in Arizona and elsewhere in the west is to protect channel banks while maintaining an alluvial channel bed. The soil cement bank protection is popular because it is economical and it preserves the natural soil appearance.

The Rillito River flows through the City of Tucson as shown in Fig. 1; it has a total drainage area of 935 square miles at the confluence with the Santa Cruz River. The Rillito River underwent significant changes during the October, 1983 flood, which reached 100-year magnitude at certain places in Pima County. River channel changes near the Dodge Boulevard bridge are shown in the aerial photo in Fig. 2 taken right after the flood. Lateral migration and channel

¹ Professor of Civil Engineering, San Diego State University, San Diego, California.

² Manager, Flood Control Design Section, Dept. of Transportation and Flood Control District, Pima County, Arizona.

³ Manager, Flood Control Section, Dept. of Transportation and Flood Control District, Pima County, Arizona.

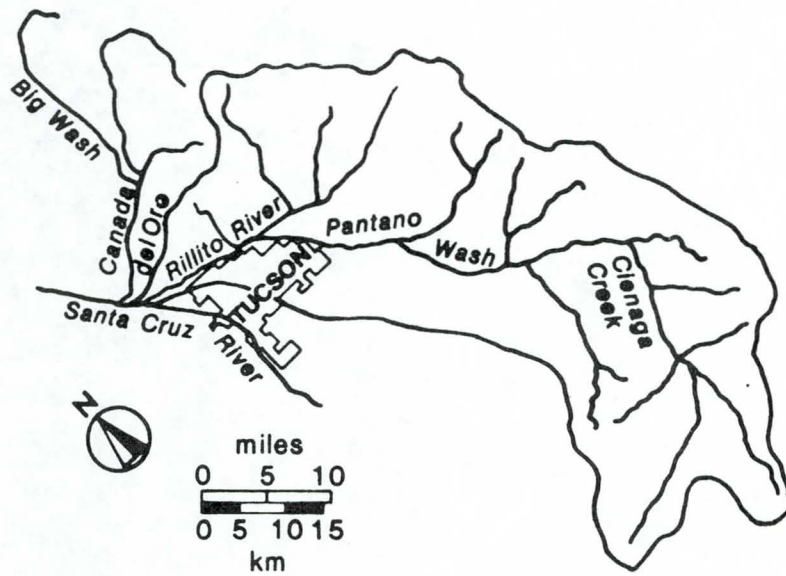


Fig. 1.- Location and Drainage Basin of the Rillito River

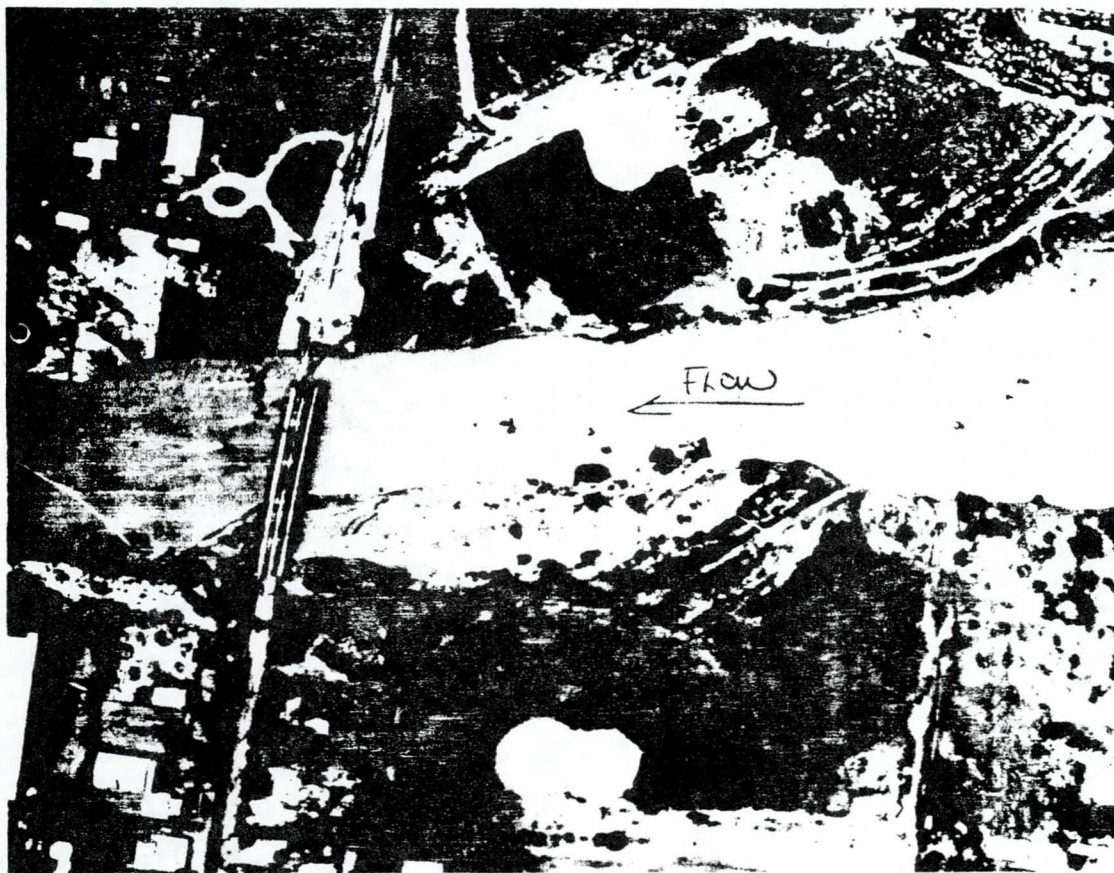


Fig. 2.- Damages Caused by Oct., 1983 Flood near Dodge Boulevard

widening resulted in the failure of one bridge abutment and endangered other adjacent properties. The river reach for which bank protections were considered started from the La Cholla bridge at 2.75 miles upstream of the confluence to the Craycroft bridge at 11.94 miles upstream. A study was made to determine the appropriate designs for channel geometry, slope, and bank protection for this river reach. Certain portions of the river channel already had soil cement bank protection, either along one bank or along both banks. These existing structures would be utilized as much as feasible. Because of the alluvial channel bed, the potential scour and fill (or long-term degradation and aggradation) needed to be considered. Such information was also essential for the design of bank protection which must contain the design flood and extend below the potential scour.

MATHEMATICAL MODEL FOR CHANNEL DESIGN

While the alluvial bed is subject to scour and fill that are induced by the imbalance in longitudinal (streamwise) sediment discharge, such channel-bed development may also be caused by transverse sediment movement due to channel curvature. Despite the bank protection, the channel still has certain freedom in width adjustment within the constraints; particularly, the width between rigid banks varies at different locations. Therefore, scour and fill due to longitudinal sediment imbalance and curvature effects as well as width changes need to be considered in the simulation study. The latest version of FLUVIAL-11 for water and sediment routing through curved channels contains the necessary features for river channel changes during a flood(1). Briefly, this model, for a given flood hydrograph, simulates time and spatial variations in flood level, sediment transport and bed topography. In the prediction of river channel changes, scour and fill are tied in with width variation and the effect of secondary currents under the changing channel curvature. In the model, scour and fill are computed on the basis of longitudinal imbalance in sediment discharge. Through a curved reach, the effects of secondary currents consist of moving sediment away from the concave bank until the transverse bed slope balances such sediment movement. At the same time, the variation in channel width is simulated such that the flow moves in the direction of equal power expenditure, i.e. equal energy gradient, subject to the physical constraint of rigid banks. If the energy gradient is approximated by the water-surface slope, then equal energy gradient is equivalent to the straight water-surface profile along the channel. In response to any design or control scheme, the river channel evolves in such a way that uniformity in sediment discharge and straight water-surface profile are approached subject to the given constraints.

CHANNEL DESIGN CONFIGURATION

The 100-year flood hydrograph for the Rillito River as shown in Fig. 3 has a peak discharge of 34,000 cfs. For this design flood, the final channel design configuration was arrived at from a preliminary assumed configuration defined by cross sections following the HEC-2 format. For the initial assumed configuration, river channel changes were evaluated using the FLUVIAL-11 Model. The simulated results

served as a feedback to be used as a guide in revising the design. The final configuration was selected based upon the major design considerations in flood control, flow velocity, river channel changes, material balance, and economy. Except for certain existing bank protections, the design channel cross section is trapezoidal in shape, with a bottom width of 320 feet and 1 on 1 side slopes. At the 100-year discharge of 34,000 cfs, the average depth of flow is about 8.5 feet. Longitudinal alignment of the channel design consists of straight reaches and simple curves as exemplified in Fig. 4 together with the longitudinal profile of design channel bed. Because of the slight decrease in sediment size from upstream to downstream, the channel slope is designed to decrease gently downstream.

SIMULATED RESULTS

In the FLUVIAL computation, the Manning coefficient of 0.03 was used for the channel. Selected simulation results are shown in Figs. 4 and 5. The computed water-surface profile at the peak discharge based upon the FLUVIAL program is shown in Fig. 4 together with the respective channel-bed profiles at the peak discharge and at the end of flood. It is important to point out that the channel-bed profile at the end of flood does not reflect the effect of extended low flow which usually develops an incised small channel. The cross sectional profiles shown in Fig. 5 include those of the design (the initial), at the peak discharge and at the end of flood (again, excluding the incised low flow channel). Within a river bend, the channel-bed profile is characterized by a transverse bed slope, with greater flow depth and scour near the concave bank as shown in Fig. 5 for Sections 6.35 and 6.66. The transverse bed slope as well as the scour depth,

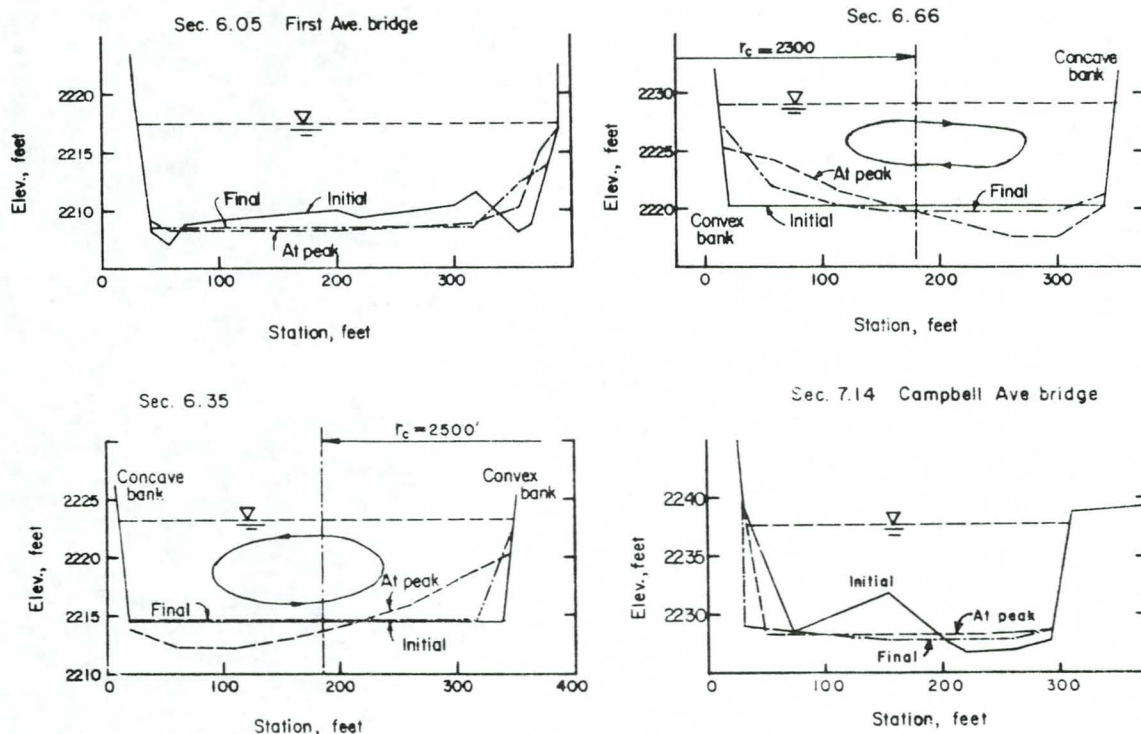


Fig. 5. - Simulated Results for Sample Cross Sections

is directly related to the channel curvature and water discharge. The nonuniform channel-bed profile at the peak discharge shown in Fig. 4 is primarily attributed to spiral motion associated with the curvature which grows as the flow enters a bend and decays after the bend exit. However, this kind of scour is at least partially eliminated during the falling limb of the hydrograph. This explains why an observer of the post-flood channel bed may fail to recognize the severe scour under the muddy flowing water at high flow.

The FLUVIAL profile for the water surface is nearly a straight-line because it includes the river channel changes. The water-surface profile computed based upon the HEC-2 program which is a fixed-bed model is less uniform; it shows backwater effects upstream of bridges. In reality, one would expect such bridge obstructions to be at least partially compensated by channel-bed scour.

TOP AND TOE ELEVATIONS OF BANK PROTECTIONS

The top and toe elevations of bank protections were selected on the basis of the simulated results and other considerations described below. The top elevations as shown in Fig. 4 are two feet above the peak water-surface profile based upon the FLUVIAL model, plus the superelevation. The toe elevations as shown in Fig. 4 were determined based upon the computed maximum channel-bed scour plus one half of the wave height for antidunes and a safety margin of about 6 feet. The wave height for antidunes was computed from the equation(2)

$$h = 2\pi (0.14) V^2/2g \quad (1)$$

in which h = wave height; V = mean velocity; and g = gravitational acceleration. For the maximum velocity of 13 feet per second, the wave height is about 2.3 feet.

An important feature of this design is the fact that variable toe elevations were used to account for the variation in scour depth between the concave and convex banks as shown in Fig. 4. Needless to say, this design scheme provides more effective protection against channel-bed scour.

ACKNOWLEDGEMENTS

This study was sponsored by the Department of Transportation and Flood Control District, Pima County, Arizona under the project title "Rillito River Bank Protection" (Contract No. 07-04-10051-0984).

APPENDIX I. REFERENCES

1. Chang, n. n., "Water and Sediment Routing Through Curved Channels," Journal of Hydraulic Engineering, ASCE, Vol. 111, No. 4, April, 1985.
2. Kennedy, J. F., "Stationary Waves and Antidunes in Alluvial Channels," Rept. KH-R-2, California Institute of Technology, 1961.